RNA Localization in *Drosophila* Oogenesis and Early Embryogenesis

Thesis by
Kellie L. Whittaker

In Partial Fulfillment of the Requirements
for the Degree of
Doctor of Philosophy

California Institute of Technology
Pasadena, California
1997
(Submitted May 30, 1997)

ACKNOWLEDGMENTS

The art of mentoring requires a delicate balance between providing guidance and advice and allowing a young scientist the latitude to find one's own way of doing things. I thank my advisor, Dr. Howard Lipshitz, for providing all of the above plus a steady dose of encouragement and the chance to live in Toronto for over a year of my graduate career. In his lab I experienced the joy of science, the excitement of fitting together pieces of a scientific puzzle, the pleasure of figuring out the implications of that puzzle and how best to convey my work to others, and what it truly meant to have camaraderie in the work environment.

All graduate students experience both ups and downs during the quest for the doctorate, and I was no exception. I want to thank each and every one of my thesis committee members--Drs. Howard Lipshitz, Barbara Wold, Elliot Meyerowitz, John Abelson, and Paul Sternberg, for listening to me and giving me support during the most difficult of those times. Each one of you provided encouragement and helped me to make the decision to persevere until I finished. Was it worth it to stick it out? Unequivocally, yes.

To the many members of the Lipshitz lab and the Lewis lab, both past and present--you have all enriched my life, both personal and professional, in immeasurable ways. To the Caltech members of the Lipshitz lab: Drs. Dali Ding, Susan Halsell, Richard Yip, Terry Strecker, Michele Zaccai and Michele Lamka, and Jim Angus and Bill Fisher: you helped to make the rigors of graduate school seem like fun. To the Toronto members of the Lipshitz lab: Arash Bashirullah, Angelo Karaiskakis, Peter Becker, Ramona Cooperstock, Ronit Wilk, Dr. Leonora Rochwerger, Dr. Bruce Reed, Weili Fu and Kent Wang: you are a great group of people both to do science with and to hang out with. The experience of being the senior graduate student in the Toronto lab was especially important to me. To the Lewis lab: Dr. Jo Topol, Dr. Sue Celniker, John Knafels, Beth Turner, and Dr. Ed Lewis: Thanks for all the support, and for making me feel welcome in your lab during the last few

months of my time at Caltech. Jo, thank you for the many years of friendship and for gluing my lucky frog back together the week before my thesis was finished. I also deeply appreciate Dr. Ed Lewis' giving me a "home," desk space in his lab, and extensive use of his computer during the time of writing up my dissertation.

I am particularly grateful to Dr. Jo Topol, Dr. Sue Celniker, Dr. Susan Halsell, Peter Becker, Bill Fisher, and of course Dr. Howard Lipshitz, for extensive and insightful scientific and editorial comments on my Adducin-like chapter.

My off-campus support and morale team included Kate and Aidan Bird, Alice Dennison, Dr. Ed Dennison, Marti Brande, Bob Fisher, Irene Hayman, John Helgeson, and Patty Byler. Kate, thanks for always sparking my scientific curiosity and excitement through our many discussions, for sharing your love of the natural world with me, for all the times you encouraged me to keep going, and for sustaining our friendship through the years of my living in the lab. Alice and Ed, your love and support and eagerness to listen have meant a lot to me. Marti, thanks for being my cheerleader and reminding me that graduate school is only one small part of life. Bob and Irene, your gallons of freshly squeezed orange juice kept me healthy during the critical last months of dissertation writing. John and Patty, the encouragement and confidence-boosting you did helped me to get over the last hurdles.

To Bill Fisher: You are the best. Your love and support (both technical and emotional!) have meant more to me than I can possibly tell you.

Finally, I am grateful to have a family who encouraged my curiosity about the world in many ways and my decision to go for a Ph.D. in science. I appreciate the constant love and support from my brother, Jim Whittaker II, and my grandmother, June H. Oshel. In particular, I want to give special thanks to my parents, Dr. James O. Whittaker and Sandra J. Whittaker, for your unflagging love, support, and encouragement, for the financial and emotional help during the tough times of graduate school, for cheering me on, and for making the world seem my oyster.

ABSTRACT

Localization of maternal mRNAs is an important developmental strategy for providing spatially restricted synthesis of the encoded proteins. Much of the work done on localized RNAs in *Drosophila* development has focused on identification of pattern determinants, but not all localized maternal RNAs encode such patterning specifiers. *Adducin-like*, also known as *hu-li tai shao*, represents the only example to date of a transcript which is both localized throughout *Drosophila* oogenesis and encodes a cytoskeletal protein. *Adducin-like* encodes the *Drosophila* homologue of mammalian adducin, which in humans is a membrane-cytoskeletal protein that contributes to local cytoskeletal assembly, particularly at sites of cell-cell contact and communication. We show here that *Adducin-like* generates a family of transcripts through alternative mRNA splicing. The splice variants of *Adducin-like* share sequence in the open reading frame (ORF) but are truncated at different points and have unique 3' ORF sequences plus different 3'UTRs. One of these transcript classes, R1, encodes an Adducin-like protein isoform with a MARCKS-related element and represents the first *Drosophila* orthologue of mammalian adducin. R1 Adducin-like activity is likely to be regulated by signal transduction pathways similar to those affecting human adducins. Another *Adducin-like* transcript class, N4, is localized specifically to and within the developing *Drosophila* oocyte and early embryo. *Cis*-acting signals for N4 RNA localization are contained within the 3'UTR. We have mapped these signals and identified a unique *cis*-acting element capable of directing early transport of mRNA into the oocyte. *swallow* is required for the localization of *Adducin-like* mRNA, and we present evidence that *swallow* acts through the *Adducin-like* N4 3'UTR to promote *Adducin-like* N4 mRNA localization in mid- to late oogenesis. We consider the possible functions of alternative splicing in development.

Another non-pattern-specifying maternal RNA localized in early *Drosophila* development is the mitochondrial 16S large ribosomal RNA (16S RNA). The 16S RNA is

localized to the posterior of the early embryo and appears to be a constituent of polar granules, since maternal effect mutations which disrupt the polar granules also abolish 16S RNA localization. We show that 16S RNA localization does not appear to be necessary for pole cell formation or function.

TABLE OF CONTENTS

CHAPTER 1

Mechanisms and Functions of RNA Localization to the Anterior Pole of the *Drosophila* Oocyte and Early Embryo

This chapter has been published in:

Localized RNAs (ed. H.D. Lipshitz). R.G. Landes/Springer-Verlag Press, 1995.

MECHANISMS AND FUNCTIONS OF RNA LOCALIZATION TO THE ANTERIOR POLE OF THE *DROSOPHILA* OOCYTE AND EARLY EMBRYO

Kellie L. Whittaker, Howard D. Lipshitz

INTRODUCTION

The first molecularly cloned localized RNA encoded by a gene with a known developmental function was *bicoid*, which is localized to the anterior pole of the *Drosophila* oocyte and early embryo.[1-3] Identification of *bicoid* as an anterior localized RNA represented the first convincing evidence in any organism or cell type that RNA localization serves a key functional role: in this case, specification of cell fates in the anterior of the early embryo.[3-6] The fact that *bicoid* was identified as an anterior-localized RNA in a molecular screen for genes that encode proteins with a shared motif (the PRD-domain)[1] before this RNA was definitively shown to be encoded by the *bicoid* locus,[3] exemplifies the power of combining molecular and genetic approaches. Since then, several additional anterior localized RNAs have been identified in the *Drosophila* oocyte and early embryo. Four of these are encoded by genetic loci that were molecularly cloned because of their interesting developmental phenotypes (*Bicaudal-D*, *fs(1)K10*, *gurken*, *oskar*).[7-11] Others were identified in molecular screens (*Adducin-like/hu-li tai shao*, *orb*, *yemanuclein-α*),[12-15] and a subset of these have subsequently been shown to be encoded by loci with interesting mutant phenotypes.

Since an extensive description has been given in chapter 2 of *Drosophila* oogenesis and early embryogenesis, those topics will not be reviewed again here. Rather, we will proceed directly to a description of the anterior RNAs, the mechanisms of their localization, and their functions.

Localized RNAs, edited by Howard D. Lipshitz.

DYNAMICS OF ANTERIOR RNA LOCALIZATION

RNAs that exhibit anterior localization during *Drosophila* oogenesis fall into one of several categories on the basis of their localization dynamics (Figs. 3.1-3.3, Table 3.1): (1) concentration at the oocyte's anterior pole and maintenance at the anterior through early embryogenesis (*bicoid*, *Adducin-like/hu-li tai shao*); (2) concentration at the oocyte's anterior pole, followed by loss of localization by the end of oogenesis (*fs(1)K10*, *yemanuclein-α*, *Bicaudal-D*); or (3) initial concentration at the oocyte's posterior pole, followed by anterior localization (*gurken, orb*).

Class 1: RNAs Localized to the Anterior of the Oocyte and Early Embryo

bicoid

bicoid encodes a homeodomain protein that plays a key role in establishing the anterior-posterior axis of the embryo (see below).[2,3] *bicoid* transcripts first accumulate

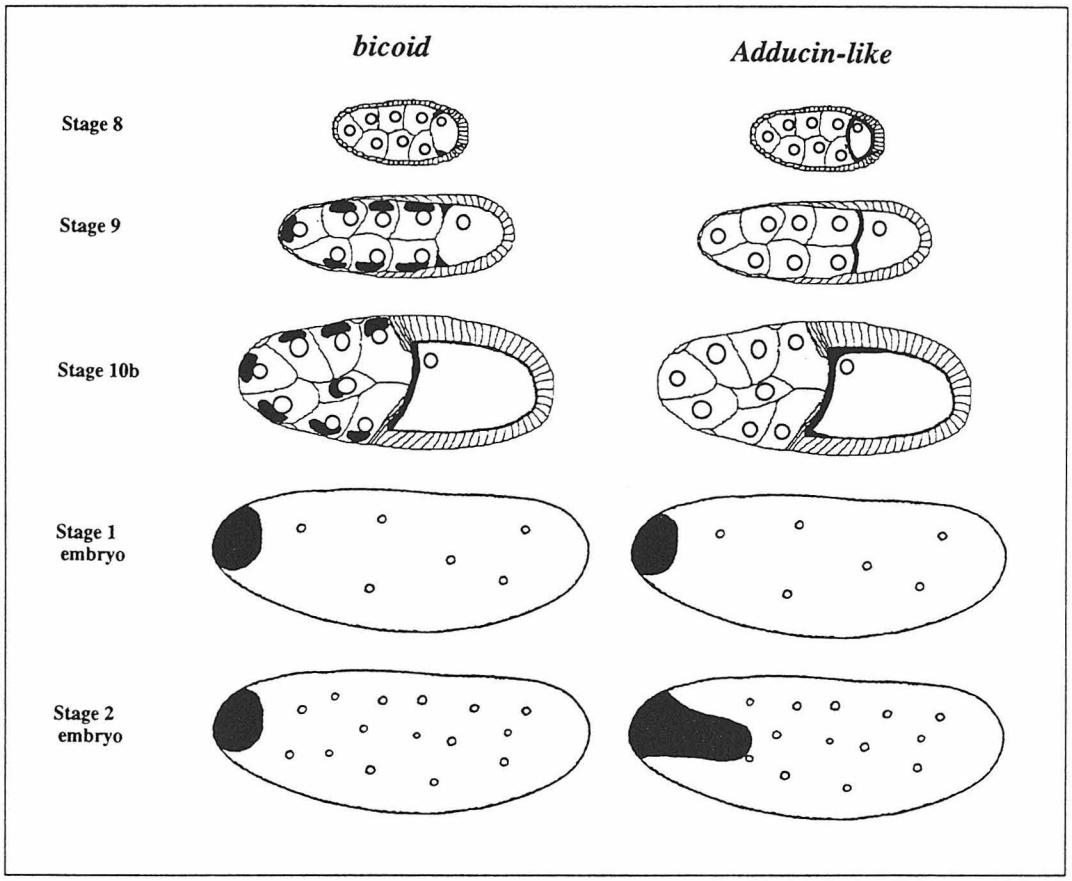

Fig. 3.1. Localization dynamics of bicoid *and* Adducin-like/hu-li tai shao *RNAs. Representative stages during which the two RNAs become localized to the anterior are shown. (A)* bicoid *RNA is localized as a ring at the anterior of stage 8 oocytes. In stage 9 oocytes,* bicoid *RNA is also localized within nurse cells, apical to the nuclei. At stage 10B, the anterior distribution broadens to cover the entire anterior cortex. In stage 1 and stage 2 embryos,* bicoid *RNA is maintained at the anterior. (B)* Adducin-like *RNA is restricted to the cortex of the oocyte in stage 8. At stage 9,* Adducin-like *RNA begins to concentrate at the anterior cortex. In stage 10 oocytes* Adducin-like *RNA is found only in the anterior cortex with the highest concentration antero-dorsally. Newly fertilized eggs (stage 1 embryos) show an anterior distribution of* Adducin-like *RNA that is very similar to the* bicoid *RNA distribution. However,* Adducin-like *RNA is released from the anterior at stage 2 and diffuses posteriorly. It disappears shortly thereafter (not shown), again unlike* bicoid. *See the text for additional stages at which these RNAs are expressed.*

in the oocyte at stage 5-6 of oogenesis in patches that seem to correspond with the locations of the four ring canals that connect the oocyte to the nurse cells (Figs. 3.1 and 3.2, Table 3.1) (see chapter 2 for description of the nurse cell-oocyte complex).[6] The patches of *bicoid* RNA merge into a ring at the anterior cortex and remain as an anterior ring from about stages 7-9.[6,16] During stages 9-10A, *bicoid* RNA is also localized within nurse cells in distinct patches apical to the nuclei.[3,6,16] During stages 10B-11, apical localization of *bicoid* RNA in the nurse cells disappears, while

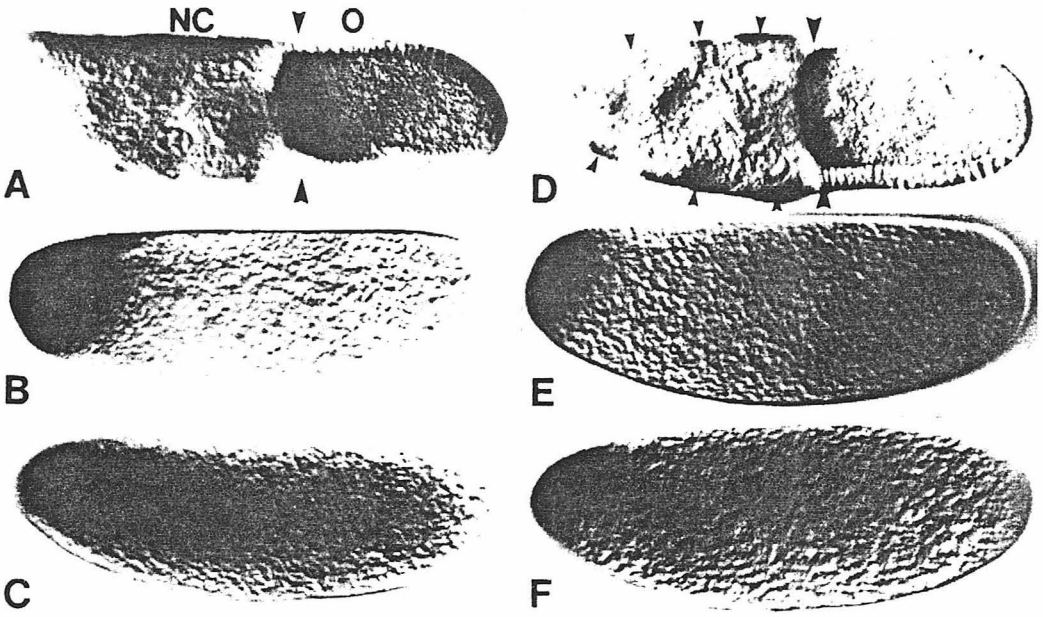

Fig. 3.2. Visualization of bicoid *and* Adducin-like/hu-li tai shao *RNA localization by whole mount in situ hybridization. (A) In stage 10 oocytes,* Adducin-like *transcripts are localized to the anterior cortex (large arrowheads) with the highest concentration antero-dorsally. Shading of the dorsal edge of the nurse cells and the posterior follicle cells is due to DIC optics and does not reflect transcripts. NC, nurse cells; O, oocyte. (B)* Adducin-like *RNA is concentrated at the anterior of stage 1 embryos. (C) In stage 2 embryos,* Adducin-like *RNA is released from the anterior and diffuses posteriorly. (D) In stage 10 egg chambers,* bicoid *transcripts are confined to the anterior pole of the oocyte (large arrowheads) and apical to the nurse cell nuclei (small arrowheads). (E) In stage 1 embryos,* bicoid *RNA is localized at the anterior. (F) In stage 2 embryos,* bicoid *RNA is retained at the anterior in contrast to* Adducin-like *RNA (cf. C). In all cases, anterior is to the left and dorsal is towards the top of the page. Figures courtesy of D. Ding.*

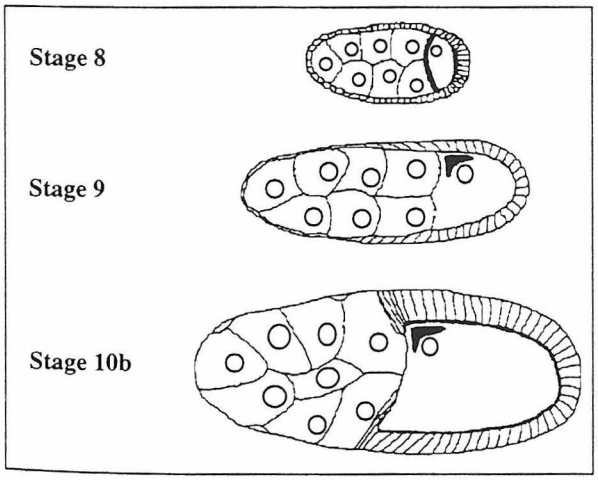

Fig. 3.3. Localization of gurken *RNA to the antero-dorsal tip of the oocyte.* gurken *RNA is found transiently at both poles in early stage 8 oocytes. In late stage 8 to early stage 9 oocytes, when the oocyte nucleus has migrated to just below the anterodorsal surface,* gurken *RNA is tightly restricted anterodorsally between the oocyte nucleus and the plasma membrane.*

Table 3.1. Dynamics of anterior RNA localization

Gene (homology and function)	Germarium	Stages 2-6	Stages 7-8	Stages 9-10A	Stages 10B-11	Stages 12-14	Cleavage Stage Embryo	Syncytial Blastoderm Embryo	Ref.
Adducin-like (adducin; cytoskeletal spectrin-actin binding protein)	region 2-3: concentrated in oocyte	Stage 2-6: RNA fills oocyte Stage 2-6; low levels in nurse cells	cortex of oocyte; low levels in nurse cells	cortex of oocyte Stage 10A: expression in nurse cells	anterior of oocyte Stage 10B: expression in nurse cells	antero-dorsal of oocyte	Stage 1: antero-dorsal of oocyte Stage 2: released from anterior and diffuses posteriorly	no maternal RNA	12, 13
Bicaudal-D (coiled-coil motif; protein protein interaction)	region 1: all 16 cells region 2A: enriched in oocyte	in oocyte	Stage 7: in oocyte Stage 8: anterior of oocyte; nurse cells	nurse cells, anterior of oocyte	Stage 10B: anterior of oocyte; nurse cells Stage 11: delocalization begins	delocalized	delocalized	delocalized	7
bicoid (homeodomain transcription factor)	no RNA	Stage 5-6: concentrated in oocyte	ring at anterior of oocyte	ring at anterior of oocyte; apical patches in nurse cells	cortical cap at anterior of oocyte	anterior of oocyte	anterior of embryo	anterior of embryo	3, 6, 16, 46
fs(1)K10 (helix-turn-helix motif DNA binding protein)	region 1: RNA fills all 16 cystocytes region 2-3: concentrated in oocyte	Stage 2-6: RNA concentrated in oocyte	Stage 7: throughout oocyte Stage 8: anterior of oocyte	anterior of oocyte; nurse cells	anterior of oocyte; nurse cells	absent	absent	absent	27, 74
gurken (TGF-α motif; secreted ligand for EGF-like receptor)	region 2B-3: concentrated in oocyte	concentrated in oocyte	Stage 7: posterior of oocyte Stage 8: anterior and posterior poles of oocyte; late Stage 8, anterodorsal only	anterodorsal, between oocyte nucleus and plasma membrane	anterodorsal, between oocyte nucleus and plasma membrane Stage 11: delocalization begins	not reported	not reported	not reported	9, 33

orb (RNP/RRM motif RNA binding protein)	region 2A-3: concentrated in oocyte region 3: low levels in nurse cells	concentrated in oocyte; low levels in nurse cells	Stage 7: posterior of oocyte Stage 8: anterior of oocyte	anterior of oocyte	Stage 10B: anterior of oocyte Stage 11: delocalized	delocalized	posterior of embryo; accumulates preferentially in pole cells when they form	pole cells	14
yemanuclein-α (novel; DNA binding protein)	no RNA	Stage 2-5: no RNA Stage 6: in oocyte, distributed around nucleus	Stage 7: in oocyte, around nucleus Stage 8: anterior, around nucleus	anterior of oocyte	delocalized in oocyte; expressed in nurse cells	delocalized	delocalized	delocalized	15, 31

in the oocyte it is localized as a cap covering the entire anterior cortex.[6,16] In early cleavage stage embryos, maternally synthesized *bicoid* RNA is present in a spherical[6] or cone-shaped[3] distribution that extends into the interior of the embryo from the anterior pole (see chapter 2 for a description of early embryogenesis). *bicoid* transcript levels begin to drop after nuclear migration to the periphery of the embryo is completed and become restricted to the anterior cortex before disappearing.[3,6] This restriction to the cortex could be accomplished either through an active RNA localization process or, alternatively, as a consequence of a uniform rate of degradation gradually revealing a higher level of *bicoid* RNA in the cortex than in the interior of the embryo. *bicoid* RNA disappears completely during the process of blastoderm cellularization.[6]

Although *bicoid* RNA is localized at the anterior of oocytes for three days (stages 5-14 of oogenesis), it is not translated until after fertilization.[4,5] This fact excludes the possibility that *bicoid* RNA is localized co-translationally (see below). Diffusion of Bicoid protein from the anterior source of translation creates an inverse exponential protein gradient with a maximum at the anterior pole and extending posteriorly through the anterior half of the embryo.[4,5] The functional significance of anterior localization of *bicoid* RNA will be discussed below.

Adducin-like/hu-li tai shao

The *Adducin-like/hu-li tai shao* gene[12,13] encodes a family of proteins most of which exhibit strong similarity to mammalian adducin, a membrane cytoskeletal protein that promotes the assembly of F-actin at actin-spectrin junctions.[17-20] Southern blots have shown that *Adducin-like* is a single-copy gene,[13] but cDNA sequence analysis has indicated that there are at least four different spliced forms of ovarian *Adducin-like* RNA with distinct 3'UTRs (see below).[21] These alternatively spliced RNAs encode proteins that share amino-domains of homology to mammalian adducin but that differ in their carboxy-region.[21] It should be noted that, since the probes used for RNA tissue in situ hybridization[12,13] detect all known splice variants of *Adducin-like* RNA, all readily detectable forms of *Adducin-like* RNA in the nurse cell-oocyte complex are localized as described below.

Adducin-like/hu-li tai shao RNA is targeted to the oocyte four days before *bicoid* RNA; it can readily be detected in the presumptive oocyte in region 2 of the germarium (Figs. 3.1 and 3.2, Table 3.1).[12,13] From stages 1–6 of oogenesis the RNA fills the oocyte, and during stages 7–9 it begins to be concentrated in the cortex.[13,22] At stage 10, *Adducin-like* RNA begins to concentrate at the anterior pole of the oocyte and it is more highly con-

centrated antero-dorsally from stages 10 through 14 (Figs. 3.1 and 3.2).[13] At stage 10 accumulation can also be detected in the nurse cells.[12,13] In very early cleavage stage embryos, *Adducin-like* transcripts are localized at the anterior pole in a pattern similar to that of *bicoid* transcripts.[13] At slightly later cleavage stages the RNA is released from the anterior pole and diffuses posteriorly.[13] By the syncytial blastoderm stage maternally synthesized *Adducin-like* RNA has disappeared.[12,13]

One isoform of Adducin-like protein (60 kD) has no homology to mammalian Adducin and is localized at the ring canals.[23] At least three isoforms (140, 95, 87 kD) with homology to mammalian Adducin are synthesized during oogenesis. All of these appear first in germarial region 1 in the fusome,[22,24] a spectrin-containing cytoskeletal structure that is involved in germarial cyst formation (see chapter 2). At least two of these isoforms (95 and 87 kD) are present in the nurse cell cytoplasm through stage 11 and the 87 kD form is also localized to the oocyte cortex from stages 9 through 10B.[22] By stage 12, this isoform is found at the anterior pole of the oocyte. *Adducin-like* RNA and protein localization thus roughly parallel each other both temporally and spatially, the former preceding the latter as expected.

Class 2: RNAs with Anterior Localization During Mid-Oogenesis Followed by De-localization Late in Oogenesis

fs(1)K10

The *fs(1)K10* gene functions in the pathway that specifies the dorso-ventral axis of the oocyte.[25] It encodes a protein containing a helix-turn-helix domain with an octapeptide repeat that has been proposed to be DNA-binding.[8,26] However, recent evidence suggests that the postulated DNA-binding domain is dispensable for K10 protein function (see chapter 7). *fs(1)K10* transcripts fill all 16 cystocytes in germarial region 1 (Table 3.1).[27] Accumulation in the nurse cells drops to background levels in germarial regions 2 and 3, leaving *fs(1)K10* RNA concentrated in the oocyte.[27] *fs(1)K10* RNA is found throughout the oocyte from stage 1-7 egg chambers. It is localized to the anterior cortex of the oocyte from stage 8 at least through the end of stage 10.[27] *fs(1)K10* transcripts accumulate in the nurse cells again at stages 9-11; these transcripts are transferred into the oocyte as the nurse cell contents are dumped beginning at stage 10B/11.[27] *fs(1)K10* RNA is absent from 0-2 hour embryos, implying that the transcripts are degraded between stage 10B and fertilization (chapter 7).

K10 protein is present in the oocyte nucleus starting at stage 1 and continuing through stage 11 of oogenesis.[8] The *fs(1)K10* gene is considered in detail in chapter 7

Bicaudal-D

Bicaudal-D (Bic-D) encodes a protein with a region of homology to the coiled-coil domains of myosin heavy chain, kinesin, and intermediate filament proteins such as keratin and lamin.[7,28] *Bicaudal-D* RNA is first detected in germarial region 1 in all 16 cystocytes but accumulates at higher levels in the oocyte through stage 7 (Table 3.1).[7] Nurse cell accumulation of *Bicaudal-D* RNA is high during stages 8-11. From stages 8-10, *Bicaudal-D* RNA is localized as a cap to the anterior of the oocyte. At stage 11, the RNA begins to delocalize. From stage 13 through the end of oogenesis and in early embryos, *Bicaudal-D* RNA is uniformly distributed.[7] By the syncytial blastoderm stage the level of RNA begins to drop and, by the cellular blastoderm stage, *Bicaudal-D* RNA is no longer detectable.

Translation of *Bicaudal-D* RNA is coincident with its transcription. Bicaudal-D protein is detectable in germarial region 1 in all 16 cystocytes.[29] In germarial region 2A, the protein begins to accumulate preferentially in the presumptive oocyte, and this enrichment in the cytoplasm of the oocyte relative to the nurse cells persists through oogenesis. In

early embryos the protein is concentrated in the cytoplasm basal to the nuclei but is uniformly distributed with respect to the anterior-posterior axis.[28] The *Bic-D* gene and its functions are considered in detail in chapter 5.

yemanuclein-α

yemanuclein-α encodes a DNA-binding protein that is concentrated in the oocyte nucleus.[30] The *yemanuclein-α* transcript is first detectable by stages 6-7 in the cytoplasm of the oocyte, at the periphery of the nucleus (Table 3.1).[15,31] By early stage 8, when the nucleus begins to migrate to the anterior dorsal region of the oocyte, *yemanuclein-α* mRNA also begins to show anterior localization with the highest concentration found around the nucleus. During stages 9-10A, anterior enrichment is maintained and a gradient forms along the anterior-posterior axis. In stage 10B, localization is abolished and *yemanuclein-α* RNA is uniformly distributed in the cytoplasm of both the oocyte and nurse cells. This uniform distribution persists through the remainder of oogenesis and into early embryogenesis. At the syncytial blastoderm stage the transcript begins to disappear and is no longer detectable by the completion of gastrulation.[15]

The *yemanuclein-α* RNA is apparently translated as soon as it appears in the cytoplasm at stages 6-7. Yemanuclein-α protein is restricted to the oocyte nucleus throughout the rest of oogenesis.[30]

Class 3: RNAs Initially Localized to the Posterior Pole, Followed by Anterior Localization

gurken

The *gurken* gene encodes a TGF-α-related extracellular signal involved in specification of the dorso-ventral axis of the oocyte.[9,32] Accumulation of *gurken* RNA can first be detected in region 2B of the germarium (Fig. 3.3, Table 3.1).[9] In stage 1-7 egg chambers, the RNA is localized to the oocyte and, at stage 7, *gurken* RNA is found predominantly as a crescent at the posterior. At stage 8, when the oocyte nucleus begins its migration from the center of the oocyte to the antero-dorsal tip, *gurken* RNA is localized at both the anterior and posterior poles. By late stage 8/early stage 9, the oocyte nucleus reaches the antero-dorsal region and *gurken* is restricted antero-dorsally, to the cytoplasm between the nucleus and the oocyte plasma membrane. This distribution is maintained from late stage 8 through at least stage 10B.[9] Transverse sections through stage 9 egg chambers have shown that *gurken* RNA is concentrated dorsally, above the oocyte nucleus.[33] No data have yet been reported for *gurken* transcript distributions during later oogenesis and early embryogenesis; neither have protein distributions been reported.

orb

The *orb* gene encodes an RNP/RRM-family RNA-binding protein.[14,34,35] *orb* RNA localization has been discussed in chapter 2, since it is localized to the posterior pole of the oocyte; for clarity, the dynamics of *orb* RNA localization are summarized here again (Table 3.1). *orb* RNA is targeted to the oocyte in region 2A of the germarium.[14] From stages 1-6 the RNA fills the oocyte but, by stage 7, *orb* RNA is found as a posterior crescent. However, in stage 8-10 oocytes, *orb* transcripts are localized to the anterior.[14] From stages 11-14, *orb* RNA is uniformly distributed through the oocyte. *orb* transcripts are concentrated at the posterior of early embryos and they accumulate in the pole cells when these cells form.[14] Somatic transcript levels drop at the syncytial blastoderm stage while the levels remain high in the pole cells at least through gastrulation.[14]

Orb protein shows a complex distribution pattern during oogenesis (chapter 6).[14,34,35] Although Orb protein can first be detected in all germline cells of 8- and 16-cell germarial cysts, the protein then becomes preferentially concentrated in the cytoplasm of the presumptive oocyte. During stage 7, Orb protein is found mostly at the posterior cortex of the oocyte.

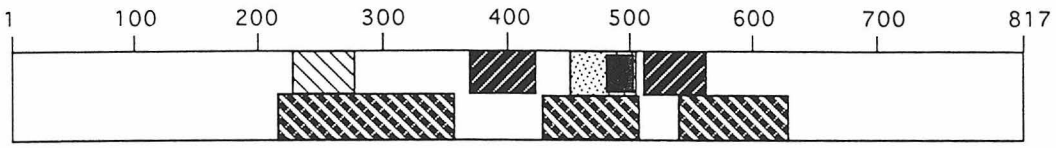

Fig. 3.4. Localization signals and protein binding sites within the bicoid *3'UTR. Within the 817 nucleotide (nt)* bicoid *3'UTR, several cis-acting signals have been mapped which direct* bicoid *RNA localization at various stages of oogenesis. Top, light diagonal striped box: sequence required for anterior localization at stage 10 and later (Δ7, nt 229-281).[37] Top, dark diagonal striped boxes: deletion of these sequences impairs but does not completely prevent anterior localization of* bicoid *RNA at stage 10 (Δ11, nt 383-419; Δ16, nt 512-565).[37] Top, stippled box: sequence directing initial* bicoid *RNA transport to the oocyte and subsequent localization of* bicoid *to the anterior (Δ14, nt 455-504, defining BLE1 sequence, for* bicoid *localization element 1).[37] Top, small gray box: sequence containing a binding site for EXL protein (nt 482-504).[38] Bottom, cross-hatched boxes: sequences containing binding sites for Staufen protein (nt 211-360, 421-510, 541-630). See chapter 8.*

During stages 8-9, Orb protein starts to accumulate at the anterior of the oocyte although high levels are still present at the posterior and throughout the cortex. At stage 10, Orb protein is concentrated in the anterior oocyte cortex.[35] No Orb protein distributions have been reported for later stages of oogenesis or for early embryogenesis. The *orb* gene and its functions are considered in chapter 6.

COMPONENTS OF THE ANTERIOR RNA LOCALIZATION MECHANISM

Cis-Acting Tags in the Anterior Localized RNAs

Methods for mapping cis-acting sequences within localized *Drosophila* RNAs have been described in chapter 2. Of the seven anterior-localized RNAs discussed here, the cis-acting sequences that tag them for transport into, and localization to the anterior of, the oocyte have been analyzed in four (*bicoid, Adducin-like, fs(1)K10, orb*). In all four cases the cis-acting signals have been found to reside within the 3'UTR of the RNA.

bicoid

Regulatory elements directing *bicoid* RNA localization were initially mapped to a 628 nucleotide (nt) region of the 817 nt *bicoid* 3'UTR (from nucleotides 93–720).[36] Reporter transcripts carrying the 628 nt region are localized to the anterior of the early embryo, indicating that this region is sufficient to direct anterior localization. Subsequently, finer-scale mapping was achieved using transgenes consisting of intact *bicoid* 5'UTR and protein coding sequence, fused to a mutated *bicoid* 3'UTR containing sequential small deletions 18 to 102 nt in size.[37] These constructs were introduced into a *bicoid* mutant background and assayed for functional rescue of the mutant phenotype, or were additionally tagged with a reporter sequence close to the polyadenylation sequence, and the resulting transcripts assayed for localization (Fig. 3.4). One deletion of 53 nucleotides (nt 451-503; Δ14, defining BLE1 for *bicoid* localization element 1) disrupts transport into, and localization within, the oocyte throughout oogenesis. To establish that BLE1 itself could confer localization, one or two copies were fused to a construct lacking almost all of the *bicoid* 3'UTR and completely deficient in RNA localization. Although a single copy of BLE1 is insufficient to drive transcript localization, the construct containing two copies of BLE1 ('2X BLE1') localizes normally until stage 10A: 2X BLE1 transcripts are properly targeted to the oocyte during stages 5-7, and at stage 8 they are localized to the anterior of the oocyte and to apical regions of nurse cells. However, these transcripts are delocalized at stage 10A and later stage oocytes and early embryos show a uniform distribution of 2X BLE1 transcripts. Thus BLE1 is necessary for *bicoid*

transcript localization, but is sufficient only for localization from stages 5 through 9. Interestingly, a binding site for EXL protein–which appears to function in *bicoid* RNA localization at stage 9–has been mapped to the 3' part of BLE1 (see below).[38]

While BLE1 is the only element whose deletion abolishes localization and mutant rescue, several other deletions produce impaired localization and/or impaired rescue of the *bicoid* mutant phenotype (Fig. 3.4).[37] Transgenes carrying these deletions (Δ7, Δ11, Δ16, Δ18, Δ19) show no functional rescue when present in a single copy but show full rescue when present in two copies. The implication of these results is that the altered transcript is sufficiently impaired in localization (or function) to lower the absolute amount of Bicoid protein synthesized at the anterior below that which is needed to properly specify head development (see below). Two copies of the transgene can, however, provide functional levels of Bicoid protein at the anterior. Direct analysis of the localization patterns of tagged transcripts carrying these deletions in the 3'UTR showed that Δ7 transcripts localize normally until stage 9-10A. Subsequently, however, the Δ7 transcripts delocalize from the anterior margin and spread along the cortex through the anterior half of the oocyte. Later, Δ7 transcripts are uniformly distributed throughout the cortex and yolk in the anterior third of the embryo. The Δ7 sequence might therefore represent a binding site for a protein that mediates tight maintenance of anterior localization. The Δ7 deletion is encompassed by a Staufen binding site (Fig. 3.4);[39] Staufen mediates anterior retention of *bicoid* RNA in the early embryo (see below). The functions of the sequences deleted by Δ11, Δ16, Δ18 and Δ19 remain unclear. Δ11 and Δ16 transcript localization resemble wild-type although levels are lower and some degree of de-localization occurs. No data have been reported for Δ18 and Δ19.

Redundancy has been invoked to explain why a deletion of part of the *bicoid* 3'UTR was found to abolish localization in one study[36] but not in another.[37] In the first study, deletion of the first 120 nucleotides of the 630 nt fragment of the 3'UTR abolished anterior transcript localization.[36] In the second study the full length (817 nt) 3'UTR carried the same 120 nucleotide internal deletion, but the resulting transcript could successfully rescue *bicoid* mutant embryos.[37] Possible impairment of localization was, however, not tested.

A nine nucleotide localization element has been reported to reside near the 5' end of the *bicoid* 3'UTR (nt 52-60).[40] Partial mislocalization occurs when in vitro transcribed RNA lacking this sequence is injected into the anterior cortex of the embryo, and it was speculated that this might be caused by elimination of a Staufen-binding region. However, removal of the entire region has recently been shown to have no effect on binding of Staufen protein to *bicoid* RNA.[39] Further, a subset of the *bicoid* 3'UTR that lacks this sequence is sufficient to direct normal anterior localization of heterologous RNAs such as *oskar* and *nanos* (chapter 2).[41,42] Thus, it seems unlikely that this nonamer functions in *bicoid* mRNA localization.

There is a significant body of evidence that the secondary structure of the *bicoid* 3'UTR may be important for RNA localization.[36,43] In particular, *bicoid* 3'UTRs from several *Drosophila* species (*D. melanogaster*, *D. simulans*, *D. teissieri*, *D. virilis*) have diverged extensively in primary sequence but have similar predicted secondary structures. Furthermore, chimeric transgenes consisting of the *D. melanogaster bicoid* 5'UTR and coding region fused to the *bicoid* 3'UTR from any of these species are capable of directing proper transcript localization in *D. melanogaster*.[43] An examination of the 53 nucleotide BLE1 localization element shows that 52 of the 53 nucleotides are completely conserved among all the four species of *Drosophila* tested for proper *bicoid* localization, and 22 of the last 24 are identical when one includes *bicoid* sequences from *D. heteroneura*, *D. picticornis*, and *D. sechellia*.[43] However,

despite this sequence conservation, a single copy of BLE1 is insufficient to direct transcript localization and two tandem copies must be used (see above). A single copy of BLE1 might be unable to form sufficient secondary structure for recognition by the appropriate trans-acting factor(s).[37]

Adducin-like

As described above, there are at least four distinct splice-variants of *Adducin-like/ hu-li tai shao* RNA, each with a different 3'UTR.[12,13,21] Two of these, the N4[13] and the R16[21] forms, have been analyzed for their spatial distributions during oogenesis and early embryogenesis. The N4 form is expressed in the nurse cells, transported into the oocyte, localized to the oocyte's cortex and then its anterior.[13] In contrast, the R16 form is expressed in the nurse cells but is never transported into the oocyte.[21] Chimeric reporter transgenes consisting of an *Hsp26* maternal nurse cell enhancer fused to the *Sgs-3* promoter,[44] a *lacZ* sequence tag, and the 351 nt *Adducin-like* N4 3'UTR produce transcripts that are properly transported into and localized within the oocyte, indicating that the N4 3'UTR is sufficient for these processes.[21]

fs(1)K10

Sequences responsible for early targeting of the *fs(1)K10* RNA to the oocyte are located in its 1.4 kb 3'UTR.[27] Recent analyses have identified a 75 nt region within the 3'UTR that is sufficient to direct *fs(1)K10* RNA transport into, and anterior localization in, the oocyte (see chapter 7).

orb

Localization of *orb* RNA to the oocyte is controlled by a specific subset of its 1.2 kb 3'UTR (see Fig. 2.6 and chapter 6).[45] A 280 nt segment of the *orb* 3'UTR (referred to as segment CE, containing nt 330-610) is sufficient to direct the normal, dynamic localization pattern observed for the endogenous *orb* transcripts. Targeting to the oocyte can be accomplished equally well with non-overlapping elements (segment HX, containing nt 1-425; and segment XN, containing nt 425-815), implying that redundant oocyte targeting tags exist. While XN by itself could direct posterior localization through stage 7, HX by itself only produces occasional weak accumulation at the posterior pole in earlier egg chambers. Neither HX nor XN alone direct anterior localization at stages 8-10, suggesting that the anterior localization element spans nucleotide position 425 or that multiple elements–at least one in HX and at least one in XN–are necessary for anterior RNA targeting.

Trans-Acting Factors that Function in Anterior RNA Localization

All cis-acting anterior RNA localization signals identified to date reside in the 3'UTRs of the transcripts. It remains to be shown definitively whether the specific information is contained in the primary RNA sequence, in its secondary structure or in a combination of these. In any case, these signals must be recognized by trans-acting factors that bind and mediate transport and anchoring (Table 3.2). Thus, it is possible that combinatorial use of localization tags and their recognition proteins might regulate the detailed stepwise spatial and temporal localization events for different RNAs. Ultimately it is expected that the cytoskeleton and associated 'motors' must also be involved (see also chapters 2 and 4).

THE ROLE OF THE CYTOSKELETON AND ASSOCIATED PROTEINS

Microtubules, Microfilaments and the Oocyte Nucleus

A detailed consideration of the functions of the cytoskeleton in RNA localization is given in chapter 4; consequently only a summary is presented here. The role of cytoskeletal elements in RNA localization and anchoring can be inferred from the ability of cytoskeleton-disrupting drugs to perturb RNA localization processes,[46,47]

and from the association of specific transcripts with the detergent-insoluble fraction of oocyte cytoskeletal extracts.[48]

Studies with microtubule polymerization inhibitors, such as colchicine, colcemid, nocodazole, or tubulazole, have shown that microtubules are required at four discrete points in oogenesis: (1) oocyte determination and growth in stages 1-6;[49] (2) migration of the oocyte nucleus from the center to the antero-dorsal corner at stages 8-9;[50] (3) positioning of *bicoid* RNA and other RNAs at stages 9-12;[46,47,51] (4) ooplasmic streaming during stages 10B-12.[52]

In contrast, microfilament polymerization inhibitors such as cytochalasin B and cytochalasin D apparently perturb only slow specific transport of nurse cell macromolecules through the ring canals[53] as well as the bulk transfer of nurse cell cytoplasm to the oocyte at stage 11.[54] Cytochalasin treatment does not affect *bicoid* transcript localization at any stage during oogenesis[46] and thus microfilaments appear not to play a role in specific RNA transport and anchoring during most stages of *Drosophila* oogenesis.

All of the anterior localized RNAs examined to date require microtubules for their transport into the oocyte, for their initial anterior localization in the oocyte, and for the maintenance of this localization (chapter 4). *bicoid, fs(1)K10, Bicaudal-D* and *orb* RNAs are all sensitive to disruption of localization by microtubule inhibitors but are not affected by microfilament inhibitors.[46,48] All of these RNAs are also found in the detergent-insoluble fraction of oocyte cytoskeletal extracts.[48] Early targeting of cyclin B and 65F transcripts to the oocyte is also disrupted by microtubule inhibitors.[47]

The effects of cytoskeletal inhibitors on *bicoid* RNA localization are understood in the most detail. Injection of colchicine directly into the abdomens of young adult female flies results in failure of *bicoid* RNA targeting to the oocyte at stage 5, or localization at any stage.[46] Incubation of stage 10 or older egg chambers directly in

Table 3.2. Trans-acting factor requirements for RNA localization

	BIC-D	CAPU	EGL	EXU	K10	ORB	SPIR	SQD	STAU	SWW
Adducin-like		-13		-13		+35	-13		-13	+13
Bicaudal-D	+7		+7			+35			-72	
bicoid		-75		+3, 6		-34	-75		+6	+3, 6
fs(1)K10	+7	+27	+7			+34, 35	+27		-72, 76	-76
gurken		+9			+9, 33	+33, 34	+9	+9, 33	-72	
orb	+14		+14			+35			-72	

[+], trans-acting factor is necessary for proper localization of this RNA; [-], trans-acting factor is not required for correct localization of the specified RNA; blank, untested whether trans-acting factor affects localization of this RNA. Numbers in superscripts refer to the relevant references.

colchicine, nocodazole, or tubulazole causes *bicoid* RNA de-localization in both the oocyte and the nurse cells.[46] When the microtubule inhibitor is washed out of the egg chamber by incubation in drug-free medium, *bicoid* RNA relocalizes to the anterior. Taxol treatment, which inhibits microtubule disassembly and results in the formation of abnormal microtubule arrays, results in aberrant localization of *bicoid* RNA around the oocyte nucleus and in the cortex.[46,48] In contrast, disruption of actin filaments by cytochalasin B and D have no effect on *bicoid* localization.[46] Thus, the microtubule-based cytoskeleton is required for the initial transport and localization of *bicoid* RNA as well as for its subsequent anchoring.

A recent report has shown that *spindle-C* mutants form a mirror-symmetric microtubule cytoskeleton in the oocyte, with the minus ends of the microtubules now located at each end of the oocyte and plus ends in the center of the oocyte.[55] This contrasts with the normal situation in which the minus ends are at the anterior and the plus ends at the posterior (see chapters 2 and 4). In these mutants, *oskar* mRNA localizes to the center of the oocyte while *bicoid* localizes at both ends. Movement of the oocyte nucleus to the anterior dorsal surface is a microtubule-dependent process, and in *spindle-C* mutants the nucleus may migrate to either "anterior" pole. Regardless of which pole contains the nucleus, *gurken* transcripts still accumulate only at that end above the nucleus. Thus, *gurken* RNA localization is dependent on the nucleus and microtubules.[55]

cappuccino and *spire*

In oocytes from *cappucino* and *spire* mutant mothers, the *fs(1)K10* RNA fails to localize to the anterior oocyte pole at stage 8 and remains de-localized through oogenesis (also see chapter 7).[27] *gurken* transcripts accumulate in an anterior ring from stage 9 onward, rather than being tightly restricted to the antero-dorsal tip (Table 3.2).[9,33] The premature ooplasmic streaming in *cappuccino* and *spire* mutant oocytes beginning at stage 8 of oogenesis[51] has been described in chapter 2 with particular attention to the microtubule cytoskeleton and its role in *oskar* RNA localization to the posterior pole of the oocyte. Defects in the anterior RNA localization and/or tethering machinery are likely to be the basis for the observed abnormalities in *fs(1)K10* and *gurken* RNA localization. Note, however, that Cappuccino and Spire play no role in anterior *Adducin-like/hu-li tai shao* RNA localization,[13] and are also unlikely to participate in *bicoid* RNA localization since *cappuccino* and *spire* mutations do not disrupt anterior embryonic pattern[56] (Table 3.2). Thus their role in the assembly of the microtubule cytoskeleton and RNA localization is not general but exhibits some specificity.

Factors that Might Interact Directly with the RNAs or Mediate their Interaction with the Cytoskeleton

Candidates for trans-acting factors that might be intermediaries between anterior-localized RNAs and the cytoskeletal network have been identified for several of the RNAs discussed in this review (Table 3.2). As described in chapter 2 for factors involved in posterior RNA localization, most of these were initially identified in genetic screens for maternal effect mutations that affect embryonic development[57] and only later shown to be required for RNA localization.[3,6] More recently, biochemical and molecular approaches have begun to yield additional candidates. Such intermediary factors might interact directly with the localized RNAs and serve to bind the RNAs or RNA-protein complexes (RNPs) to the cytoskeletal-associated transport machinery. In addition, they might function to maintain RNA localization by binding the RNAs to the desired cytoplasmic destination.

Swallow

Localization of both *bicoid* RNA to the anterior pole[3,6] and *Adducin-like* RNA to the oocyte cortex and then its anterior

pole,[13] requires the Swallow protein (Table 3.2), which possesses weak similarity to the RNP/RRM-family of RNA binding proteins as well as an amphipathic α-helical domain that might be involved in protein-protein interaction.[58] In *swallow* mutant ovaries *bicoid* RNA is targeted to the oocyte at the appropriate stage, accumulates at its anterior pole through stage 10A, and exhibits apical localization within the nurse cells at stage 9/10A.[6] However, during stages 10B-11, the anterior ring of *bicoid* RNA becomes much more diffuse than normal and, by stage 12, *bicoid* RNA is de-localized.[6] In oocytes and embryos derived from *swallow* mutant females, *Adducin-like* RNA is also de-localized—first from the cortex and then from the anterior pole—beginning at stage 8 of oogenesis, some 12 hours earlier than any effect on *bicoid* RNA.[13,59] Whether Swallow protein binds directly to the 3'UTRs of *bicoid* or *Adducin-like* RNAs remains unclear. Recent analyses suggest that monomeric Swallow protein is not a component of the cytoskeletal fraction of oocytes but that a high molecular weight form of Swallow is.[48] This may be indicative of the presence of Swallow protein in a specialized structure such as an RNA transport- or localization-related RNP particle.

Exuperantia and Exu-like (EXL)

bicoid RNA requires functional Exuperantia for anterior localization[3,6,57] while *Adducin-like* does not (Table 3.2).[13,59] Initial accumulation of *bicoid* RNA during stages 5-7 is normal in *exuperantia* mutant oocytes.[6] Anterior localization of *bicoid* during stages 8-10A is slightly perturbed in *exuperantia* oocytes as *bicoid* RNA appears more diffuse than in wild-type oocytes. At stage 10 *bicoid* RNA fails to become localized to the apical regions of the nurse cells, instead remaining uniform in the nurse cell cytoplasm. At this stage the transcripts also delocalize in the oocyte. Localization of the 2X BLE1 RNA (see above) is disrupted in *exuperantia* mutants in a manner resembling that of full-length *bicoid* RNA, consistent with Exuperantia acting through BLE1 in *bicoid* RNA localization.[37] In late oogenesis and early embryogenesis *bicoid* RNA is uniformly distributed in *exuperantia* mutants, although a shallow anterior to posterior gradient can be seen at the syncytial blastoderm stage, probably due to degradation of *bicoid* RNA in the posterior region of the embryo.[3] The *exuperantia* gene encodes a 531 amino acid protein with a basic domain, which initially led to the suggestion that it might bind to RNA directly.[60,61] However, recent data suggests that Exuperantia protein may not interact directly with *bicoid* RNA since the basic domain is dispensable for Exuperantia function[62] and Exuperantia can only bind RNA non-specifically.[38] Recently, the transport of Exuperantia-containing particles from the nurse cells into the oocyte has been observed in living embryos, and these particles have, in turn, been shown to co-localize with microtubules in normal and drug-treated ovaries.[62] This likely represents the direct visualization of a class of RNA transport particles.

A 115 kD protein referred to as EXL (Exu-like) has been identified in a search for proteins in oocyte extracts that can be UV crosslinked specifically to 2X BLE1 and not 1X BLE1 RNA (see above).[38] 2X BLE1 dimers carrying only the 3' 23 nucleotides retain EXL binding ability, while loss of the 3'-most 10 nucleotides eliminates EXL binding, as do several point mutations in the 3' region. These mutants were tested in vivo using a *lacZ* reporter construct. Point mutations that eliminate EXL binding cause RNA localization defects resembling those seen for wild-type 2X BLE1 RNA in *exuperantia* mutants.[38] These data argue that EXL is responsible for *bicoid* RNA localization at stage 9. Because of the striking similarity between the defects in 2X BLE1 localization caused by loss of functional Exuperantia and by mutations that prevent EXL binding, it is possible that EXL binds specifically to BLE1 and also interacts with Exuperantia protein (which does not, itself, bind specifically to RNA) in a *bicoid* RNA-EXL-Exuperantia localization complex.[38]

Staufen

The *staufen* gene encodes a double-stranded RNA-binding protein[63] that functions in localization of RNAs to the posterior polar plasm (see chapter 2) as well as in maintaining anterior localization of *bicoid* RNA (but not *Adducin-like*, *gurken*, *fs(1)K10*, *orb* and *Bicaudal-D* RNAs) (Table 3.2). In *staufen* mutant ovaries, *bicoid* RNA is localized at the anterior of the oocyte until stage 12 but, unlike the situation in wild-type, it is released from the anterior either late in oogenesis or early in embryogenesis.[6] In contrast, *Adducin-like* RNA is released from the anterior pole of wild-type early embryos, and *staufen* mutations have no effect on *Adducin-like* RNA localization.[13,59]

It has recently been demonstrated that Staufen protein co-localizes with *bicoid* RNA at the anterior of early embryos and that this localization depends on its association with the mRNA.[39] In vitro transcribed *bicoid* RNA injected into early embryos associates specifically with Staufen protein, and the sequences within the *bicoid* 3'UTR that are required for this interaction correlate well with regions predicted to form stem-loop structures.[36,39,43] The complexes of *bicoid* RNA and Staufen protein are particulate and both the formation and the transport of these particles is microtubule-dependent.[39] The functions and mechanisms of RNA localization by Staufen are reviewed in detail in chapter 8.

Orb

The Orb RNP/RRM-motif containing RNA-binding protein plays several roles during oogenesis, all of which can be explained on the basis of a possible role in RNA transport and targeting. First, strong *orb* mutants have defects in germarial cysts consistent with the observed defects in transport of key oocyte-localized RNAs (*Adducin-like/hts (hu-li tai shao)*, *Bicaudal-D*, *fs(1)K10*) into the presumptive oocyte in region 2 of the germarium (Table 3.2).[34,35] Weaker *orb* alleles result in dorso-ventral pattern defects in embryos, consistent with the observed de-localization of *fs(1)K10* RNA and the failure to localize *gurken* RNA dorsally near the oocyte nucleus (see below).[9,33] In addition, *orb* mutations produce defects in abdominal pattern consistent with failure to localize *oskar* RNA to the posterior pole of the oocyte. A detailed discussion of the *orb* gene and its functions is presented in chapter 6, and some discussion of its role in posterior RNA localization is also given in chapter 2.

Bicaudal-D

The *Bicaudal-D* gene encodes a protein with a region of homology to the coiled-coil domains of several cytoskeletal proteins.[7,28] The Bicaudal-D protein functions in the early choice between nurse cell and oocyte fate in the germarium and in transport and anchoring of transcripts including *Bicaudal-D* RNA itself,[29] *orb* RNA,[35] *oskar* RNA and *fs(1)K10* RNA[29] in the presumptive oocyte at this stage (Table 3.2 and chapter 5). For example, in loss of function *Bicaudal-D*^{PA66} mutants in which Bic-D protein does not accumulate in a single cystocyte and no oocyte differentiates, *orb* RNA is uniformly distributed in all 16 cystocytes instead of being concentrated in a single cell. In *Bicaudal-D*^{R26} mutants, *orb* RNA is correctly targeted to the pro-oocyte in region 2 cysts and in stage 1-3 egg chambers, but the localization is subsequently lost. Just as *orb* RNA targeting into the presumptive oocyte is dependent on *Bicaudal-D* function, so *Bicaudal-D* RNA targeting into the oocyte is dependent on *orb* function. These effects can be interpreted either as a secondary effect of misspecification of oocyte identity or as evidence for a more direct role for Bicaudal-D and Orb in RNA targeting into the oocyte, the disruption of which then results in failure to specify oocyte identity. The *Bicaudal-D* gene and its functions are considered in detail in chapter 5.

Squid

The *squid* gene encodes a protein that belongs to the hnRNP family of RNA-binding proteins.[64] Two isoforms of Squid protein (Squid-A and Squid-B) are

expressed in the oocyte during oogenesis. *squid* mutations result in dorsalization of the embryo and it has been shown that Squid is required, not for transport of the *gurken* RNA into the oocyte, but for its correct dorso-anterior localization (Table 3.2). For example, in *squid* mutant ovaries, *gurken* RNA is restricted to the anterior margin of the oocyte from stage 9 through the later stages, but it never becomes sharply limited to the dorsal tip.[9] This implicates Squid in the localization of *gurken* RNA to the dorsal anterior region, possibly through direct interaction with the *gurken* transcript.

egalitarian

In *egalitarian*[11] egg chambers, *Bicaudal-D*,[29] *orb*[35] and *fs(1)K10*[11] RNAs never accumulate in a single cell (*egalitarian* mutants fail to differentiate an oocyte), instead remaining uniform in all germline cells (Table 3.2). Interestingly, in *egalitarian* mutants these RNAs do not co-precipitate with the cytoskeletal fraction of oocytes but remain in the supernatant.[48] It remains to be determined whether the defects in RNA localization in *egalitarian* mutants are a consequence of a direct role for the *egalitarian* gene product in RNA transport or whether they are a secondary effect of failure to specify oocyte identity.

FUNCTIONS OF ANTERIOR LOCALIZED RNAS

Having described the dynamics of anterior RNA localization, the nature of the cis-acting signals directing their localization and trans-acting factors involved in their localization, we now turn to questions of function. Specifically, (1) what functions are served by the proteins that the localized RNAs encode, and (2) to what extent does this function necessitate RNA localization at a given time and place?

These functions are clearly defined for the anteriorly localized RNAs involved in dorso-ventral (*orb*, *fs(1)K10*, *gurken*) and anterior-posterior (*bicoid*) axis specification. However, at this point it is not clear what functions might be served by anterior localization of the other three RNAs: *Bicaudal-D* is discussed in depth in chapter 5; no detailed mutant phenotypes that relate to their anterior localization have been reported for *Adducin-like/hts* and *yemanuclein-α* RNAs although a preliminary phenotype has been described recently for *Adducin-like/hts*.[22] We restrict our discussion in this section to the *orb*, *fs(1)K10*, *gurken* and *bicoid* RNAs.

SPECIFICATION OF THE DORSO-VENTRAL AXIS OF THE OOCYTE: *ORB*, *FS(1)K10* AND *GURKEN*

The *gurken* RNA encodes a TGF-α-related secreted ligand that binds to and activates the *Drosophila* EGF-receptor homolog (DER/Torpedo), which is expressed on all the follicle cells surrounding the oocyte.[9] The localized nature of the Gurken ligand—a consequence of the tight localization of the *gurken* RNA to the antero-dorsal tip of the oocyte—restricts reception of the signal to the antero-dorsal follicle cells. Follicle cells that receive the Gurken signal adopt dorsal fates while the other follicle cells adopt ventral fates. One consequence of this is the asymmetric production of two egg coverings–the chorion and the vitelline membrane–by the follicle cells. A second consequence is inhibition of production of active ligand for the TOLL receptor dorsally; active TOLL ligand is produced only in the ventral regions of the perivitelline space surrounding the early embryo. The establishment of the ventral source for active TOLL ligand may involve lateral inhibitory interactions among the cells in the follicular epithelium, initiated as a result of Gurken/DER-mediated signaling in the dorsal follicle cells.[33] Ventral activation of the TOLL receptor initiates a cytoplasmic signal transduction cascade that ultimately results in transcriptional control of zygotic dorso-ventral pattern genes and specification of cell fates along the dorso-ventral embryonic axis.[65]

The necessity for the tight restriction of *gurken* RNA to the antero-dorsal tip of the oocyte is shown in two recent studies. First, if the copy-number of the *gurken* gene

is increased, hence increasing the amount of Gurken protein, dorsalized eggs are produced.[66] This indicates that increasing the amount of wild-type Gurken ligand is sufficient to induce a greater number of follicle cells to follow a 'dorsal' fate with drastic consequences for the deposition/activation of dorso-ventral signals read by the early embryo. Second, alteration of *gurken* RNA localization from its normal dorso-anterior position to a more general anterior distribution results in a 90 degree shift in the embryonic dorso-ventral axis, which then becomes coincident with the normal antero-posterior axis.[33] This is presumably a consequence of all anterior follicle cells, rather than just the dorso-anterior ones, receiving the Gurken signal and indicates why the *gurken* RNA is localized not just to the anterior but to the dorso-anterior of the oocyte.

At least two anterior localized RNAs (*orb* and *fs(1)K10*) encode products important for the dorso-anterior localization of *gurken* RNA and thus play a key role in dorso-ventral axis specification. *fs(1)K10* resides upstream of *gurken* genetically[67] while *orb* mutations interact synergistically with *gurken* alleles.[34] *fs(1)K10* and *orb* function are required respectively for the anterior and the antero-dorsal localization of *gurken* RNA.[9,33] Consequently defects in dorso-ventral pattern occur in embryos produced by *fs(1)K10* and *orb* females (see above). It is unclear whether the role of these proteins in *gurken* RNA localization is direct or indirect. For example, since Orb is an RNA binding protein, it is possible that there is a direct interaction between Orb protein and *gurken* RNA. Alternatively, *orb* mutations might disrupt the dorso-ventral polarity of the oocyte and the mislocalization of *gurken* RNA could be a secondary consequence of this perturbed polarity. If K10 functions as a transcription factor in the oocyte nucleus, it must be assumed to regulate genes in the oocyte that are important either for oocyte polarity or directly for *gurken* transcript localization. No such genes have been identified. An alternative model for K10 function is that it negatively regulates *gurken* transcription[67] or transcript stability. The functions of *orb* and *fs(1)K10* are considered in detail in chapters 6 and 7.

Specification of the Anterior-Posterior Axis of the Embryo: *bicoid*

Of all known localized RNAs, the function of anterior localization of *bicoid* RNA and the function of its encoded protein are the best understood (Fig. 3.5). *bicoid* transcripts are localized to the anterior of the egg during oogenesis and are translated after fertilization.[3-6] Because the early embryo is syncytial, Bicoid protein diffuses away from the site of translation, forming an anterior-posterior gradient extending through the anterior half of the embryo.[4] The peak of this gradient is at the anterior tip. Bicoid protein, a transcription factor containing a DNA-binding homeodomain, activates zygotic genes that establish anterior pattern in the developing embryo, in a concentration-dependent manner.[5] That is, certain genes regulated by Bicoid can be activated at relatively low concentrations of Bicoid protein (e.g. *hunchback*) while others are postulated to require higher concentrations of Bicoid (e.g. *orthodenticle*, *empty spiracles*).[68-70] In this way, the latter class of genes are only activated in the more anterior region of the embryo while genes such as *hunchback* are activated throughout the anterior half of the embryo. Localization of *bicoid* RNA to the anterior pole of the oocyte and early embryo thus serves a key role in the establishment of the gradient of Bicoid protein that is used to specify distinct anterior cell fates. It has also been shown that mislocalization of *bicoid* RNA and protein to the posterior of the early embryo results in misspecification of posterior cells to adopt anterior fates.[71] Thus anterior localization of *bicoid* RNA serves the dual roles of promoting anterior fates in the anterior of the embryo and preventing misspecification of cells in the posterior regions of the embryo as anterior in fate.

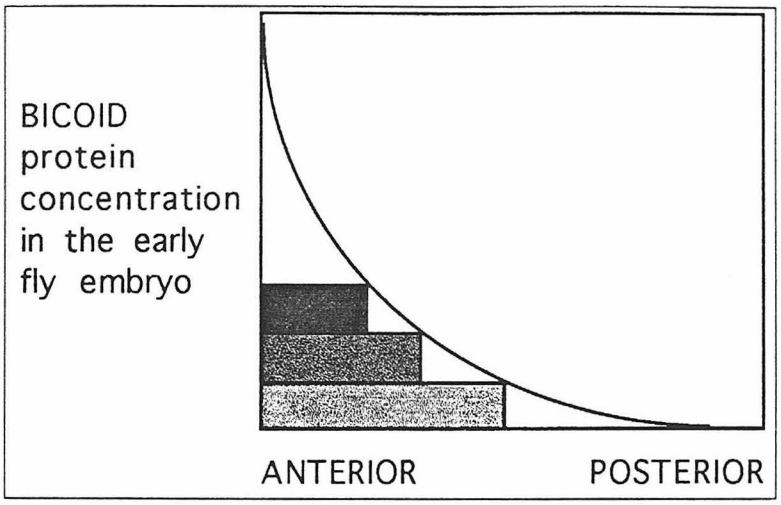

Fig. 3.5. A gradient of Bicoid protein activates target genes in a concentration-dependent manner. Translation of anteriorly localized bicoid *RNA and subsequent diffusion of Bicoid protein results in an exponentially decreasing gradient of Bicoid protein in the early embryo, with the highest level of protein present at the anterior tip. Dark shading: Because the* orthodenticle *gene is activated only by high levels of Bicoid,* orthodenticle *expression is confined to the anterior of the early embryo. Intermediate shading: The* empty spiracles *gene is turned on by high and intermediate levels of Bicoid protein. Light shading: High, intermediate and low levels of Bicoid protein can activate* hunchback, *which is therefore expressed more posteriorly than either* orthodenticle *or* empty spiracles. *(Adapted from: St Johnston D. et al. Development 1989; 107 (suppl):13-19; and Lipshitz HD. Curr Opin Cell Biol 1991; 3:966-975.)*

SUMMARY AND PROSPECTS

The *Drosophila* oocyte and early embryo is particularly well suited as a model system for the study of RNA localization. The egg and early embryo are large enough to enable leakage or transplantation of cytoplasm, localized injection of RNA or protein, and purification of RNA or protein from only a subset of the anterior-posterior or dorso-ventral axes. The facility with which genetic and molecular screens can be conducted have resulted in the identification of a number of localized gene products, several of which are essential for proper oogenesis and/or cell fate specification in the early embryo. Furthermore, the ease with which transgenic flies can be generated has allowed the molecular characterization of the cis-acting tags required for RNA localization in an appropriate in vivo context. Analyses of RNA distributions in mutant backgrounds have allowed identification of potential trans-acting factors and the biochemical isolation of factors that can bind to defined cis-acting tags is expected to increase this collection. Finally, detailed functional descriptions of the *Drosophila* microtubule system and microtubule-associated motors are emerging. It is anticipated that these genetic, molecular, biochemical and cellular descriptions of RNA localization will fuse into a unified understanding of the mechanisms of RNA localization and the functions of the localized RNAs during early *Drosophila* development.

REFERENCES

1. Frigerio G, Burri M, Bopp D et al. Structure of the segmentation gene *paired* and the *Drosophila* PRD gene set as a part of a gene network. Cell 1986; 47:735-746.
2. Frohnhöfer HG, Nüsslein-Volhard C. Organization of anterior pattern in the

Drosophila embryo by the maternal gene *bicoid*. Nature 1986; 324:120-125.

3. Berleth T, Burri M, Thoma G et al. The role of localization of *bicoid* RNA in organizing the anterior pattern of the *Drosophila* embryo. EMBO J 1988; 7:1749-1756.
4. Driever W, Nüsslein-Volhard C. A gradient of *bicoid* protein in *Drosophila* embryos. Cell 1988; 54:83-93.
5. Driever W, Nüsslein-Volhard C. The *bicoid* protein determines position in the *Drosophila* embryo in a concentration-dependent manner. Cell 1988; 54:95-104.
6. St Johnston D, Driever W, Berleth T et al. Multiple steps in the localization of *bicoid* RNA to the anterior pole of the *Drosophila* oocyte. Develop 1989; 107 (Suppl):13-19.
7. Suter B, Romberg LM, Steward R. *Bicaudal-D*, a *Drosophila* gene involved in developmental asymmetry: localized transcript accumulation in ovaries and sequence similarity to myosin heavy chain tail domains. Genes Dev 1989; 3:1957-1968.
8. Prost E, Derychere F, Roos C et al. Role of the oocyte nucleus in determination of the dorsoventral polarity of *Drosophila* as revealed by molecular analysis of the *K10* gene. Genes Dev 1988; 2:891-900.
9. Neuman-Silberberg FS, Schupbach T. The Drosophila dorsoventral patterning gene gurken produces a dorsally localized RNA and encodes a TGF-α-like protein. Cell 1993; 75:165-174.
10. Kim-Ha J, Smith JL, Macdonald PM. *oskar* mRNA is localized to the posterior pole of the *Drosophila* oocyte. Cell 1991; 66:23-35.
11. Ephrussi A, Dickinson LK, Lehmann R. *oskar* organizes the germ plasm and directs localization of the posterior determinant *nanos*. Cell 1991; 66:37-50.
12. Yue L, Spradling AC. *hu-li tai shao*, a gene required for ring canal formation during *Drosophila* oogenesis, encodes a homolog of adducin. Genes Dev 1992; 6:2443-2454.
13. Ding D, Parkhurst SM, Lipshitz HD. Different genetic requirements for anterior RNA localization revealed by the distribution of *Adducin*-like transcripts during *Drosophila* oogenesis. Proc Natl Acad Sci USA 1993; 90:2512-2516.
14. Lantz V, Ambrosio L, Schedl P. The *Drosophila orb* gene is predicted to encode sex-specific germline RNA-binding proteins and has localized transcripts in ovaries and early embryos. Develop 1992; 115:75-88.
15. Aït-Ahmed O, Thomas-Cavallin M, Rosset R. Isolation and characterization of a region of the *Drosophila* genome which contains a cluster of differentially expressed maternal genes (*yema* gene region). Developmental Biology 1987; 122:153-162.
16. Stephenson EC, Pokrywka NJ. Localization of *bicoid* message during *Drosophila* oogenesis. Curr Topics Dev Biol 1992; 26:23-35.
17. Joshi R, Gilligan DM, Otto E et al. Primary structure and domain organization of human alpha and beta adducin. J Cell Biol 1991; 115:665-675.
18. Gardner K, Bennett V. A new erythrocyte membrane-associated protein with calmodulin binding activity. J Biol Chem 1986; 261:1339-1348.
19. Gardner K, Bennett V. Modulation of spectrin-actin assembly by erythrocyte adducin. Nature 1987; 328:359-362.
20. Kaiser HW, O'Keefe E, Bennett V. Adducin: Ca^{++}-dependent association with sites of cell-cell contact. J Cell Biol 1989; 109:557-569.
21. Whittaker KL, Ding D, Fisher WW et al. Differential splicing of distinct 3'-exons controls transport and localization of *Adducin*-like RNAs encoding different protein isoforms in the *Drosophila* oocyte. In preparation.
22. Zaccai M, Lipshitz HD. Two isoforms of the *Drosophila Adducin*-like protein exhibit distinct spatial distributions during oogenesis and embryogenesis and are differentially affected by *swallow* mutations. in preparation.
23. Robinson DN, Cant K, Cooley L. Morphogenesis of *Drosophila* ring canals. Development 1994; 120:2015-2025.
24. Lin H, Yue L, Spradling A. The *Drosophila* fusome, a germline-specific organelle, contains membrane skeletal proteins and functions in cyst formation. Development 1994; 120:947-956.
25. Wieschaus E. *fs(1)K10*, a female sterile mutation altering the pattern of both egg coverings and the resultant embryos in

Drosophila. In: Le Douarin N, ed. Cell Lineage, Stem Cells and Cell Determination, INSERM Symposium 10. Amsterdam: Elsevier, 1979:291-302.

26. Suzuki M, Neuhaus D, Gerstein M et al. Solution structure of the DNA-binding octapeptide repeat of the *K10* gene product. Protein Engineering 1994; 7:461-470.
27. Cheung H-K, Serano TL, Cohen RS. Evidence for a highly selective RNA transport system and its role in establishing the dorsoventral axis of the *Drosophila* egg. Develop 1992; 114:653-661.
28. Wharton RP, Struhl G. Structure of the *Drosophila* Bicaudal-D protein and its role in localizing the posterior determinant *nanos*. Cell 1989; 59:881-892.
29. Suter B, Steward R. Requirement for phosphorylation and localization of the Bicaudal-D protein in Drosophila oocyte differentiation. Cell 1991; 67:917-926.
30. Aït-Ahmed O, Bellon B, Capri M et al. The *yemanuclein-alpha* — a new *Drosophila* DNA-binding protein specific for the oocyte nucleus. Mech Develop 1992; 37:69-80.
31. Thomas-Cavallin M, Aït-Ahmed O. The random primer labeling technique applied to in situ hybridization on tissue sections. J Histochem Cytochem 1988; 36:1335-1340.
32. Schüpbach T. Germ line and soma cooperate during oogenesis to establish the dorsoventral pattern of egg shell and embryo in *Drosophila melanogaster*. Cell 1987; 49: 699-707.
33. Roth S, Schüpbach T. The relationship between ovarian and embryonic dorsoventral patterning in *Drosophila*. Develop 1994; 120:2245-2257.
34. Christerson LB, McKearin DM. *orb* is required for anteroposterior and dorsoventral patterning during *Drosophila* oogenesis. Genes Dev 1994; 8:614-628.
35. Lantz V, Chang JS, Horabin JI et al. The *Drosophila orb* RNA-binding protein is required for the formation of the egg chamber and establishment of polarity. Genes Dev 1994; 8:598-613.
36. Macdonald PM, Struhl G. *Cis*-acting sequences responsible for anterior localization of *bicoid* mRNA in *Drosophila* embryos. Nature 1988; 336:595-598.
37. Macdonald PM, Kerr K, Smith JL et al. RNA regulatory element BLE1 directs the early steps of *bicoid* mRNA localization. Develop 1993; 118:1233-1243.
38. Macdonald PM, Leask A, Kerr K. EXL protein specifically binds BLE1, a *bicoid* mRNA localization element, and is required for one phase of its activity. submitted.
39. Ferrandon D, Elphick L, Nüsslein-Volhard C et al. Staufen protein associates with the 3'UTR of *bicoid* mRNA to form particles that move in a microtubule-dependent manner. Cell 1994; 79:1221-1232.
40. Gottlieb E. The 3' untranslated region of localized maternal messages contains a conserved motif involved in messenger-RNA localization. Proc Natl Acad Sci USA 1992; 89:7164-7168.
41. Ephrussi A, Lehmann R. Induction of germ cell formation by *oskar*. Nature 1992; 358:387-392.
42. Gavis ER, Lehmann R. Localization of *nanos* RNA controls embryonic polarity. Cell 1992; 71:301-313.
43. Macdonald PM. *bicoid* mRNA localization signal: phylogenetic conservation of function and RNA secondary structure. Develop 1990; 110:161-171.
44. Serano TL, Cheung H-K, Frank LH et al. P element transformation vectors for studying *Drosophila melanogaster* oogenesis and early embryogenesis. Gene 1994; 138: 181-186.
45. Lantz V, Schedl P. Multiple *cis*-acting targeting sequences are required for *orb* mRNA localization during *Drosophila* oogenesis. Molec Cell Biol 1994; 14:2235-2242.
46. Pokrywka NJ, Stephenson EC. Microtubules mediate the localization of *bicoid* RNA during *Drosophila* oogenesis. Develop 1991; 113:55-66.
47. Theurkauf WE, Alberts BA, Jan YN et al. A central role for microtubules in the differentiation of *Drosophila* oocytes. Develop 1993; 118:1169-1180.
48. Pokrywka NJ, Stephenson EC. Localized RNAs are enriched in cytoskeletal extracts of *Drosophila* oocytes. Dev Biol 1994; 166:210-219.
49. Koch EA, Spitzer RH. Multiple effects of colchicine on oogenesis in *Drosophila*: In-

duced sterility and switch of potential oocyte to nurse-cell developmental pathway. Cell and Tissue Res 1983; 228:21-32.

50. Gutzeit HO. The role of microtubules in the differentiation of ovarian follicles during vitellogenesis in *Drosophila*. Roux's Arch Dev Biol 1986; 195:173-181.
51. Theurkauf WE. Premature microtubule-dependent cytoplasmic streaming in *cappucino* and *spire* mutant oocytes. Science 1994; 265:2093-2096.
52. Gutzeit HO, Koppa R. Time-lapse film analysis of cytoplasmic streaming during late oogenesis in Drosophila. J Embryol Exp Morphol 1982; 67:101-111.
53. Bohrmann J, Biber K. Cytoskeleton-dependent transport of cytoplasmic particles in previtellogenic to mid-vitellogenic ovarian follicles of *Drosophila*: time-lapse analysis using video-enhanced contrast microscopy. J Cell Sci 1994; 107:849-858.
54. Gutzeit HO. The role of microfilaments in cytoplasmic streaming in *Drosophila* follicles. J Cell Sci 1986; 80:159-169.
55. González-Reyes A, St Johnston D. Role of oocyte position in establishment of anterior-posterior polarity in *Drosophila*. Science 1994; 266:639-642.
56. Manseau L, Schüpbach T. *cappuccino* and *spire*: two unique maternal-effect loci required for both anteroposterior and dorsoventral patterns of the *Drosophila* embryo. Genes Dev 1989; 3:1437-1452.
57. Frohnhöfer HG, Nüsslein-Volhard C. Maternal genes required for the anterior localization of *bicoid* activity in the embryos of *Drosophila*. Genes Dev 1987; 1:880-890.
58. Chao Y-C, Donahue KM, Pokrywka NJ et al. Sequence of *swallow*, a gene required for the localization of *bicoid* message in *Drosophila* eggs. Dev Genetics 1991; 12:333-341.
59. Ding D, Lipshitz HD. Localized RNAs and their functions. BioEssays 1993; 10: 651-658.
60. Macdonald PM, Luk SKS, Kilpatrick M. Protein encoded by the *exuperantia* gene is concentrated at sites of *bicoid* messenger-RNA accumulation in *Drosophila* nurse cells but not in oocytes or embryos. Genes Dev 1991; 5:2455-2466.
61. Marcey D, Watkins WS, Hazelrigg T. The temporal and spatial-distribution pattern of maternal *exuperantia* protein—evidence for a role in establishment but not maintenance of *bicoid* messenger-RNA localization. EMBO J 1991; 10:4259-4266.
62. Wang S, Hazelrigg T. Implications for *bcd* mRNA localization from spatial distribution of *exu* protein in *Drosophila* oogenesis. Nature 1994; 369:400-403.
63. St Johnston D, Brown NH, Gall JG et al. A conserved double-stranded RNA-binding domain. Proc Natl Acad Sci USA 1992; 89:10979-10983.
64. Kelley RL. Initial organization of the *Drosophila* dorsoventral axis depends on an RNA-binding protein encoded by the *squid* gene. Genes Dev 1993; 7:948-960.
65. Chasan R, Anderson KV. Maternal control of dorsal-ventral polarity and pattern in the embryo. In: Bate M, Martinez Arias A, eds. The Development of *Drosophila melanogaster*. Cold Spring Harbor, NY: Cold Spring Harbor Laboratory Press, 1993:387-424.
66. Neuman-Silberberg FS, Schüpbach T. Dorsoventral axis formation in *Drosophila* depends on the correct dosage of the gene *gurken*. Develop 1994; 120:2457-2463.
67. Forlani S, Ferrandon D, Saget O et al. A regulatory function for K10 in establishment of dorsoventral polarity in the *Drosophila* egg and embryo. Mech Develop 1993; 41:109-120.
68. Driever W, Nüsslein-Volhard C. The *bicoid* protein is a positive regulator of *hunchback* transcription in the early *Drosophila* embryo. Nature 1989; 337:138-143.
69. Driever W, Thoma G, Nüsslein-Volhard C. Determination of spatial domains of zygotic gene expression in the *Drosophila* embryo by the affinity of binding sites for the *bicoid* morphogen. Nature 1989; 340:363-367.
70. Struhl G, Struhl K, Macdonald PM. The gradient morphogen *bicoid* is a concentration-dependent transcriptional activator. Cell 1989; 57:1259-1273.
71. Driever W, Siegel V, Nüsslein-Volhard C. Autonomous determination of anterior structures in the early *Drosophila* embryo by the *bicoid* morphogen. Develop 1990; 109: 811-820.
72. González-Reyes A. Role of *staufen* in the

localization of *oskar* and *bicoid* RNAs. In: Lipshitz HD, ed. Localized RNAs. Austin: RG Landes, 1995: in press.

73. Lipshitz HD. Axis specification in the *Drosophila* embryo. Curr Opin Cell Biol 1991; 3:966-975.
74. Haenlin M, Roos C, Cassab A et al. Oocyte-specific transcription of *fs(1)K10*: a *Drosophila* gene affecting dorsal-ventral developmental polarity. EMBO 1987; 6:801-807.
75. Stephenson EC. Cytoskeletal mechanisms of RNA localization during *Drosophila* oogenesis. In: Lipshitz HD, ed. Localized RNAs. Austin: RG Landes, 1995: in press.
76. Serano TL, Cohen RS. mRNA localization and function of the *Drosophila fs(1)K10* gene. In: Lipshitz HD, ed. Localized RNAs. Austin: RG Landes, 1995: in press.

(blank page)

INTRODUCTION

The targeting of specific mRNAs to distinct subcellular compartments is an important mechanism for generating asymmetry in many cell types, including fibroblasts, neurons, and oocytes (reviewed in 46, 75, 14). RNAs localized within the oocyte generally encode proteins which play spatially restricted roles in early embryonic development. For instance, specification of the anterior body plan in early *Drosophila* embryos requires targeting of *bicoid* mRNA to the anterior pole of the oocyte (6). Mutations which result in *bicoid* mRNA delocalization in oocytes disrupt the anterior-posterior gradient of Bicoid protein and result in embryos with severe defects in head and thoracic structures (73, 23, 24, 17). Similarly, the posterior determinant Nanos is encoded by an RNA localized to the posterior pole of the oocyte, and mutations disrupting *nanos* RNA localization produce embryos with abdominal defects (84, 29).

Localization of RNA can be accomplished in one of two ways, either by translocation of a specific RNA to a particular subcellular location, or by degrading a ubiquitous RNA everywhere except a particular region (15). The majority of localized RNAs studied to date use the first mechanism, i.e., where the RNA remains intact but is physically moved to its target destination. This targeting requires sequences within the RNA (*cis*-acting signals) as well as cellular machinery, which includes *trans*-acting factors that are able to recognize the *cis*-acting elements, direct the RNA to its appropriate destination, and tether it there. *Cis*-acting localization signals have so far been found to reside within the 3' untranslated region (UTR) of mRNAs (e.g., 57, 28, 49).

In *Drosophila*, the oocyte itself can be thought of as a specific subcellular compartment, because it develops as part of a syncytial egg chamber (44, reviewed in 72). Each egg chamber contains a single oocyte plus 15 nurse cells, with the nurse cell-oocyte complex surrounded by a monolayer of somatically-derived follicle cells. The oocyte is connected to the nurse cells by cytoplasmic bridges known as ring canals, through which

RNAs and other synthetic products of the nurse cells are transported into the oocyte. However, during early to mid-oogenesis, only a subset of maternal mRNAs are strongly enriched within the oocyte as compared to the nurse cells (74). Thus *cis*-acting elements may serve at least two functions in localizing mRNAs during *Drosophila* oogenesis: first, to target an mRNA specifically to the developing oocyte within the nurse cell-oocyte complex, and second, to direct that mRNA to its destination within the oocyte itself.

Much of the work done on localized RNAs in *Drosophila* development has focused on identification of pattern determinants, but not all localized maternal mRNAs encode such patterning specifiers. Since one aspect of cell and oocyte asymmetry is the organization of the cytoskeleton, it might be expected that some localized RNAs would encode cytoskeletal proteins. Many of the localized RNAs identified in somatic cells encode cytoskeletal proteins and/or cytoskeletal-associated proteins such as actin, myosin heavy chain, and MAP-2 (50, 9, 65, 27). Although some cytoskeletal proteins are known to be asymmetrically distributed in the early mouse embryo (21, 58, 63), few developmentally localized RNAs encoding cytoskeletal proteins have been characterized in *Drosophila*. *Adducin-like*, also known as *hu-li tai shao* (*hts*), represents the only example to date of a transcript which is both localized throughout *Drosophila* oogenesis and encodes a cytoskeletal protein (15, 88).

At least one class of *Adducin-like* mRNA is found within the germarium as early as region 1 (88). *Adducin-like* mRNA is localized within the presumptive oocyte beginning at region 2B of the germarium (15, 88). In early egg chambers, *Adducin-like* transcripts fill the oocyte until stage 7-8, when they are restricted to the oocyte cortex. At stage 8-9, *Adducin-like* transcripts are further restricted to the anterior cortex of the oocyte, where they remain through the end of oogenesis. In the early embryo, maternal transcripts are found at the anterior during stages 1-2 (15, 88). During stage 2, *Adducin-like* mRNA is released from the anterior, begins to diffuse posteriorly, and forms an anteroposterior

gradient. By stage 4 (syncytial blastoderm) maternal *Adducin-like* transcripts are no longer detectable within the embryo (15).

Adducin-like encodes the *Drosophila* homologue of mammalian adducin, which is a membrane-cytoskeletal protein that contributes to local cytoskeletal assembly, particularly at sites of cell-cell contact and communication (39, 68). Human adducin binds spectrin-actin complexes, recruits spectrin to spectrin-actin-adducin complexes, bundles actin filaments, and is also capable of regulating actin filament length by capping the barbed end of actin (25, 61, 5, 47). Although the *Drosophila Adducin-like* gene is single copy (15, 88), the mammalian adducin genes encode α, β, and γ subunits (38, 40), and the subunits associate as αβ heterodimers or tetramers (38, 37) or αγ heterodimers (16). There is no information yet as to whether *Drosophila* Adducin-like proteins are present as monomers or multimers.

Multiple signal transduction pathways appear to be regulating human adducin activity, including calmodulin binding and phosphorylation by PKA and PKC. The main site of calmodulin binding and phosphorylation is an element with MARCKS (myristoylated alanine-rich C-kinase substrate) homology (25, 59). Since the human α– and β-adducin genes have been reported to encode multiple isoforms by alternative splicing, and not all of these subunit isoforms include the MARCKS-related element, regulation of adducin function is both subunit-specific and isoform-specific (38, 77, 30, 51, 80).

We show here that *Adducin-like* also generates a family of transcripts through alternative mRNA splicing. The *Adducin-like* splice variants share sequence in the open reading frame (ORF) but are truncated at different points and have unique 3' ORF sequences plus different 3'UTRs. One of these transcript classes, the R1 class, encodes an Adducin-like protein isoform with a MARCKS-related element and thus represents the *Drosophila* orthologue of mammalian adducin. Another *Adducin-like* transcript class, the N4 class, is localized specifically to and within the developing *Drosophila* oocyte. *Cis*-acting signals for N4 RNA localization are contained within the 3'UTR. We have mapped

those signals and identified a unique *cis*-acting element capable of directing early transport of mRNA into the oocyte. *swallow* is required for the localization of *Adducin-like* mRNA and protein and is therefore a candidate *trans*-acting localization factor (15, 90). We present evidence that *swallow* acts through the *Adducin-like* N4 3'UTR to promote *Adducin-like* N4 mRNA localization in mid- to late oogenesis. Finally, we consider the possible functions of alternative splicing in development.

MATERIALS AND METHODS

cDNA preparation and sequence analysis

An ovarian cDNA library (λRAT1 library, 15) and a 0- to 4-hr embryonic cDNA library (Nick Brown library, 7) were screened with a 2.2 *Eco*RI-*Pst*I genomic fragment as previously described (15). Eight cDNA clones were isolated, which were then separated into four classes. Sequence analysis of the Adducin-like cDNA clones was done using the GELASSEMBLE, FASTA and BLAST programs of the Genetics Computer Group package (GCG). RNA folding was modeled by the GCG MFOLD program.

In situ hybridization to whole-mount ovaries

Young adult females (1-2 days old) were fed on yeast for two to three days. Ovaries from these females were dissected in 1X Ringer's and transferred to fresh 1X Ringer's kept on ice. After half an hour of dissecting ovaries, the ovaries were transferred to siliconized RNase-free Eppendorf tubes (Sorenson Bioscience) and washed with 1X phosphate-buffered saline (PBS). For each line, ovaries were split into two tubes. One sample was fixed (10% EM-grade formaldehyde (Ted Pella), 10% DMSO, 50 mM EGTA, 1X PBS) without heptane, for 20 minutes while gently rocking on a nutator. The second sample received fix (about 1 ml) and heptane and was shaken vigorously for about 15 seconds before being placed on the nutator for 20 minutes. From this point on, all samples were kept RNAse-free. Both samples were then rinsed three times with PTW (1X PBS, 0.1% Tween-20), followed by a 10-minute wash with PTW while nutating. For the second sample, ovaries were rubbed gently between the frosted parts of two slides to separate the ovarioles and devitellinize the later stage oocytes. At this point samples for a given line were combined into a single tube, which then contained both whole ovaries and individual ovarioles and egg chambers in PTW. Each combined sample was treated with proteinase K (1:1000 dilution into PTW just before use, from an 18.6 mg/ml stock

solution; BMB) for three minutes. Egg chambers were rocked on the nutator for the first minute of proteinase K digestion, and allowed to settle for the last two minutes. Digestion was stopped by two rinses of 3 minutes each in ice-cold glycine (2 mg/ml in PTW), followed by two rinses of 3 minutes each in PTW. Postfixation was done for 20 minutes on the nutator, without heptane. Samples were then given two three-minute rinses in PTW, and one ten-minute wash in PTW on the nutator. Oocytes were then dehydrated by allowing them to settle through a 1:1 ethanol: PTW solution, followed by two rinses in 100% ethanol, and then stored at -20° until hybridization.

Prior to hybridization, egg chambers were washed once with 100% ethanol and then rehydrated through freshly made ethanol: PTW (3:1, 1:1, 1:3) for two minutes each. Next, three two-minute rinses in PTW were followed by successive 10-minute washes in PTW, 1:1 hybridization buffer: PTW, and hybridization buffer alone. Oocytes were then prehybridized for 2 hours in fresh hybridization buffer at 55° for RNA probe or 45° for DNA probe. For RNA probes, hybridization buffer contained 50% deionized formamide, 4X SSC, 250 μg/ml tRNA, 250 μg/ml calf thymus DNA, 50 μg/ml heparin, 1% Tween-20. For DNA probes, hybridization buffer contained 50% deionized formamide, 5X SSC, 250 μg/ml tRNA, 250 μg/ml calf thymus DNA, 50 μg/ml heparin, 0.1% Tween-20.

After prehybridization, the supernatant was removed and 150 μl of diluted probe was added. Hybridization was carried out overnight for about 16 hours at 55° for RNA probe or 45° for DNA probe.

When hybridization was completed, RNA probes were removed and discarded (DNA probes were saved). For RNA probes, the washes were as follows: 15 minutes at 55° in hybridization buffer; two 30-minute washes at 55° in wash buffer 1 (2X SSC, 50% formamide, 1% Tween); 15 minutes at 55° in wash buffer 2 (2X SSC, 1% Tween); two 30-minute washes at 55° in wash buffer 3 (0.2X SSC, 1% Tween). Finally, the ovaries were washed twice in PTW at room temperature for 5 minutes each, on the nutator. For DNA probes, the egg chambers were washed briefly at 45° in hybridization buffer,

followed by a 10-20 minute wash on the nutator at room temperature in 1:1 hybridization buffer: PTW, three 5 minute washes in PTW while rocking at room temperature, and seven 10 minute washes in PTW while nutating at room temperature.

Antibody binding was carried out overnight at 4° while gently rocking on a nutator. Egg chambers were incubated with 1 ml. of preabsorbed anti-digoxigenin antibody (BMB), diluted 1:2000 in PTW. Subsequently, they were washed ten times for ten minutes each in PTW, with rocking. One rinse in freshly made staining buffer (100 mM Tris, pH 9.5; 100 mM NaCl; 50 mM $MgCl_2$; 0.1% Tween-20) was followed by a ten minute incubation in staining buffer, both with rocking. Finally, color buffer was added (4.5 µl NBT and 3.5 µl BCIP per 1 ml. of staining buffer). All samples were placed on the nutator and the nutator was covered with foil to exclude light. The color buffer was changed after approximately 30-33 minutes, and incubation under foil was continued for another 25 minutes while rocking. Each sample was then washed several times with PTW to stop the color reaction. At this point the whole ovaries remaining in each sample were rubbed gently between the frosted part of two slides until all ovarioles were separated, and recombined into a single tube with the previously separated egg chambers. Oocytes were mounted in JB-4 plastic mountant (Polysciences).

Antisense digoxigenin-labeled anti-*β-galactosidase* RNA probe, corresponding to the entire 3.4 kb *lacZ* sequence, was transcribed by T7 polymerase from *Hin*dIII-digested pGEM1-LZΔ1-F template. After probe synthesis using Ambion's Megascript kit, the probe was precipitated, resuspended in 100 µl RNase-free H_20, and hydrolyzed by treatment with 100 µl of 100 mM $NaCO_3$ buffer, pH 10.2 for 1 hour at 60°. Anti-*β-galactosidase* RNA probe was used at a 1:500 dilution for *in situ* hybridization of egg chambers.

Antisense N4 3'UTR digoxigenin-labeled RNA probe was transcribed using T7 polymerase from 1 µg of *Sal*I-cut pNB40-N4 DNA. Transcription reactions were performed in a 20 µl volume and consisted of 1X transcription buffer (BMB), 1X BMB digoxigenin RNA labeling mix, 37.5 mM DTT, 40 units RNasin (Promega), 1 µg

linearized template DNA, and 50 units of T7 polymerase (Gibco/BRL). The reaction was allowed to proceed for 1 hour at 37°, after which 1 µl of T7 polymerase was added and the reaction was continued for an additional hour. 2 µl of 0.2M EDTA was added to stop the transcription reaction and the reaction was then frozen at -20°. Anti-N4 probe was diluted 1:1000 into hybridization buffer and used directly for *in situ* hybridization.

Antisense R1 3'UTR digoxigenin-labeled RNA probe was transcribed using Sp6 polymerase from 1 µg of *Blp*I-cut pR1 DNA. Transcription reactions were performed as for N4 except that Sp6-specific transcription buffer (BRL) and 15 units of Sp6 polymerase (Gibco/BRL) were used. Anti-R1 probe was diluted 1:500 into hybridization buffer and used directly for *in situ* hybridization.

Digoxigenin-labeled DNA probes for each of the *Adducin-like* splice form 3'UTRs were made by random priming of gel-purified PCR products. For the N4 3'UTR, PCR primers were 5A1(5'-TAC CCT AGG TAG ATA CAT ATT ATG-3') and 3N1 (ACG GCG GCC GCT AAT GAA AAC TAT ATT T-3'). The R1 3'UTR (plus part of the coding region unique to the R1 cDNA) was amplified using primers 972-84 (5'-AAT GGC GAT CAT TCG GAG GC-3') and Sp-6-UBDT (5'-GCT GCG GCC GCA GAT TTA GGT G-3'). For the R2 3'UTR, PCR primers were Rat Add 1 (5'-CCA CCA ACC TTA AGG AGA TTG-3') and Rat Add 2 (5'-GAT TTA TGC ACA TTA CAC-3'). The N32 3'UTR was amplified with primers AddN32A (5'-GTG-CCT CAT TTA GGG ATT TGC GCT G-3') and T7 (5'-TAA TAC GAC TCA CTA TAG GG-3'). PCR amplifications were done using the following conditions: 4' at 94°, followed by 30 cycles of 94°, 1.5'; 58°, 1.5'; 72°, 2'. Additionally, the *Hin*DIII-*Not*I fragment of pNB40-N4 was gel-purified and labeled with digoxigenin by random priming, producing a full-length N4 DNA probe.

Construction of *lacZ-Adducin-like* transgenes for germline transformation

For all constructs, the parent vector was pCaSpeR4β26. This vector contains the *hsp26-Sgs-3* promoter and 5'UTR, a cassette which promotes nurse cell transcription, and the entire 3.4 kb *lacZ* sequence. To construct pCaSpeR4β26, the *hsp26-Sgs-3* cassette was cut out of pGerm6 (from Robert Cohen) with *Eco*RI and *Not*I and endfilled, then cloned into the *Stu*I site of pCaSpeR4. The *lacZ/Y* sequence was cut out of pCaSpeR-X+R+ using *Xba*I and cloned into the *Xba*I site of pCaSpeR4-26, to complete pCaSpeR4-β-26. In order to obtain a shorter *lacZ* tag, pCaSpeR4β26 was cut with *Hpa*I (which produces a blunt end) and *Not*I and the vector sequence was gel-purified away from the 3.4 kb *lacZ* insert. Subsequently, a 600-bp fragment of *lacZ* was amplified by PCR, such that the 3' primer contained a *Not*I site. This 600 bp *lacZ* fragment was digested by *Eco*RV (which produces a blunt end) at an internal site, and *Avr*II, releasing a 500 bp and a 100 bp fragment. The 500 bp *lacZ* fragment was then gel-purified. In addition, the *Adducin-like* 3'UTR was amplified from pNB40-N4,by PCR, using primers designed to have *Avr*II and *Not*I sites, and digested with *Avr*II and *Not*I. A triple ligation was performed, which joined the pCaSpeR4β26 vector to the *lacZ* sequence and the *Adducin-like* 3'UTR sequence, producing pAdd3'UTR.

PCR primers used to amplify the full-length *Adducin-like* N4 3'UTR were 5A1 (5'-TAC CCT AGG TAG ATA CAT ATT ATG-3'), which includes an engineered *Avr*II restriction site, and 3N1 (5'-ACG GCG GCC GCT AAT GAA AAC TAT ATT T-3'), which includes an engineered *Not*I restriction site. Standard PCR conditions for all reactions were as follows: 100 µl total volume, 50 mM KCl, 10 mM Tris pH 8.3, 0.01 mg/ml gelatin, 50 pmoles of each primer, 200 µM dNTPs, 1.5 mM or 7.5 mM $MgCl_2$, 100 pg-10 ng of template DNA, and 2.5 or 5 units of Taq polymerase. Except where noted, 30 cycles of amplification were carried out at 94° for 1.5', 45° for 1.5' and 72° for 2'. Some amplifications also included an extra initial denaturation step of 2-4 minutes at 94°, and an extra final extension step of 3-5 minutes at 72°.

For 5' deletion constructs (p5D-1 to p5D-6), pAdd3'UTR was digested with *Avr*II and *Not*I and the vector was gel-purified away from the full-length *Adducin-like* 3'UTR sequence. Using primers with engineered *Avr*II and *Not*I sites, the desired subset of the *Adducin-like* 3'UTR was amplified from *HinD*III-*Not*I digested pNB40-N4 and subcloned into the vector. Primers for the p5D-1 insert were 5A2AB (5'-ATA CCT AGG GGA TCC ATA TTT GAA ATC GAC-3'), which contains both an *Avr*II site and a *Bam*HI site, and 3N1. Primers for the p5D-2 insert were 5A3 (5'-ACG TAC CCT AGG GTT TAA TGA TGA TAA TTT GG-3') and 3N1. Primers for the p5D-3 insert were 5A4AB (5'-ATA CCT AGG GGA TCC ACT TCT TTG TTC TC-3'), which contains both an *Avr*II site and a *Bam*HI site, and 3N1. Primers for the p5D-4 insert were 5A5 (5'-ACG TAC CCT AGG ATG GAA ATG CAA AG-3') and 3N1. Primers for the p5D-5 insert were 5A6AB (5'-GCG CCT AGG GGA TCC ACA TCT GTG AAA TTG-3'), which contains both an *Avr*II site and a *Bam*HI site, and 3N1. Primers for the p5D-6 insert were 5A7AB (5'-GCG CCT AGG GGA TCC TCA TAT TTT TAT AAT TAA AAT AT-3'), containing both an *Avr*II site and a *Bam*HI site, and 3N1. Thus two of these constructs (p5D-2 and p5D-4) have only an *Avr*II site marking the 5' boundary of the insert, while the rest (p5D-1, p5D-3, p5D-5, and p5D-6) also have an adjacent *Bam*HI site.

For 3' deletion constructs (p3D-1 to p3D-6), pAdd3'UTR was digested with *Avr*II and *Not*I and the vector was gel-purified away from the full-length Adducin-like 3'UTR. Using primers with engineered *Avr*II and *Bam*HI sites, the desired subset of the *Adducin-like* 3'UTR was amplified from *HinD*III-*Not*I digested pNB40-N4. Since the 3' deletion constructs are missing the predicted *Adducin-like* N4 polyadenylation and transcription termination sites, the *α-tubulin* 3'UTR was appended to give stability to this set of reporter transcripts. DNA sequence corresponding to the *α-tubulin* 3'UTR was amplified from p701, a gift from Paul Macdonald, using primers designed with *Bam*HI and *Not*I sites. Subsequently the PCR product was cloned into Invitrogen's AT vector, digested with *Bam*HI and *Not*I, and the insert containing the *α-tubulin* 3'UTR was gel-purified. Triple

ligations were then performed, joining the pAdd3'UTR vector to the desired segment of the *Adducin-like* 3'UTR and the *tubulin* 3'UTR to produce various *Adducin-like* 3' deletion constructs.

PCR primers for the p3D-1 insert were 5A1 (5'-TAC CCT AGG TAG ATA CAT ATT ATG-3') and 3B1 (5'-CCG GGA TCC AAC GAA AAT CAA GAT TCG AC-3'). Primers for the p3D-2 insert were 5A1 and 3B2 (5'-CAT GGA TCC TTA AAT GTA CAA TGG TTG GC-3'). Primers for the p3D-3 insert were 5A1 and 3B3 (5'-ACG TGG ATC CAT TGT GCT TAA GTT ACA G-3'). Primers for the p3D-4 insert were 5A1 and 3B4 (5'-ACG TGG ATC CAA AAA ATG CAT TAG TTC G-3'). Primers for the p3D-5 insert were 5A1 and 3B5 (5'-ACG TGG ATC CTT AAT CTA GTT GCT TTA TAC-3'). Primers for the p3D-6 insert were 5A1 and 3B6 (5'-ACG TGG ATC CCA CAA CAA AAG CGA AG-3').

For internal deletion constructs (pΔ50-1 to pΔ50-5 and pΔ100-1 to pΔ100-3), in most (but not all) cases triple ligations were performed, joining *Avr*II-*Bam*HI cut PCR-amplified fragments of the *Adducin-like* 3'UTR to *Bam*HI-*Not*I PCR-amplified pieces of the *Adducin-like* 3'UTR, and to the *Avr*II-*Not* I cut pAdd3'UTR vector (as above). To make construct pΔ50-1, the 5A1/3B2 amplification product was digested with *Avr*II and *Bam*HI and ligated to the *Bam*HI-*Not*I digested p3D-2 vector. For pΔ50-2, the 5A1/3B3 amplification product was digested with *Avr*II and *Bam*HI and ligated to the *Bam*HI-*Not*I digested 5A6AB/3N1 PCR product, plus *Avr*II-*Not*I digested pAdd3'UTR vector. For pΔ50-3, the 5A1/3B4 amplification product was digested with *Avr*II and *Bam*HI and ligated to the *Avr*II-*Bam*HI digested and gel-purified pΔ100-3 vector. To make pΔ50-4, the 5A1/3B5 amplification product was digested with *Avr*II and *Bam*HI and ligated to the *Bam*HI-*Not*I digested 5A4AB/3N1 PCR product, plus *Avr*II-*Not*I digested pAdd3'UTR vector. For construction of pΔ50-5, the 5A1/3B6 amplification product was digested with *Avr*II and *Bam*HI and ligated to the *Bam*HI-*Not*I digested 5A3B/3N1 PCR product, plus *Avr*II-*Not*I digested pAdd3'UTR vector. To make pΔ100-1, the 5A7AB/3N1 amplification

product was digested with *Bam*HI and *Not*I and ligated to the *Bam*HI-*Not*I digested p3D-3 vector. For construction of pΔ100-2, the 5A1/3B4 amplification product was digested with *Avr*II and *Bam*HI and ligated to the *Bam*HI-*Not*I digested 5A6AB/3N1 amplification product as well as to *Avr*II-*Not*I digested pAdd3'UTR vector. To construct pΔ100-3, the 5A1/3B5 amplification product was digested with *Avr*II and *Bam*HI and ligated to the *Bam*HI-*Not*I digested 5A5B/3N1 amplification product plus *Avr*II-*Not*I digested pAdd3'UTR vector.

For construction of p50-250, primers 5A2M (5'-ACG TCC TAG GAT ATT TGA AAT CGA C-3') and 3B2 (5'-CAT GGA TCC TTA AAT GTA CAA TGG TTG GC-3') were used to amplify a 200-bp fragment of the N4 3'UTR. The *Bam*HI-*Not*I digested PCR product was ligated into *Bam*HI-*Not*I digested and gel-purified p3D-1 vector. For construction of p100-250, primers 5A3B (5'-ACG TAC GGA TCC GTT TAA TGA TGA TAA TTT GG-3') and 3B2 were used to amplify a 150-bp fragment of the N4 3'UTR. The *Bam*HI-*Not*I digested PCR product was ligated into *Bam*HI-*Not*I digested and gel-purified p3D-1 vector. pAddtag3'UTR was constructed by digesting pAdd3'UTR with *Nhe*I and ligating in a PCR product consisting of the complete *Adducin-like* 5'UTR and open reading frame (ORF), with *Nhe*I-compatible *Avr*II ends engineered into the primers Add-Avr-5 and Add-Avr-3. PCR reaction conditions were as follows: 94°, 2'; then 28 cycles of 94°, 1'; 58°, 1'; 72°, 3', followed by a final, single incubation of 5' at 72°. pORFtagtub was constructed by digesting pAddtag3'UTR with *Avr*II and blunt-ending with Klenow enzyme, then digesting with *Not*I and gel-purifying to remove the *Adducin-like* 3'UTR; simultaneously p3D-1 was digested with *Bam*HI and end-filled with Klenow, then cut with *Not*I and the *tubulin* 3'UTR gel-purified. Subsequently, the blunt-*Not*I pAddtag vector was ligated to the blunt-*Not*I *tubulin* 3'UTR insert. ptagtub3'UTR was made by digesting p3D-1 with *Bam*HI and *Not*I, gel-purifying the vector, blunting the ends by end-filling with Klenow enzyme, and religating.

Germline transformation

Germline transformation was carried out using standard procedures (67). w^{1118} embryos were coinjected with 500 μg/ml of pAdd3'UTR or the desired deletion construct, and 100 μg/ml of pHSπ helper plasmid. All lines were homozygosed or balanced over *CyO* or *TM3*.

Northern blot analysis

Ovarian RNA was prepared and selected for polyA+RNA as previously described (15).

The gelboxes and combs used for Northern blotting were prepared by soaking them in 3% hydrogen peroxide for 10 minutes, then rinsing them twice with DEPC-treated water, followed by rinsing with 100% ethanol. After pouring out the ethanol, the gelboxes were tilted on their side in a hood and allowed to air dry, then covered with foil when dry.

For Northern analysis, a low percentage formaldehyde gel and running buffer were prepared (81). The gel consisted of 1% agarose and 1.67% deionized formaldehyde in 1X MOPS buffer. For the running buffer, 1.67% formaldehyde in 1X MOPS was used. Formaldehyde was deionized by vigorously shaking 40 ml of formaldehyde with 2 g of Dower XG8 resin in a 50 ml Falcon tube on its side, for 1 hour, followed by filtration through a 0.2 micron Nalgene filter. A 15-well comb was used.

RNA samples consisted of polyA+ ovarian RNA and Gibco-BRL's 0.25-0.95 RNA molecular weight marker. 5.3 μg of polyA+ ovarian RNA was run in lanes 5,9, and 12, while 3.5 mg of RNA marker was loaded in the two outside lanes (1 and 15) of each gel. RNA samples were prepared in a total volume of 20 μl, consisting of 1X MOPS, 50% deionized formamide, 17.5% deionized formaldehyde, and RNA. 1 μg of ethidium bromide in water was added to marker RNA only, to facilitate visualization and confirmation of transfer. All samples were denatured at 68° for 15 minutes, quenched on wet ice for 2 minutes, and centrifuged, and 2 μl of 50% glycerol/0.4% bromophenol

blue/0.4% xylene cyanol was added to each sample. Samples were loaded onto the gel and electrophoresed at 5V/cm until the bromophenol blue dye had run 2/3 of the way down the gel. Each gel was then laid on a UV transilluminator, protected by Saran Wrap, and photographed using a Polaroid camera, with rulers laid alongside the markers.

Immediately after photography, the gels were set up for downward capillary transfer onto Genescreen, using 20X SSC as the transfer buffer. Since the gels contained a low percentage of formaldehyde, no pretreatment was done to get rid of the formaldehyde. After an overnight transfer, the blot was dried overnight on Whatman paper. Both sides were UV crosslinked, and the blot was then baked for 2 hours at 80° under vacuum to reverse the formaldehyde reaction.

The blots were photographed on a UV transilluminator to verify transfer of the markers, and were then cut into strips to separate the lanes. Prehybridization and hybridization were carried out in high-SDS buffer, following Boehringer Mannheim's nonradioactive Northern protocol. Prehybridization and hybridization were done at 42°, using DNA probes, with washes at 46°.

Primers were designed for amplification of the 3'UTR from all five splice forms of Adducin-like. Using the cDNA clones as templates, the 3'UTR was amplified in each case and gel-purified by running the band onto DE81 paper with subsequent elution off the paper and ethanol precipitation. An aliquot was checked on a 1% agarose gel to verify purification and estimate recovery. 100 ng of each PCR product was then labeled with digoxigenin-dUTP using Boehringer Mannheim's High Prime kit. The concentration of labeled probe was checked by comparing serial dilutions for each probe to dilutions of a labeled control DNA provided in the High Prime kit. Chemiluminescent detection using CSPD as a substrate was done according to Boehringer Mannheim's protocol. Subsequently, 25 ng of each probe was used per ml of hybridization buffer.

RT-PCR analysis

Total RNA was prepared from 25 female flies of each transgenic line, using an SDS lysis buffer (4). Newly hatched female flies were fed on yeast for several days and then homogenized in 500 μl of RNase-free SDS lysis buffer. Homogenization was done in Eppendorf tubes, using disposable plastic pestles. Lysates were transferred to screw-capped 2 ml. Sarstedt tubes, and proteinase K (BMB) was added to give a final concentration of 250 μg/ml. Lysates were digested with proteinase K for one hour at 50° and then frozen down at -70 for approximately one month. After thawing on ice, lysates were extracted with phenol-chloroform and chloroform and precipitated first with ethanol, then with LiCl. RNAse-free DNAse I (BRL, amplification grade) was used to remove contaminating genomic DNA. First-strand cDNA synthesis was primed from 3 μg total RNA with oligo-$dT_{12\text{-}18}$,using the Superscript II Preamplification kit (Gibco/BRL). In order to minimize negative effects of secondary structure on first-strand cDNA synthesis, the oligo-dT primer was heated to 70° and immediately transferred to 50°; simultaneously, the reverse transcription mix was prewarmed to 50° before the primer was added. After first-strand cDNA synthesis was complete, RNase H was used to remove RNA from the RNA/DNA hybrids. Hot Start PCR was performed in a volume of 50 μl, with 200 μM dNTPs and 0.2 μM primers. PCR amplification began with a 3' denaturation step at 94°, and was followed by 34 cycles of 1' at 94°, 1' at 54°, and 2' at 72°. For amplification of the transgene from the beginning of the lacZ tag sequence through the Adducin-like 3'UTR , primers TG1 and 3N1 were used, which produced an 874 bp product for the full-length 3'UTR transgene and correspondingly shorter products for deletion transgenes. The TG1 sequence was as follows: 5'-ATC CTG CTG ATG AAG CAG AAC AAC-3'. The 3N1 sequence was: 5'-ACG GCG GCC GCT AAT GAA AAC TAT ATT T-3'.

Fly strains

For injection, w^{1118} stocks were used (53). In order to ascertain whether reporter transcripts bearing the N4 3'UTR were localized properly in a *swallow* (*sww*) mutant background, ovaries were collected from mothers that were sww^1/sww^1; pAdd3'UTR/pAdd3'UTR or sww^1/sww^6; pAdd3'UTR/pAdd3'UTR. *sww* alleles have previously been described; sww^1 (which is also known as *fs(1) A1497*) is a strong allele while sww^6 (also known as *fs(1) A384*) is weaker (36). Flies were cultured at 25°.

RESULTS

The *Adducin-like* gene produces at least four classes of transcripts via alternative splicing, which encode three polypeptides

In flies, *Adducin-like* is a single-copy gene which produces multiple forms of transcripts through alternative exon splicing (88, 15). Four distinct classes of *D. melanogaster* Adducin-like cDNAs have been identified (Figure 1). These cDNA classes have been designated as N4, R2, N32, and R1, with the letters N or R referring to the cDNA library (Nick Brown or λRAT1) from which the clones were recovered. Three clones each were recovered for the N4 class (N4, R8, N1) and the R2 class (R2, R10, R16). The N32 and R1 classes are each represented by a single clone. The sequence of the cDNA encoding the longest open reading frame, N4, has previously been published (15), but the other three cDNA sequences are reported here for the first time (Figure 2). Excluding the polyA tail, the N4 cDNA is 4.2 kb long, while R2 is 1.9 kb, N32 is 2.4 kb, and R1 (which may be incomplete at both ends) is approximately 2.6 kb long.

All of the cDNA classes share at least some 5'UTR sequence (Figure 1, Figure 2). The R1 5'UTR is identical to nucleotides (nt) 85-397 of the N4 5'UTR and may simply reflect incomplete cloning of the 5' end of R1. The R2 5'UTR is identical to nt 73-127 and 332-397 of the N4 5'UTR, so that part of exon 1 is spliced to a complete exon 2. However, there is no consensus splice donor sequence (GT) at N4 positions 128-129 as would be expected for an intra-exon splice site, leaving it unclear as to whether the R2 5'UTR sequence represents a cloning artifact or a valid splice variant. The sequence of the N32 5'UTR suggests that there is another exon upstream of the known Adducin-like genomic sequence. The N32 5'UTR begins with a novel sequence and then is identical to the N4 sequence, such that the novel sequence is spliced to the start of exon 2.

The 3' untranslated regions (3'UTRs) differ for each cDNA class (Figure 1, Figure 2). N4 and R1 have unique 3'UTRs. The N4 3'UTR is 345 nt, including the stop codon.

The 3' end of the R1 cDNA may not be full length, because the 3'UTR sequence is relatively short (151 nt) and has neither a consensus polyadenylation signal (AAUAAA) nor its most common variant (AUUAAA). In addition, the R1 cDNA terminates with a run of only 12 A's; this polydA sequence may be internal rather than corresponding to the polyA tail of the R1 RNA. Alternatively, R1 may be one of a small class of mRNAs which has a nonconsensus polyadenylation signal (83, 87, 71).

The N32 3'UTR is 700 nt while the R2 3'UTR is 314 nt, and the N32 and R2 transcripts share 3'UTR sequence. R2 carries a truncated version of the N32 3'UTR, making use of an alternate polyadenylation signal. For R2, there are actually several potential polyadenylation signals which overlap; we have not determined which one may be used preferentially. In addition to the mid-3'UTR AAUAAA signal(s) used by R2, there are two potential polyadenylation signals at the end of the N32 cDNA, and we have not defined which of these polyadenylation signals is the one functional for N32.

Our cDNA sizes do not all match up with previously reported Northern blot data, which indicate (using the entire N4 coding region as a probe) that there is one major ovarian transcript of 4.5 kb (15, 88) and two minor ovarian transcripts of 3.7 and 3.8 kb (88). The 3.7 and 3.8 kb minor ovarian transcripts are strongly upregulated in 0-24 hour embryos (88). The 4.5 kb transcript matches the expected size for a polyadenylated N4 transcript. We have not found Adducin-like cDNAs that fall into the 3.7 and 3.8 kb size category, and thus we expect that there are additional cDNAs. Since R1, R2, and N32 sizes do not match the reported Northern blot data, it is likely that they represent rare transcripts. Using the N4 coding region as a probe might be expected to bias detection in favor of N4 clones, since the N4 open reading frame has about 1500 nt that are not shared with R1, R2 and N32 transcripts.

All four classes of Adducin-like cDNAs share sequence in their open reading frames, such that all of the Adducin-like protein isoforms described here are identical over the first 473 amino acids (cDNAs, Figures 1 and 2; protein isoforms; Figure 3). N4

encodes the longest protein, with a predicted length of 1156 amino acids (AA) and predicted molecular mass of 128 kD (88, 15). The C-terminal 498 AA of N4 do not show homologies to any known proteins (15, 88, 66; K.W., unpublished data). Previous analysis of the genomic structure indicates that N4 consists of ten exons (88; Figure 1, Table 1). The R1 cDNA is alternatively spliced after exon 9, to yield a predicted R1 protein of 718 AA with an expected molecular mass of 79 kD. R1 is identical to N4 for the first 658 AA and then diverges in sequence, as R1 has a 60 AA C-terminal coding extension (Table 1). The R1 coding extension contains a region with MARCKS (myristoylated alanine-rich C-kinase substrate) homology, and will be discussed further in the following section. In contrast, the R2 and N32 cDNAs are alternatively spliced at the 3' end of exon 5, and thus encode a protein with a predicted length of 495 AA and predicted molecular mass of 55 kD. R2 and N32 are identical to R1 and N4 for the first 473 AA, but both R2 and N32 protein isoforms have a C-terminal coding extension of 22 AA that lacks homology to any known protein (Table 1).

The protein encoded by the R1 class of *Adducin-like* RNA is the *Drosophila* orthologue of mammalian adducin

Sequence comparison of the predicted *Drosophila* Adducin-like protein isoforms with human α-, β-, and γ-adducin proteins reveals that the *Drosophila* R1 class shows the highest homology to human adducins (Figure 4). R1 is about the same length (718 AA) as human adducin polypeptides (α–adducin, 737 AA, 38, β–adducin, 726 AA, 38, γ–adducin, 674 AA, 40) and is equally homologous to all three human adducin subunits (39-40% amino acid identity, and 59-61% similarity). In contrast, R2 and N32 are considerably shorter proteins (495 AA), while N4 is a much longer protein (1156 AA). Most importantly, the R1 protein contains a motif at the C-terminal end which is highly conserved with α-, β-, and γ- forms of human adducin (Figure 5A), but which does not exist in the N4, R2, or N32 proteins. This motif is highly polybasic, shows MARCKS

homology (Figure 5B, MARCKS peptide sequence from 35), and is likely to represent a phosphorylation substrate for protein kinase A (PKA) and protein kinase C (PKC), as well as a binding site for calmodulin. The MARCKS-related sequence has been shown to be the major calmodulin-binding site and the major phosphorylation site for PKA and PKC in both human α- and β-adducin (59). Phosphorylation occurs within the MARCKS-related sequence at Ser-726 for human α-adducin, and Ser-713 for human β-adducin (59). The corresponding residues in human γ-adducin (Ser-660) and *Drosophila* R1 Adducin-like (Ser-705) are conserved but have not been tested for their ability to be phosphorylated.

Another major PKA phosphorylation site specific to human α-adducin (Ser-481, 59) may be conserved in *Drosophila* R1 and N4 Adducin-like proteins (Figure 6). However, the sequence conservation between human and *Drosophila* adducins in this region is weak enough that it is questionable whether this is a functional PKA site in *Drosophila*. The truncated R2 and N32 proteins lack this potential phosphorylation site.

Human α-adducin also shows strong PKA-dependent phosphorylation at Ser-408 and Ser-436, and weak PKA-dependent phosphorylation at Ser-59. In human β-adducin, the minor PKA phosphorylation site is at Thr-55, the residue corresponding to α-adducin Ser-59 (59). However, none of these PKA sites are present in any of the *Drosophila* Adducin-like proteins described here.

Adducin-like transcripts bearing different classes of 3'UTRs show distinct distribution patterns during oogenesis

The early events of oogenesis will be reviewed briefly here, before proceeding to the rest of the Results (for a more extensive review, see 72). Formation and maturation of oocytes in *Drosophila* take place in the ovariole, which is essentially an egg chamber assembly line. Each *Drosophila* ovary consists of a bundle of 15-20 ovarioles, and each ovariole is a linear filament that consists of a connected series of increasingly older and more mature egg chambers. The ovariole is conventionally divided into two regions: the

germarium, where germline and somatic stem cells reside, germline cysts are formed, and egg chambers are first assembled, and the vitellarium, where egg chambers develop and mature. In the germarium, oogenesis begins with the asymmetric division of a germline stem cell into a daughter stem cell and a cystoblast. Within region 1 of the germarium, the cystoblast undergoes four rounds of mitotic division to produce 16 cystocytes, which do not fully separate into individual cells but remain joined by specialized cytoplasmic bridges called ring canals. In germarial region 2, this 16-cell germline cyst is enveloped by a monolayer of somatically derived follicle cells. During this stage, one of the 16 germline cells becomes the oocyte, by a process which is still not fully understood, while the remaining 15 cells become highly polyploid nurse cells. Specific transport into the oocyte of a number of RNAs (*Adducin-like/hts*, *cyclin B*, *65F*, *orb*, *oskar*, *tudor*, *Bic-D*, *fs(1)K10*, *gurken*) begins at this stage (reviewed in 86, 34). In region 3 the oocyte moves to the posterior of the germline cyst, so that the anterior of the oocyte is facing towards the nurse cells, and the assembly of the egg chamber is complete at this point. Egg chambers found in region 3 of the germarium are referred to as stage 1 egg chambers, and are ready to enter the vitellarium, where the remainder of oogenesis (stages 2-14) will take place.

In order to assess the pattern of expression of each endogenous *Adducin-like* transcript class during oogenesis, whole-mount *in situ* hybridizations were carried out on w^{1118} ovaries using DNA probes specific for each 3'UTR (Figure 7). Transcripts with the N4 3'UTR accumulate within the prospective oocyte in region 2 of the germarium and are subsequently targeted specifically to the oocyte within early egg chambers. As oogenesis progresses, RNAs recognized by the N4 3'UTR probe are restricted to the oocyte cortex at stage 8, and further restricted to the anterior oocyte cortex from stages 9-14. The *in situ* localization pattern visualized by the N4 3'UTR probe corresponds to what has been reported for N4 coding region probes (for N4 coding region probes, see Figure 8, panels A-F; 15, 89). N4 coding region probes are expected to recognize R1, R2 and N32 transcripts as well as N4 transcripts, because there is extensive shared sequence. As

previously noted in this chapter, however, using the N4 coding region as a probe might bias detection in favor of N4 transcripts, since the N4 open reading frame has about 1500 nt that are not shared with R1, R2 and N32 transcripts.

In contrast to N4, transcripts bearing the R1 3'UTR accumulate within the germarium, where they do not appear to be localized, and are restricted to the follicle cells thereafter. Since follicle cells first migrate to surround developing germline cysts in region 2 of the germarium (72), the R1 distribution pattern within the germarium is consistent with expression within the initial population of follicle cells. R1 transcripts appear to be expressed throughout stage 1-6 egg chambers. Since a monolayer of somatic follicle cells now envelops the egg chamber, it is likely that this expression pattern actually reflects the presence of R1 transcripts within surrounding follicle cells and not within the nurse cell-oocyte complex. The level of expression of transcripts with the R1 class of 3'UTR seems to be lower in stage 7-9 egg chambers, with strong expression detectable in the follicle cells from early stage 10 onwards.

The R2 class of 3'UTR appears to be expressed in nurse cells and is excluded from the oocyte until late oogenesis, when transcripts from this class are dumped into the oocyte. R2 transcripts are not localized within the oocyte. Both R2 and N32 transcripts should be recognized by the R2 probe, since the first 314 nt of the R2 and N32 3'UTRs are identical. We did not examine the unique portion of the N32 3'UTR for its patterns of localization in egg chambers. Northern blots of ovarian polyA+ RNA hybridized with DNA probes specific for each 3'UTR class confirm that transcripts bearing each class of *Adducin-like* 3'UTR described here are present in ovarian RNA (data not shown). Thus, different *Adducin-like* 3'UTRs are associated with distinct mRNA localization patterns within the egg chamber.

The N4 class of 3'UTR is able to direct RNA transport to the oocyte in early oogenesis and localization within the oocyte at later stages

To test whether the 3'UTR of the N4 transcript is capable of directing transport to the oocyte and localization within the oocyte, a reporter construct was made in pCaSpeR4 (79) which consists of the *hsp26-Sgs-3* regulatory cassette (70) fused to a short *lacZ* sequence (0.5 kb), followed by the N4 *Adducin-like* 3'UTR (Figure 9). Detection of transcripts produced by the reporter construct can be achieved by use of an antisense *β-galactosidase* RNA probe. The regulatory cassette consists of two copies of the *hsp26* nurse cell enhancer (22) followed by the *Sgs-3* glue gene promoter (26, 60). These *hsp26* elements activate ovarian (but not heat-inducible) transcription specifically within the nurse cells (11).

The reporter construct, called pAdd3'UTR, was injected into w^{1118} embryos. Transgenic offspring were selected and homozygous transgenic lines were set up. Whole-mount *in situ* hybridizations were performed using an antisense *β-galactosidase* RNA probe on ovaries collected from homozygous transgenic flies. Three different lines were analyzed, two with the transgene inserted onto the second chromosome and one with the transgene carried on the third chromosome, and the results were the same for all three lines. Localization of pAdd3'UTR reporter transcripts in transgenic egg chambers was found to be identical to that of endogenous *Adducin-like* transcripts in w^{1118} egg chambers (Figure 8). For both endogenous *Adducin-like* transcripts and reporter transcripts, four stages of localization occur: (1) early transport of RNA into the presumptive oocyte, filling the oocyte (stages 1-7); (2) restriction of RNA to the oocyte cortex (stage 8); (3) further restriction of RNA to the anterior oocyte cortex (stages 9-10a); and (4) maintenance of RNA in the anterior cortex of late stage oocytes (stages 10b-14). We conclude that the N4 3'UTR is capable of directing *Adducin-like* N4 RNA localization to the oocyte in early oogenesis and within the oocyte at later stages.

The 3'UTR is the only region within the *Adducin-like* N4 transcript that is capable of directing localization during oogenesis

We have shown that the N4 3'UTR is sufficient to direct localization of transcripts bearing this 3'UTR to the oocyte. To examine whether localization signals might also exist in other regions of the transcript, two additional reporter constructs, pAddtag3'UTR and pORFtagtub, were made. pAddtag3'UTR carries the full-length Adducin-like N4 cDNA sequence, with the *lacZ* tag inserted between the coding region and the N4 3'UTR, and the resulting reporter transcript of approximately 5.5 kb is localized in the normal N4 pattern (Figure 10). pORFtagtub carries the *Adducin-like* N4 5'UTR and coding region and the *lacZ* tag, but replaces the N4 3'UTR with the *α-tubulin* 3'UTR, so that the pORFtagtub reporter transcript is approximately 6 kb. The *α-tubulin* 3'UTR has been shown to promote RNA stabilization and polyadenylation but does not direct RNA localization (57, 78). Whole-mount *in situ* hybridizations, using an antisense *β-galactosidase* RNA probe on ovaries from flies transgenic for pORFtagtub, showed that the reporter transcripts were present in nurse cells at stages 10-11 but were not localized within the oocyte at any stage of oogenesis (Figure 10). Clearly there are no elements capable of directing N4 localization outside of the 3'UTR.

Localization signals for early transport of *Adducin-like* RNA into stage 1-7 oocytes map to the central region of the N4 3'UTR (ALE1 element, nt 150-250)

To determine the nature of the localization tags within the N4 3'UTR sequence, a series of reporter constructs containing successive 5' or 3' deletions in the N4 3'UTR was made (Figure 11). In addition, reporter constructs with internal deletions of 50 bp or 100 bp were also made. Each reporter construct contained the *hsp26-Sgs3* cassette and a short *lacZ* tag, fused to a mutated N4 3'UTR. Constructs were made using a PCR cloning strategy (see Materials and Methods).

Early transport of reporter RNA from the nurse cells into the oocyte is normal when the reporter transgene (pAdd3'UTR) contains the complete 345 nt N4 3'UTR (see Figure 9). Deletion of the first 150 nt of the N4 3'UTR has no effect on the transport of the reporter transcript to the oocyte at stages 1-7 of oogenesis (Figure 12). However, deletion of another 50 nt, so that the first 200 nt are missing, abolishes transport of the reporter transcript. Within the resolution of this analysis, this places the 5' boundary of the localization tag affecting early transport at nt 150. Consistent with this result, further 5' deletions also abolish localization.

It is important to note that although we are assuming here that the effect of these deletions is to abolish early transport and localization, it is also possible that what we are actually seeing is the effect of deletion of an element responsible for stability of the RNA in the oocyte. RT-PCR was used to verify that full-length reporter RNA from selected transgenes is present even when no localization is detectable in the oocyte, and these experiments are detailed later in the Results.

Successive deletions inward from the 3' end of the N4 3'UTR show that deletion of the last 95 nt of the 3'UTR, leaving nt 1-250 intact, has no effect on reporter transcript localization in early oogenesis. Removal of additional 50 nt increments from the 3' end abolishes reporter RNA localization. The 3' boundary of the localization tag affecting early transport can therefore be mapped to nt 250.

Analysis of 5' and 3' deletions of the 3'UTR thus shows that the localization element responsible for directing early transport of *Adducin-like* RNA into the oocyte is found between nt 150-250. Internal deletions of 50 nt (Δ50-1, Δ50-2, Δ50-3, Δ50-4, and Δ50-5) and 100 nt (Δ100-1, Δ100-2, and Δ100-3) were also generated and their effects on early transport of the reporter RNA into the oocyte were examined by whole-mount *in situ* hybridization (Figure 12). Deletions which leave the presumptive "early transport element" intact (Δ50-1, Δ50-4, Δ50-5) have no effect on early transport of reporter RNA to the oocyte. However, all internal deletions which overlap the presumptive "early transport

element" abolish localization (Δ50-2, Δ50-3, Δ100-1, Δ100-2, Δ100-3). We have named this element ALE1 (*Adducin-like* localization element 1), and it extends from nt 150-250.

The localization tag responsible for early transport of *Adducin-like* RNA into the oocyte is defined by the deletion analysis as residing at or within nt 150-250. While deletion analysis shows which parts of the 3'UTR are necessary for localization to the oocyte, it cannot address what region of the 3'UTR is sufficient for early transport and localization. To test for sufficiency, ovaries from flies transgenic for a reporter construct including nt 100-250 of the N4 3'UTR were examined. Whole-mount *in situ* hybridizations of these transgenic ovaries with antisense *β-galactosidase* RNA probe showed that nt 100-250 of the N4 3'UTR could successfully direct proper localization of reporter RNA in early oogenesis (Figure 12, panel U). Our conclusion that ALE1 is the early transport element for *Adducin-like* N4 mRNA is supported by these results.

The element directing cortical restriction of *Adducin-like* RNA within stage 8 oocytes maps to the same region of the N4 3'UTR (ALE1) as the region affecting early transport

Stage 8 oocytes normally contain *Adducin-like* RNA restricted to the cortex as a thin layer just beneath the plasma membrane. All deletion transgenes in which the 3'UTR region from nt 150 to 250 (ALE1) remained intact were able to produce correctly localized reporter transcripts in stage 8 egg chambers (Figure 13). Conversely, deletions which overlapped ALE1 abolished localization at stage 8.

Reporter transcripts bearing only nt 100-250 of the N4 3'UTR are fully capable of correct localization to the cortex in stage 8 oocytes. Thus for stage 8 localization, the 150-250 element is necessary, and the 100-250 region is sufficient.

Localization signals affecting initial anterior restriction of *Adducin-like* RNA within stage 9-10a oocytes map to ALE1 plus two partially redundant elements between nt 50-100 and between 100-150 of the N4 3'UTR

At stages 9-10a, reporter RNA carrying the full 345 nt N4 3'UTR is tightly confined to the anterior of the oocyte. Deletion of nt 1-50 of the N4 3'UTR has no effect on transcript localization at stages 9-10a (Figure 14). Removing nt 1-100 results in decreased levels of anteriorly localized RNA, while deletion of nt 1-150 abolishes localization entirely. Deletions overlapping ALE1 (nt 150-250) also abolish localization. 3' deletions of nt 250-345 do not affect anterior localization at stages 9-10a.

Removal of both the 50-100 and 100-150 sequences (5'Δ3) abolishes localization entirely, whereas deletion of each region individually does not have that effect. Having nt 50-100 but not 100-150 results in a diminished level of anteriorly localized reporter transcript at stages 9-10a (Δ50-4). Having nt 100-150 but not 50-100 results in either a diminished level of anteriorly localized reporter transcript (5'Δ2, 100-250) or does not affect the level of anteriorly localized reporter transcript (Δ50-5).

Stage 9-10a localization signals thus are additive to those directing early transport; both the ALE1 element (nt 150-250) and the 50-150 region are necessary for initial anterior localization of reporter RNA at stage 9-10a. Deletions of subregions 50-100 or 100-150 affect the amount of localized RNA but not the pattern (with the exception of transgene Δ50-5, which contains a deletion of nt 50-100 but directs completely normal anterior localization). However, while the region from nt 50-150 is necessary for initial anterior localization, it is not sufficient to drive normal anterior localization by itself. Reporter transcripts from transgenes containing nt 1-100 (3'Δ5) or 1-150 (3'Δ4) do not show anterior localization at stage 9-10a.

The 100-250 region by itself is partially sufficient to direct wild-type anterior localization of reporter RNA at stages 9-10a. While the pattern of localization is normal (tight anterior localization), the level of reporter RNA is diminished.

Localization signals affecting maintenance of *Adducin-like* RNA at the anterior of stage 10b-11 oocytes map throughout the 3'UTR

At stage 10b-11, the nurse cells begin bulk transfer of their cytoplasmic contents to the oocyte, including RNAs not previously transported. *Cis*-acting localization signals functioning during this time period are therefore likely to be affecting tethering of *Adducin-like* N4 RNA at the anterior of the oocyte, or stability of the transcript, rather than directing specific transport. Deletion analysis reveals that multiple elements contribute to localizing *Adducin-like* N4 transcripts to the anterior of stage 10b-11 oocytes (Figure 15), and that the entire N4 3'UTR is required for proper localization at stage 10b-11. Successive 50-nt deletions from the 5' end (5'Δ1, 5'Δ2, 5'Δ3) result in changes in both pattern and level of reporter RNA. Removal of the first 50 nt (5'Δ1) produces reporter transcripts that are localized to the anterior but not as tightly as normal. Removal of another 50 nt (5'Δ2) also results in a slight diffusion of the mRNA from the anterior, similar to 5'Δ1, and a lower level of localized mRNA as well. As is the case for stage 9-10a, separate deletions of nt 50-100 and nt 100-150 impair localization, but deletion of both regions at the same time abolishes localization (5'Δ3).

Successive deletions from the 3' end (3'Δ1, 3'Δ2) show increasingly abnormal reporter RNA distribution at stages 10b-11, until localization is abolished by deletion of nt 200-345. All deletions that overlap ALE1 (nt 150-250) also prevent reporter mRNA localization.

Only the 100-250 region is sufficient to direct anterior localization by itself at stage 10b-11. However, the 100-250 region is not completely sufficient, as these transgenic oocytes show some impairment of reporter transcript localization. Reporter transcripts do show enrichment at the anterior but are also slightly delocalized or ectopically localized in addition. Transgenes bearing various regions from nt 1-150 (3'Δ4, 3'Δ5, 3'Δ6) and 250-345 (5'Δ5, 5'Δ6) are not able to produce localized reporter trancripts. Thus none of the elements outside of ALE1 are able to independently direct localization at stage 10b-11.

Localization signals affecting maintenance of *Adducin-like* RNA at the anterior of stage 12-14 oocytes map throughout the 3'UTR

The entire N4 3'UTR contributes to maintaining *Adducin-like* N4 transcripts at the anterior of stage 12-14 oocytes (Figure 16). All deletions which overlap ALE1 (nt 150-250) abolish reporter transcript localization in late stage oocytes. Transgenes with deletions of the first 50 nt (5'Δ1) are still able to produce anteriorly-localized RNA but there is also delocalized RNA visible throughout the oocyte. Deletion of nt 50-100 (5'Δ2, Δ50-5) results in a drop in the levels of localized RNA and sometimes in a change in pattern, from anterior to dorsal anterior. Deletion of nt 100-150 results in either complete delocalization (5'Δ3) or anterior localization of reporter RNA plus slight delocalization throughout the oocyte (Δ50-4). These results are similar to the mapping results from stage 9-10a; there may be two redundant elements at nt 50-100 and 100-150, since loss of either one alone impairs but does not abolish localization, while loss of both simultaneously does abolish localization. Deletion of nt 250-300 produces some impairment of anterior localization, which appears as a slight diffusion of RNA from the entire anterior cortex (100-250, Δ50-1), or as a delocalization from all but the anterior dorsal "corner" of the oocyte cortex (Δ50-1), or as relatively normal but weak anterior localization (3'Δ2). The last 45 nt seem to be the least important in terms of directing stage 12-14 localization, since removal of nt 300-345 results either in no effect, or in a slight delocalization from the anterior, depending on the specific transgenic line. Stage 1 embryos transgenic for deletions of the first 150 nt (5'Δ1, 5'Δ2, 5'Δ3) or last 45 nt (3'Δ1) were also examined for localization, since late stage oocytes are difficult to prepare and stain well. Deletion of the first 50 nt (5'Δ1) had the effect of significantly reducing the level of localized RNA, but anterior localization remained intact. No reporter RNA was detected in stage 1 embryos transgenic for 5'Δ2 or 5'Δ3. Deletion of the last 45 nt (3'Δ1) had little to no effect on either level or pattern of localization in stage 1 embryos (data not shown).

As is the case for other stages, the 100-250 region is the only one capable of directing anterior localization at stages 12-14. None of the other regions of the N4 3'UTR can confer localization by themselves. 100-250 reporter transcript localization is not fully normal, as it is not as tightly maintained at the anterior of stage 12-14 oocytes.

Early transport vs. late transport of reporter RNA

Figure 17 presents a summary of *in situ* hybridization results for all deletion constructs through all stages of oogenesis. The stages of localization are abbreviated as T (for early transport from the nurse cells into the oocyte), C (for cortical localization within the oocyte at stage 8), and A (for anterior localization at stages 9-14). Stages 1-7 are designated either as T++ or T-, indicating that early transport is either normal or does not occur. Stage 8 is designated as either C++ or T-, to show that either localization shows the normal restriction to the cortex, or that there is no reporter RNA within the oocyte. Stages 9-10a are coded as either A++ or A+, depending on whether anterior localization is normal or slightly impaired, or T-, to indicate that no reporter RNA has been transported to the oocyte. For stages 10b-14, the code changes to A++, A+, A+*, or A- , to indicate whether anterior localization is normal, slightly impaired, normal plus ectopic, or completely absent.

The change in code for later stages marks an important issue with respect to transport into the oocyte. RNA transport from the nurse cells to the oocyte during stages 1-10 appears to be a highly selective process. Tritiated uridine studies suggest that most maternal RNAs are synthesized by and retained within the highly polyploid nurse cells at this time, while the oocyte is transcriptionally quiescent, with the caveat that the bulk of RNA synthesis detected by this method would be ribosomal RNA (45). Microtubule inhibitors administered in early oogenesis disrupt oocyte growth as well as early transport and localization of *bicoid* RNA (64). The selectivity of the RNA transport process probably lasts only until stage 10b-11, when the nature of nurse-cell-to-oocyte transport changes radically. At the end of stage 10 and the beginning of stage 11, the nurse cells

begin to rapidly dump their cytoplasmic contents into the oocyte, completing the non-specific transfer of cytoplasm, RNAs, and non-nuclear organelles in approximately thirty minutes (72). Nurse cell dumping is not affected by microtubule inhibitors, but is prevented by cytochalasin, which disrupts actin polymerization (33, 32). Clearly there are different mechanisms operating during the two phases of transport. During the stages when early transport is operating, reporter RNA is not likely to be present in the oocyte unless specifically targeted there. At later stages, when the cytoplasmic contents of the nurse cells are transferred to the oocyte, reporter RNA will be present in the oocyte whether or not early transport has occurred. Our coding scheme reflects this separation of early and late transport.

Summary of localization elements found in the *Adducin-like* N4 3'UTR

The N4 3'UTR localization elements are summarized and schematically depicted in figure 18. The 100-250 region is completely sufficient to drive early transport of reporter RNA in stages 1-7 and cortical localization at stage 8. Of this region, only nt 150-250 (the ALE1 element) is necessary for early transport and cortical localization. We would like to know whether the ALE1 element alone has the capability to direct reporter RNA localization. That will require additional experiments, which are currently in progress. For initial anterior localization (stages 9-10a) and later maintenance at the anterior (stages 10b-14), the 100-250 region is only partially sufficient. Reporter RNA from the 100-250 transgene is localized to the anterior of the oocyte at the appropriate time, but either at a lower level (stage 9-10a) or not as tightly as normal (stages 11-14). Also, in a small percentage of the late-stage 100-250 transgenic oocytes, reporter RNA is dispersed throughout the oocyte in addition to being enriched at the anterior. However, since endogenous *Adducin-like* is being localized concurrently with reporter RNA to the anterior of transgenic oocytes, the dispersed reporter RNA may simply reflect overloading of the localization apparatus.

The observations from the 100-250 transgene show that there are likely to be additional binding sites outside of the 100-250 region necessary for correct anterior localization and maintenance. The results from deletion analysis support this conclusion. Removal of any region outside of nt 100-250 produces impairment in either the pattern or level of anterior localization or both, with one exception: deletion of nt 50-100 in transgene Δ50-5 has no effect on either pattern or level of anteriorly localized reporter RNA. There also appears to be an element within nt 50-150, probably within 100-150, that is essential for anterior localization from stages 9-14.

The predicted secondary structure for the N4 3'UTR includes five stem-loops

The N4 3'UTR is predicted to have extensive secondary structure (Figure 19). The most energy-efficient structure generated by the GCG MFOLD program shows five stem-loops organized around a common center. ALE1 is part of predicted stem-loop 3.

RT-PCR of selected transgenes shows that reporter transcripts from both localized and non-localized lines are full-length

To verify that full-length reporter RNA was present but delocalized (as opposed to prematurely truncated and therefore undetectable due to degradation, or unstable due to misfolding or deletion of an element conferring stability), total RNA was prepared from whole female flies homozygous for selected transgenes (pAdd3'UTR, 5'Δ2, 5'Δ4, 5'Δ6), and used as a substrate for RT-PCR. All transgenes used in this analysis were derived from pAdd3'UTR and are transcribed only in ovaries, as the *hsp26* promoter is nurse-cell specific (22). Reporter transcripts which contained either the full-length *Adducin-like* N4 3'UTR (pAdd3'UTR) or deletions of the first 150 nt or less of the N4 3'UTR (5'Δ2) were successfully localized to the oocyte in stage 1-7 egg chambers. Those reporter transcripts

which contained larger deletions of the N4 3'UTR (5'Δ4, 5'Δ6) were not detectable by whole-mount *in situ* hybridization at early stages of oogenesis.

The upstream PCR primer amplifies from the 5'-most end of the *lacZ* tag of the reporter construct, while the downstream primer amplifies from the 3'-most end of the complete N4 3'UTR just prior to the polyA tail. For the positive control, RNA was prepared from homozygous pAdd3'UTR female flies, which are expected to contain oocytes producing reporter transcripts with the full-length N4 3'UTR. A single PCR product of 874 bp was predicted for the positive control. For each of the experimental lines, which used RNA prepared from homozygous 5'Δ2, 5'Δ4, and 5'Δ6 female flies respectively, single PCR products of 774, 674, and 574 bp were predicted. In each case, a single band of the expected size was detected (Figure 20).

Transgenes pAdd3'UTR and 5'Δ2 are able to direct localization of the resulting reporter transcript but transgenes 5'Δ4 and 5'Δ6, which delete the first 200 and 300 bp of the 345 nt 3'UTR, are not able to direct localization. Nevertheless, RT-PCR indicates that these transgenes produce RNA of the appropriate length, showing that the lack of *in situ* signal is due to the reporter RNA being present but unlocalized. Presumably this result can be generalized, meaning that reporter RNA should also be present but unlocalized in transgenic oocytes carrying other N4 3'UTR deletions which do not succeed in producing localized transcripts. We cannot exclude the possibility that there are stage-specific stability effects which are not revealed by this type of analysis (since RNA from all stages is combined), but it seems unlikely.

swallow acts through the *Adducin-like* 3'UTR

swallow (*sww*) is known to be required for *Adducin-like* RNA localization during oogenesis (15). Since the *Adducin-like* RNA localization signals are contained within the 3'UTR, the Swallow protein may influence *Adducin-like* localization by direct or indirect interaction with the 3'UTR. To test this possibility, flies transgenic for pAdd3'UTR were

crossed into a *sww* mutant background. Two alleles of *sww* were used: sww^1, one of the strongest *sww* alleles and sww^6, a weaker allele (36). Females were selected which were homozygous for pAdd3'UTR and also carried either sww^1/sww^1 or sww^1/sww^6. We were not able to obtain homozygous sww^6/sww^6 females, as our stock seems to have accumulated an unrelated lethal mutation. Localization of reporter transcripts in egg chambers from *sww* mutant females was examined by whole-mount *in situ* hybridization using an antisense *β-galactosidase* RNA probe (Figure 21).

sww^1 has no detectable effect on the first three stages of pAdd3'UTR reporter transcript localization. Reporter RNA is correctly transported into early stage oocytes from sww^1/sww^1 mothers, restricted to the oocyte cortex at stage 8, and further restricted to the anterior oocyte cortex at stages 9-10. The effects of sww^1 on reporter RNA localization are first visible in late stage 9 oocytes, which show anterior expression that is less tightly restricted than normal. In stage 10b oocytes, transcripts are detectable only at the anterior dorsal corner rather than along the entire anterior of the oocyte. By stages 11-12 reporter transcripts have been completely delocalized within the oocyte and remain delocalized through the rest of oogenesis.

The effect of the two *sww* alleles in trans to one another differs only slightly from the effect sww^1 has when homozygous. In oocytes from mothers with a sww^1/sww^6 background, the first two stages of reporter RNA localization are normal. Initial anterior RNA localization is somewhat abnormal; while reporter RNA is clearly detectable at the anterior, it is more diffuse and not as tightly localized as normal. Localization begins to disappear at stages 11-12 and is completely gone by the end of oogenesis.

sww thus plays a role in maintenance of reporter RNA at the anterior of the oocyte (15), once anterior localization has been established in mid-to-late oogenesis. Our results show that *sww*'s effect on RNA localization is exerted through the 3'UTR of the transcript. If Swallow does in fact act through the 3'UTR, then deletion of the site(s) through which Swallow acts should produce the mutant phenotype described above: normal early transport

into the oocyte during stages 1-7, cortical localization of reporter RNA at stage 8, followed by anterior localization that may be normal or somewhat diffuse at stages 9-10, a failure to maintain tight anterior localization at stages 10b-12, and delocalization in late oogenesis. None of the deletion transgenes yield *in situ* results that completely fit this phenotypic description. Possible explanations are: first, there may be multiple sites through which Swallow acts in the *Adducin-like* N4 3'UTR, and no deletion overlapped enough sites to produce a phenotype, or second, Swallow target sites may lie within ALE1. At present we cannot distinguish between these alternatives.

DISCUSSION

Alternative splicing: The *Drosophila* Adducin-like family of proteins

We have recovered four classes of Adducin-like cDNAs (R1, N4, R2, N32) from ovarian and early embryonic cDNA libraries, representing alternatively spliced *Adducin-like* transcripts encoding three polypeptides. Whole mount *in situ* hybridizations using probes specific to the R1, N4, and R2/N32 3'UTRs show that transcripts bearing these 3'UTRs are directed to separate locations within the developing egg chamber (the follicle cells, the oocyte and the nurse cells, respectively). All three predicted Adducin-like protein isoforms have the same N-terminal region but are different lengths and have different C-termini.

Four *Drosophila* adducin-related proteins (Add-140, Add-95, Add-87, and Add-60) have been reported (52, 89, 66). Of these adducin-related proteins, only two can be correlated with our cDNAs so far. Add-140 is most likely encoded by N4, and Add-60 is probably processed from Add-140 (66). More work is needed to establish conclusively whether Add-87 and Add-95 are isoforms of Adducin-like or represent other adducin-related proteins, since neither signal diminishes in *Adducin-like* mutant ovaries (*hts*^{1}, L. Cooley, pers. comm.).

It is likely that we have not recovered all the Adducin-like cDNAs, since our cDNAs do not all correlate with previously published Northern blot band sizes, and since there are Adducin-like protein isoforms that do not all match up to our cDNAs. In addition, we expect that there may be other isoforms specific to later development or adulthood and to the brain.

The R1 class of *Adducin-like* RNA encodes the *Drosophila* orthologue of human adducin

Of all the *Drosophila* Adducin-like proteins, the one predicted to be encoded by the R1 class of *Adducin-like* RNA shows the highest homology to human adducins and most closely matches the human adducins in size. R1 is the only *Drosophila* Adducin-like protein predicted to contain a MARCKS-related motif at the C-terminal end. The core sequence of the MARCKS-related motif is identical in R1 and human adducins, including the serine residue which has been shown to be the target for PKA and PKC phosphorylation in human adducins.

The MARCKS-related sequence also functions in human adducins to bind calmodulin (59). Calmodulin-binding and phosphorylation are reciprocally inhibitory processes for human adducins (59). Both calmodulin and PKA phosphorylation of human adducin also inhibit binding of adducin to spectrin-actin complexes and recruitment of additional spectrin molecules to the complexes by adducin (25, 59). Calmodulin binding downregulates the ability of adducin to act as a barbed-end capping protein for actin (47). PKC phosphorylation of human adducin redistributes adducin away from cell-cell contact sites in cultured epithelial cells (39). R1 Adducin-like activity is likely to be regulated by signal transduction pathways similar to those affecting human adducins.

Given that *Drosophila* R1 *Adducin-like* transcripts appear to be localized to the follicle cells throughout oogenesis, what might the function of R1 protein be during *Drosophila* oogenesis? Adducin and Adducin-like proteins which contain a MARCKS-related site are likely to have some functions in common with MARCKS proteins. Human MARCKS proteins are thought to contribute to phagocytosis, neurosecretion and actin-based cell motility by promoting highly localized rearrangements and destabilization of the actin cytoskeleton (2, 1, 3). Human adducins are also capable of promoting local cytoskeletal rearrangements and dynamic changes in actin-spectrin cytoskeletal stability at cell-cell contact junctions and are candidates to mediate synaptic plasticity (39, 68).

Drosophila R1 Adducin-like is likely to be involved in similar processes involving cytoskeletal remodeling of follicle cells, since they undergo extensive shape changes, migrations, secretory processes, and alterations of cell surface properties during *Drosophila* oogenesis (the roles follicle cells play in oogenesis are reviewed in 72). At the beginning of oogenesis, the progeny of somatically-derived stem cells migrate from the wall of the germarium to surround the 16-cell germinal cysts. During later oogenesis, specific subpopulations of follicle cells migrate to separate the anterior of the oocyte from the nurse cells, secrete vesicles containing components of the vitelline membrane, undergo rapid cell shape change to accommodate the elongation of the egg chamber, lay down the chorion (eggshell) and participate in forming distinct chorion structures such as the micropyle and dorsal appendages. All of these processes require substantial, dynamic, and coordinated cytoskeletal change. The R1 isoform of *Drosophila* Adducin-like, with its potential for regulation through multiple signal transduction pathways, is an excellent candidate for mediating some of these extensive cytoskeletal changes within the follicle cells during oogenesis.

Organization of the *Adducin-like* N4 3'UTR localization signals

The *Adducin-like* N4 transcript is targeted specifically to the oocyte within the nurse-cell oocyte complex, and then localized within the oocyte. By analyzing the distributions of reporter transcripts containing systematic deletions of the N4 mRNA, we have shown that the signals responsible for directing all phases of localization reside within the 345 nucleotide (nt) 3'UTR of the *Adducin-like* N4 transcript, and that the 3'UTR is both necessary and sufficient to direct N4 mRNA localization.

Early transport of *Adducin-like* N4 mRNA to the oocyte is directed by a *cis*-acting element within nt 150-250 of the 3'UTR. We have named this *cis*-acting signal ALE1. Deletions overlapping this region abolish reporter trancript localization. Interestingly, the transient cortical restriction of N4 RNA at stage 8 is also directed by ALE1. It is not clear

whether there are two separable signals within the 150-200 region or whether early transport and cortical restriction are driven by the same process and therefore directed by the same localization signal. Further dissection of the ALE1 region by deletion analysis would help to resolve this issue.

In contrast to the signals directing early transport, those directing anterior localization of N4 transcripts during stages 9-14 are more complex and show functional redundancies. ALE1 is required for anterior localization during stages 9-14. Deletion analysis shows that there are also two separable and redundant signals contained within nt 50-100 and 100-150 of the 3'UTR. Removal of both these signals abolishes localization during stages 9-14, as does removal of ALE1, with one exception: the Δ50-5 transgene, in which nt 50-100 are removed, produces reporter transcripts that are localized normally to the anterior at stage 9-10a. Thus the more important of the two elements seems to be contained within nt 100-150. At stages 10b-11, deletion of any part of the 3'UTR either impairs or abolishes localization and so the entire 3'UTR is necessary for normal stage 10b-11 anterior localization. At stages 12-14, all but the first 50 and last 45 nt of the 3'UTR play a role in anterior localization. Although elements other than ALE1 are necessary for late localization to the anterior, none of them are able to function autonomously.

In addition, we have shown that a reporter transcript containing only nt 100-250 of the *Adducin-like* N4 3'UTR (nt 100-150 plus ALE1) is capable of correct localization in early stages (1-8) of oogenesis. However, the 100-250 region is not completely sufficient to direct stage 9-14 anterior localization. Stage 9-14 oocytes bearing this transgene show a slight change in either pattern or level of anterior localization of reporter mRNA; reporter mRNA is enriched at the anterior but either not as tightly as normal or there is not as much of it as normal. This suggests that ALE1 is necessary but not sufficient to direct the correct pattern and level of *Adducin-like* N4 localization, since additional *cis*-acting elements are required for wild-type late localization.

In a small percentage of oocytes carrying the 100-250 transgene, reporter RNA is dispersed throughout the oocyte in addition to being enriched at the anterior. While it is likely that *cis*-acting elements other than ALE1 are necessary for late anterior localization, an alternative explanation is that the dispersed reporter RNA may simply reflect saturation of the localization apparatus, since endogenous *Adducin-like* is being localized concurrently with reporter RNA to the anterior of transgenic oocytes.

How do *Adducin-like* N4 localization signals compare to those found in other *Drosophila* oocyte-localized RNAs?

Is there likely to be a single early transport pathway for all *Drosophila* oocyte-localized RNAs, and thus a common early transport element in *Drosophila*? *Adducin-like*, *orb* , *K10*, *oskar*, *cyclin B, gurken, Bic-D,* and *tudor* mRNAs undergo early transport at about the same time, as all of these mRNAs are first localized to the presumptive oocyte within the germarium (48, 10, 15, 18, 42, 12, 62, 76, 31). For a subset of these mRNAs (*Adducin-like*, *orb*, *K10*, and *oskar*), 3'UTR early transport localization signals have been at least partially mapped (49, 10, 69, 43).

The *orb* 3'UTR is 815 nt; division of this 3'UTR into two non-overlapping halves leaves each half with the ability to direct early transport (49). Clearly there are at least two elements within the *orb* 3'UTR capable of directing early transport to the oocyte. A central sequence of 280 nt which overlaps the two regions described above has been defined as completely sufficient to produce normal *orb* localization throughout oogenesis, and may contain both of the early transport elements (49). One of the *orb* early transport elements has been defined: a 42 nt sequence which is predicted to fold into a stem-loop and can direct early transport and anterior localization through stage 9 (69; R.S. Cohen, pers. comm.).

K10 possesses a 44 nt stem-loop sequence which is capable of directing early transport (the TLS element, for transport and localization sequence) and contains a region

in the stem that is strongly homologous to the *orb* early transport signal (69). In fact, the *orb* early transport element was first identified by its similarity to the *K10* sequence (69). Although *K10* and *orb* have very similar early transport elements, these signal sequences do not resemble the ALE1 element of *Adducin-like* in terms of primary sequence. However, all three are predicted to form stem-loop structures (*K10* and *orb*, 69; ALE1, see Figure 19). Mutagenesis of the *K10* TLS element shows that the stem rather than the loop is the functional part of the localization element, and also suggests that base-pairing is more important than primary sequence (69). This is similar to what has been shown for Staufen binding sites within the *bicoid* 3'UTR (20).

The *oskar* 3'UTR is 1043 nt (43). For *oskar*, two adjacent deletions (olc 15 and 16, or oskar localization construct) within the 3'UTR of 148 and 111 nt each severely impair early transport (43). Finer-scale mapping has not yet been done for *oskar* early transport elements.

With the exception of the localization element common to *K10* and *orb*, there does not seem to be a shared element responsible for early transport of specific mRNAs into the *Drosophila* oocyte. This may reflect a difference in subsequent localization patterns and pathways, and thus the need for different *trans*-acting localization factors.

Distribution patterns of localized RNAs in later oogenesis vary considerably, and deletion analysis shows that the signals for later stage localization are correspondingly complex. For example, two separate deletions (olc 13 and olc 17) impair the transient phase of anterior *oskar* localization at stage 9 (43). The posterior localization of *oskar* mRNA in late oogenesis can be abolished by deletion of the region corresponding to olc 21 (43). The olc 21 region also contains redundant signals, since its two components (olc 11 and 12) can individually be deleted without much effect on posterior localization. This redundancy is similar to what is seen in *Adducin-like* localization, since the signals at nt 50-100 and 100-150 can individually be deleted with minor effects on stage 9-14 anterior localization, but abolish localization when deleted simultaneously.

Deletion analysis and the complexity of 3'UTR localization elements

The TLS element of *K10* (69), the BLE1 element of *bicoid* (54), and the ALE1 element of *Adducin-like* N4 are all*cis*-acting localization elements within *Drosophila* mRNA 3'UTRs. Each is sufficient to direct a particular pattern of RNA localization when attached to a heterologous reporter RNA (although BLE1 is only sufficient when present in two copies; 54). Localization elements are likely to consist of binding sites for RNA-binding proteins (or possibly other RNAs), and it has been proposed that localization pathways result from combinatorial use of such binding sites (43, 54, 49). Why, then, has it not yet been possible to obtain precise definition of many of these localization elements?

First, the apparent complexity of the localization signals present in 3'UTRs may be due to the three-dimensional structure of the signals and their presentation to RNA-binding proteins, and to the inability of deletion analysis to fully address these aspects. RNAs can fold not only into secondary stem-and-loop structures but also into tertiary structures where loops interact (termed pseudoknots; 85). Furthermore, RNAs can form quaternary structures by interacting with each other, as has been shown for the *bicoid* 3'UTR, which dimerizes by base pairing between certain single-stranded loops (20). This means protein binding sites can potentially be composed of subelements that are far apart in the primary sequence. Staufen protein, for example, binds to three noncontiguous double-stranded stems of stem-loop structures within the *bicoid* 3'UTR (19). In addition, Staufen binds to dimerized *bicoid* mRNAs, at the double-stranded regions where base-pairing occurs between single-stranded loops of different *bicoid* mRNA molecules (20). Staufen is required to maintain anterior localization of *bicoid* at the anterior of stage 13-14 oocytes and early embryos (73).

Second, the complex and redundant nature of 3'UTR localization signals strongly suggests that multiple binding sites for a given protein may exist. When multiple binding sites exist, either one protein might fully occupy a single binding site, so that multiple binding sites would be occupied by a corresponding number of proteins, or one protein

may make multiple contacts with the folded RNA. Deletion of one of many binding sites could thus potentially have only a subtle effect (or no effect) on localization, if other binding sites are able to compensate. This might be the case for *orb*, where each half of an 815 nt subregion of the 3'UTR is able to direct early transport (49). Alternatively, if all binding sites are necessary, deletion of one of many sites would abolish localization completely. In the case of Staufen, all three of the binding sites in the *bicoid* 3'UTR are necessary; linker-scanning substitutions within any of them abolish *bicoid* localization (19).

Third, complexity in defining binding sites by deletion analysis might be due to misfolding induced by specific deletions. Removal of part of a region which normally forms a double-stranded stem leaves the other part free to base-pair in novel ways, and thus could potentially interfere with normal folding of the remainder of the 3'UTR.

Fourth, deletion analysis is a good first approach but generally does not provide high resolution, as deletions are typically 30 nt or more while actual binding sites are likely to be smaller. It is clear that more precise definition of the *cis*-acting localization signals within 3'UTRs is necessary. This requires both finer-scale mapping methods and characterization of RNA-binding proteins (*trans*-acting factors) which recognize those signals. For instance, UV-crosslinking methods have been used to identify a protein (Exl, for exuperantia-like) which binds to the *bicoid* 3'UTR via the BLE1 localization element and to further define Exl's binding site within BLE1 (55).

Trans-acting factors in *Adducin-like* RNA localization: the role of Swallow

Swallow is the only *trans*-acting factor that has been identified in the *Adducin-like* RNA localization pathway (15). *swallow* function is required for Adducin-like RNA and Add-87 protein localization and bicoid RNA localization to the anterior of the oocyte, as well as posterior polar plasm and polar granule localization (90, 6, 73, 36). Although putative RNA-recognition motifs (RRMs) have been identified in Swallow protein, these motifs are very divergent from consensus RRMs (8) and there are no data to indicate

whether Swallow is capable of binding RNA directly. We have shown here that all localization signals in the *Adducin-like* N4 transcript are contained in the 3'UTR, and that *swallow* also exerts its influence on *Adducin-like* RNA localization via the N4 3'UTR. The effects of mutations in *swallow* are first noticeable at stage 9, when reporter transcripts bearing the N4 3'UTR are not as tightly confined to the anterior as normal. By stage 10b-11, reporter RNA is localized only along the dorsal part of the anterior cortex and is also spreading dorsally. During stages 12-14, reporter RNA is increasingly delocalized until localization is lost entirely. Thus *swallow* is required for maintenance of *Adducin-like* N4 RNA localization at the anterior cortex of the oocyte, beginning at stage 9. Our assessment of the timing of the requirement for *swallow* conflicts somewhat with a previous report of *Adducin-like* localization in *swallow* oocytes, which stated that delocalization from the anterior occurred as early as stage 7-8 (15). Our data clearly indicate that reporter localization is normal through stage 8; both early transport and cortical restriction of reporter RNA occur normally in *swallow* oocytes.

Function of *Adducin-like* N4 RNA localization to the anterior of the oocyte and early embryo

Previous work has shown that localization of *Adducin-like* RNA to the anterior cortex of stage 9-14 oocytes appears to be necessary for normal embryonic development (90). Mutations of the *swallow* gene delocalize *Adducin-like* RNA and Add-87 protein in oocytes and result in embryos with disorganized F-actin and spectrin cytoskeletons, as well as defects in nuclear division, nuclear migration, and cellularization (90, 36). *swallow* mutations also produce defects in pole cell formation and abdominal pattern specification, as well as defects in head development, but these are due respectively to failure of *swallow* mutants to retain polar granules (ribonucleoprotein complexes) at the posterior pole and *bicoid* mRNA at the anterior pole (90, 24, 19, 73). Early embryos from homozygous *swallow* mothers exhibit the same cytoskeletal defects as early embryos from mothers

homozygous for the *hts*^{1e25} mutation, in which the *Adducin-like* RNA is localized normally but greatly reduced in amount (91, 90, 88). Having functional but non-localized *Adducin-like* RNA and protein (as in *swallow*) thus results in the same abnormalities as having insufficient *Adducin-like* RNA and protein (as in *hts*^{1e25}), and shows that localization of *Adducin-like* is necessary for normal early embryonic development. It is not completely clear why post-fertilization cytoskeletal reorganization (which underpins the processes of nuclear division, nuclear migration and cellularization) should specifically require anterior localization of *Adducin-like* RNA and protein. The implication is that the cytoskeletal reorganization of early cleavage may begin from the anterior of the embryo. While nuclear division is known to initiate in the anterior center of the early *Drosophila* embryo (92, 82), there is not extensive evidence to support an anterior origin for embryonic cytoskeletal reorganization.

Functions of alternative splicing in development

Many, if not most, genes seem to produce alternatively spliced transcripts, but the role of alternative splicing in development has not yet been well explored. Alternative splicing provides one way to vary function as well as spatial and temporal regulation of gene products. Through alternative splicing, a single gene such as *Adducin-like* can generate transcripts which have different 3'UTRs and which can also encode alternate protein isoforms. Since RNA localization signals usually reside within 3'UTRs, use of different 3'UTRs allows targeting of transcripts encoding specific isoforms to different locations. Related proteins that have different roles in development can thus be spatially restricted to appropriate domains of function.

In addition, spatial restriction of function is often linked to temporal restriction of function. Pattern determinants such as Oskar, Bicoid, and Nanos are required not only at a specific location but also within a specific time frame. To control the time at which protein synthesis occurs, developmentally localized RNAs are frequently subject to translational

regulation, often by repression of translation via the 3'UTR (reviewed in 56). Transcripts encoding the patterning determinant Oskar, for instance, are localized to the posterior of the *Drosophila* oocyte, and are prevented from being translated until the appropriate time through binding of Bruno protein to sites within the *oskar* 3'UTR (41). In contrast to *oskar*, the *cyclin B* gene provides an example of alternative splicing and regulation of a developmentally important gene which does not encode a pattern determinant. Two *cyclin B* transcripts of 2.3 kb and 2.7 kb with the same open reading frame but variant 3'UTRs are expressed at different times during oogenesis (12). The 2.3 kb transcript is produced by splicing out a 393 nt region from the middle of the complete 776 nt 3'UTR. This shorter *cyclin B* transcript undergoes early transport to the oocyte beginning in the germarium and continuing through stage 7 of oogenesis, after which it is no longer detectable. Beginning at stage 9 the longer *cyclin B* transcript is synthesized in nurse cells and following dumping into the oocyte at stage 11, the RNA is localized to the posterior pole of the oocyte and embryo and taken up into the pole cells when they form (12). Translation of the 2.7 kb *cyclin B* transcript is then repressed until the pole cells begin proliferation in the gonad at stage 14 of embryogenesis (13). Both posterior localization and translational repression are conferred by elements within the part of the 3'UTR that is present within the longer transcript but spliced out of the shorter transcript (12, 13). Thus use of different 3'UTRs can confer different temporal regulation as well as spatial regulation of protein isoform synthesis.

It seems likely that there are more splice forms of *Adducin-like*, since we cannot correlate all the known Adducin-like proteins with the cDNAs reported here, and our cDNAs in turn do not all correlate with previously reported *Adducin-like* transcript sizes (cf. 88). It will be interesting to elucidate whether alternate *Adducin-like* 3'UTRs confer temporal as well as spatial regulation of protein expression, where and when the different protein isoforms are translated, what roles the different isoforms play in cytoskeletal

organization during oogenesis and embryogenesis, and to discover why localization of the N4 isoform to the anterior of the oocyte is required for early embryogenesis.

ACKNOWLEDGMENTS

We thank Dali Ding for cloning and sequencing the Adducin-like cDNAs; Michele Zaccai for aligning the cDNA clones and assigning them to classes; Bill Fisher, Angelo Karaiskakis, and Weili Fu for expert technical assistance; and David Mathog for help with the GCG computer package. The plasmid p701, which encodes the *α-tubulin* 3'UTR, was a generous gift from Paul Macdonald. We thank Joanne Topol, Susan Celniker, Peter Becker, Susan Halsell, and Bill Fisher for critical reading of the manuscript. K.W. also wishes to thank the Caltech Division of Biology, Dr. Howard D. Lipshitz, and the Hospital for Sick Children for financial support.

REFERENCES

1. Aderem, A. 1992. The MARCKS brothers: a family of protein kinase C substrates. Cell **71:** 713-716.
2. Aderem, A. 1992. Signal transduction and the actin cytoskeleton: the roles of MARCKS and profilin. Trends in Biol. Sci. **17:** 438-443.
3. Allen, L.H. and A. Aderem. 1995. Protein kinase C regulates MARCKS cycling between the plasma membrane and lysosomes in fibroblasts. EMBO J. **14:** 1109-1121.
4. Andres, A.J. and C.S. Thummel. 1994. Methods for quantitative analysis of transcription in larvae and prepupae. Meth. Cell. Biol. **44:** 565-573.
5. Bennett, V., K. Gardner, and J.P. Steiner. 1988. Brain adducin: a protein kinase C substrate that may mediate site-directed assembly at the spectrin-actin junction. J. Biol. Chem. **263:** 5860-5869.
6. Berleth, T., M. Burri, G. Thoma, D. Bopp, S. Richstein, G. Frigerio, M. Noll, and C. Nüsslein-Volhard. 1988. The role of localization of *bicoid* RNA in organizing the anterior pattern of the *Drosophila* embryo. EMBO J. **7:** 1749-1756.
7. Brown, N.H. and F.C. Kafatos. 1988. Functional cDNA libraries from *Drosophila* embryos. J. Mol. Biol. **203:** 425-437.
8. Chao, Y.-C., K.M. Donahue, N.J. Pokrywka, and E.C. Stephenson. 1991. Sequence of *swallow*, a gene required for the localization of *bicoid* message in *Drosophila* eggs. Dev. Genet. **12:** 333-341.
9. Cheng, H. and M. Bjerknes. 1989. Asymmetric distribution of actin mRNA and cytoskeletal pattern generation in polarized epithelial cells. J. Mol. Biol. **210:** 541-549.

10. Cheung, H.-K., T.L. Serano, and R.S. Cohen. 1992. Evidence for a highly selective RNA transport system and its role in establishing the dorsoventral axis of the *Drosophila* egg. Develop. **114:** 653-661.

11. Cohen, R.S. and M. Meselson. 1985. Separate regulatory elements for the heat-inducible and ovarian expression of the *Drosophila hsp26* gene. Cell **43:** 737-746.

12. Dalby, B. and D.M. Glover. 1992. 3' non-translated sequences in *Drosophila cyclin B* transcripts direct posterior pole accumulation late in oogenesis and peri-nuclear association in syncytial embryos. Develop. **115:** 989-997.

13. Dalby, B. and D.M. Glover. 1993. Discrete sequence elements control posterior pole accumulation and translational repression of maternal *cyclin B* RNA in *Drosophila.* EMBO J. **12:** 1219-1227.

14. Ding, D. and H.D. Lipshitz. 1993. Localized RNAs and their functions. BioEssays **10:** 651-658.

15. Ding, D., S.M. Parkhurst, and H.D. Lipshitz. 1993. Different genetic requirements for anterior RNA localization revealed by the distribution of *Adducin-like* transcripts during *Drosophila* oogenesis. Proc. Natl. Acad. Sci. USA **90:** 2512-2516.

16. Dong, L., C. Chapline, B. Mousseau, L. Fowler, K. Ramsay, J.L. Stevens, and S. Jaken. 1995. 35H, a sequence isolated as a protein kinase C binding protein, is a novel member of the adducin family. J. Biol. Chem. **270:** 25534-25540.

17. Driever, W. and C. Nüsslein-Volhard. 1988. A gradient of bicoid protein in *Drosophila* embryos. Cell **54:** 83-93.

18. Ephrussi, A., L.K. Dickinson, and R. Lehmann. 1991. *oskar* organizes the germ plasm and directs localization of the posterior determinant *nanos*. Cell **66:** 37-50.

19. Ferrandon, D., L. Elphick, C. Nüsslein-Volhard, and D. St Johnston. 1994. Staufen protein associates with the 3'UTR of *bicoid* mRNA to form particles that move in a microtubule-dependent manner. Cell **79:** 1221-1232.

20. Ferrandon, D., I. Koch, E. Westhof, and C. Nüsslein-Volhard. 1997. RNA-RNA interaction is required for the formation of specific *bicoid* mRNA 3'UTR-STAUFEN ribonucleoprotein particles. EMBO J. **16:** 1751-1758.

21. Fleming, T.P., M. Hay, Q. Javed, and S. Citi. 1993. Localization of tight junction protein cingulin is temporally and spatially regulated during early mouse development. Develop. **117:** 1135-1144.

22. Frank, L.H., H.-K. Cheung, and R.S. Cohen. 1992. Identification and characterization of *Drosophila* female germ line transcriptional control elements. Develop. **114:** 481-491.

23. Frohnhöfer, H.G. and C. Nüsslein-Volhard. 1986. Organization of anterior pattern in the *Drosophila* embryo by the maternal gene *bicoid*. Nature **324:** 120-125.

24. Frohnhöfer, H.G. and C. Nüsslein-Volhard. 1987. Maternal genes required for the anterior localization of *bicoid* activity in the embryo of *Drosophila*. Genes Dev. **1:** 880-890.

25. Gardner, K. and V. Bennett. 1987. Modulation of spectrin-actin assembly by erythrocyte adducin. Nature **328:** 359-362.

26. Garfinkel, M.D., R.E. Pruitt, and E.M. Meyerowitz. 1983. DNA sequences, gene regulation and modular protein evolution in the *Drosophila* 68C glue gene cluster. J. Mol. Biol. **168:** 765-789.

27. Garner, C.C., R.P. Tucker, and A. Matus. 1988. Selective localization of messenger RNA for cytoskeletal protein MAP 2 in dendrites. Nature **336:** 674-676.

28. Gavis, E.R. and R. Lehmann. 1992. Localization of *nanos* RNA controls embryonic polarity. Cell **71:** 301-313.

29. Gavis, E.R. and R. Lehmann. 1994. Translational regulation of *nanos* by RNA localization. Nature **369:** 315-318.

30. Goldberg, Y.P., B.-Y. Lin, S.E. Andrew, J. Nasir, R. Graham, M.L. Glaves, G. Hutchinson, J. Theilmann, D.G. Ginzinger, K. Schappert, L. Clarke, J.M. Rommens, and M.R. Hayden. 1992. Cloning and mapping of the α-adducin gene close to D4S95 and assessment of its relationship to Huntington disease. Hum. Mol. Genet. **1:** 669-675.

31. Golumbeski, G.S., A. Bardsley, F. Tax, and R.E. Boswell. 1991. *tudor*, a posterior-group gene of *Drosophila melanogaster*, encodes a novel protein and an mRNA localized during mid-oogenesis. Genes Dev. **5:** 2060-2070.

32. Gutzeit, H. 1986. Transport of molecules and organelles in meroistic ovarioles of insects. Differentiation **31:** 155-165.

33. Gutzeit, H.O. 1986. The role of microfilaments in cytoplasmic streaming in *Drosophila* follicles. J. Cell Sci. **80:** 159-169.

34. Halsell, S.R. and H.D. Lipshitz. 1995. Mechanisms and functions of RNA localization to the posterior pole of the *Drosophila* oocyte and early embryo. in: Localized RNAs, ed. H.D. Lipshitz. R.G. Landes/Springer-Verlag: Austin, Texas, p. 9-39.

35. Harlan, D.M., J.M. Graff, D.J. Stumpo, R.L. Eddy, T.B. Shows, J.M. Boyle, and P.J. Blackshear. 1991. The human myristoylated alanine-rich C kinase substrate (MARCKS) gene (MACS). Analysis of its gene product, promoter, and chromosomal localization. J. Biol. Chem. **266:** 14399-14405.

36. Hegdé, J. and E.C. Stephenson. 1993. Distribution of swallow protein in egg chambers and embryos of *Drosophila melanogaster*. Development **119:** 457-470.

37. Hughes, C.A. and V. Bennett. 1995. Adducin: a physical model with implications for function in assembly of spectrin-actin complexes. J. Biol. Chem. **270:** 18990-18996.

38. Joshi, R., D.M. Gilligan, E. Otto, T. McLaughlin, and V. Bennett. 1991. Primary structure and domain organization of human alpha and beta adducin. J. Cell Biol. **115:** 665-675.

39. Kaiser, H.W., E. O'Keefe, and B. Bennett. 1989. Adducin: Ca++-dependent association with sites of cell-cell contact. J. Cell Biol. **109:** 557-569.

40. Katagiri, T., K. Ozaki, T. Fujiwara, F. Shimizu, A. Kawai, S. Okuno, M. Suzuki, Y. Nakamura, E. Takahashi, and Y. Hirai. 1996. Cloning, expression, and chromosome mapping of adducin-like 70 (ADDL), a human cDNA highly homologous to human erythrocyte adducin. Cytogenet. Cell Genet. **74:** 90-95.

41. Kim-Ha, J., K. Kerr, and P.M. Macdonald. 1995. Translational regulation of *oskar* mRNA by Bruno, an ovarian RNA-binding protein, is essential. Cell **81:** 403-412.

42. Kim-Ha, J., J.L. Smith, and P.M. Macdonald. 1991. *oskar* mRNA is localized to the posterior pole of the *Drosophila* oocyte. Cell **66:** 23-35.

43. Kim-Ha, J., P.J. Webster, J.L. Smith, and P.M. Macdonald. 1993. Multiple RNA regulatory elements mediate distinct steps in localization of *oskar* mRNA. Develop. **119:** 169-178.

44. King, R.C. 1970. Ovarian development in *Drosophila melanogaster*. New York: Academic Press.

45. King, R.C. and R.G. Burnett. 1959. An autoradiographic study of uptake of tritiated glycine, thymidine, and uridine by fruit fly ovaries. Science **129:** 1674-1675.

46. Kislauskis, E.H., A. Ross, V.M. Latham, X. Zhu, G. Bassell, K. Taneja, and R.H. Singer. 1995. The mechanism of mRNA localization: its effect on cell polarity. in: Localized RNAs, ed. H.D. Lipshitz. R.G. Landes/Springer-Verlag: Austin, TX, p. 185-195.

47. Kuhlman, P.A., C.A. Hughes, V. Bennett, and V.M. Fowler. 1996. A new function for adducin: calcium/calmodulin regulated capping of the barbed ends of actin filaments. J. Biol. Chem. **271:** 7986-7991.

48. Lantz, V., L. Ambrosio, and P. Schedl. 1992. The *Drosophila orb* gene is predicted to encode sex-specific germline RNA-binding proteins and has localized transcripts in ovaries and early embryos. Develop. **115:** 75-88.

49. Lantz, V. and P. Schedl. 1994. Multiple *cis*-acting targeting sequences are required for *orb* mRNA localization during *Drosophila* oogenesis. Mol. Cell. Biol. **14:** 2235-2242.

50. Lawrence, J.B. and R.H. Singer. 1986. Intracellular localization of messenger RNAs for cytoskeletal proteins. Cell **45:** 407-415.

51. Lin, B., J. Nasir, H. McDonald, R. Grahm, J. Rommens, Y.P. Goldberg, and M. Hayden. 1995. Genomic organization of the human α–adducin gene and its alternately spliced isoforms. Genomics **25:** 93-99.

52. Lin, H., L. Yue, and A.C. Spradling. 1994. The *Drosophila* fusome, a germline-specific organelle, contains membrane skeletal proteins and functions in cyst formation. Develop. **120:** 947-956.

53. Lindsley, D.L. and G. Zimm. 1992. The Genome of *Drosophila melanogaster*. San Diego: Academic Press.

54. Macdonald, P.M., K. Kerr, J.L. Smith, and A. Leask. 1993. RNA regulatory element BLE1 directs the early steps of *bicoid* mRNA localization. Develop. **118:** 1233-1243.

55. Macdonald, P.M., A. Leask, and K. Kerr. 1995. EXL protein specifically binds BLE1, a *bicoid* mRNA localization element, and is required for one phase of its activity. Proc. Natl. Acad. Sci. USA **92:** 10787-10791.

56. Macdonald, P.M. and C.A. Smibert. 1996. Translational regulation of maternal mRNAs. Curr. Op. Genet. Dev. **6:** 403-407.

57. Macdonald, P.M. and G. Struhl. 1988. *Cis*-acting sequences responsible for anterior localization of *bicoid* mRNA in *Drosophila* embryos. Nature **336:** 595-598.

58. Maro, B., C. Gueth-Hallonet, J. Aghion, and C. Antony. 1991. Cell polarity and microtubule organization during mouse early embryogenesis. Develop. **(Suppl. 1):** 17-25.

59. Matsuoka, Y., C.A. Hughes, and V. Bennett. 1996. Adducin regulation: definition of the calmodulin-binding domain and sites of phosphorylation by protein kinases A and C. J. Biol. Chem. **271:** 25157-25166.

60. Meyerowitz, E.M., K.V. Raghavan, P.H. Mathers, and M. Roark. 1987. How *Drosophila* larvae make glue: control of *Sgs-3* gene expression. Trends in Genet. **3:** 288-293.

61. Mische, S.M., M.S. Mooseker, and J.S. Morrow. 1987. Erythrocyte adducin: a calmodulin-regulated actin-bundling protein that stimulates spectrin-actin binding. J. Cell Biol. **105:** 2837-2845.

62. Neuman-Silberberg, F.S. and T. Schüpbach. 1993. The Drosophila dorsoventral patterning gene gurken produces a dorsally localized RNA and encodes a TGF-α-like protein. Cell **75:** 165-174.

63. Pinto-Correia, C., E.G. Goldstein, V. Bennett, and J.S. Sobel. 1991. Immunofluorescence localization of an adducin-like protein in the chromosomes of mouse oocytes. Dev. Biol. **146:** 301-311.

64. Pokrywka, N.J. and E.C. Stephenson. 1991. Microtubules mediate the localization of *bicoid* RNA during *Drosophila* oogenesis. Develop. **113:** 55-66.

65. Pomeroy, M.E., J.B. Lawerence, R.H. Singer, and S. Billings-Gagliardi. 1991. Distribution of myosin heavy chain mRNA in embryonic muscle tissue visualized by ultrastructural *in situ* hybridization. Dev. Biol. **143:** 58-67.

66. Robinson, D.N., K. Cant, and L. Cooley. 1994. Morphogenesis of *Drosophila* ovarian ring canals. Develop. **120:** 2015-2025.

67. Rubin, G.M. and A.C. Spradling. 1982. Genetic transformation of *Drosophila* with transposable elements. Science **218:** 348-353.

68. Seidel, B., W. Zuschratter, H. Wex, C.C. Garner, and E.D. Gundelfinger. 1995. Spatial and sub-cellular localization of the membrane cytoskeleton-associated protein α-adducin in the rat brain. Brain Research **700:** 13-24.

69. Serano, T. and R. Cohen. 1995. A small predicted stem-loop structure mediates oocyte localization of *Drosophila K10* mRNA. Develop. **121:** 3809-3818.

70. Serano, T.L., H.-K. Cheung, L.H. Frank, and R.S. Cohen. 1994. P element transformation vectors for studying *Drosophila melanogaster* oogenesis and early embryogenesis. Gene **138:** 181-186.

71. Sheets, M.D., S.C. Ogg, and M.P. Wickens. 1990. Point mutations in AAUAAA and the poly(A) addition site - effects on the accuracy and efficiency of cleavage and polyadenylation in vitro. Nucl. Ac. Res. **18:** 5799-5805.

72. Spradling, A. 1993. Developmental genetics of oogenesis. in: The development of *Drosophila melanogaster,* ed. M. Bate and A.M. Arias. Cold Spring Harbor Laboratory Press: Cold Spring Harbor, N.Y., p. 1-70.

73. St Johnston, D., W. Driever, T. Berleth, S. Richstein, and C. Nüsslein-Volhard. 1989. Multiple steps in the localization of *bicoid* RNA to the anterior pole of the *Drosophila* oocyte. Develop. **107** (Suppl.)**:** 13-19.

74. Stephenson, E.C. 1995. Cytoskeletal mechanisms of RNA localization during *Drosophila* oogenesis. in: Localized RNAs, ed. H.D. Lipshitz. R.G. Landes Co./Springer-Verlag: Austin, Texas, p. 63-76.

75. Steward, O. 1997. mRNA localization in neurons: a multipurpose mechanism? Neuron **18:** 9-12.

76. Suter, B., L.M. Romberg, and R. Steward. 1989. *Bicaudal-D*, a *Drosophila* gene involved in developmental asymmetry: localized transcript accumulation in ovaries and sequence similarity to myosin heavy chain tail domains. Genes Dev. **3:** 1957-1968.

77. Taylor, S.A.M., R.G. Snel, A. Buckler, C. Ambrose, M. Duyao, D. Church, C.S. Lin, M. Altherr, D.E. Housman, M.E. MacDonald, and J.F. Gusella. 1992. Cloning of the α-adducin gene from the Huntington's disease candidate region of chromosome 4 by exon amplification. Nature Genet. **2:** 223-227.

78. Theurkauf, W.E., H. Baum, J. Bo, and P. Wensink. 1986. Tissue-specific and constitutive α-tubulin genes of *Drosophila melanogaster* code for structurally distinct proteins. Proc. Natl. Acad. Sci. USA **83:** 8477-8481.

79. Thummel, C.S. and V. Pirrotta. 1991. New pCaSpeR P element vectors. Dros. Inf. News. **2:** 19.

80. Tisminetzky, S., G. Devescovi, G. Tripodi, A. Muro, G. Bianchi, M. Colombi, L. Moro, S. Barlati, R. Tuteja, and F.E. Baralle. 1995. Genomic organization and chromosomal localization of the gene encoding human beta-adducin. Gene **167:** 313-316.

81. Tsang, S.S., X. Yin, C. Guzzoarkuran, V.S. Jones, and A.J. Davison. 1993. Loss of resolution in gel-electrophoresis of RNA-a problem associated with the presence of formaldehyde gradients. Biotechniques **14:** 380-381.

82. von Dassow, G. and G. Schubiger. 1994. How an actin network might cause fountain streaming and nuclear migration in the syncytial *Drosophila* embryo. J. Cell Biol. **127:** 1637-1653.

83. Wahle, E. and W. Keller. 1992. The biochemistry of 3'-end cleavage and polyadenylation of messenger-RNA precursors. Ann. Rev. Biochem. **61:** 419-440.

84. Wang, C., L.K. Dickinson, and R. Lehmann. 1994. Genetics of *nanos* localization in *Drosophila*. Dev. Dynamics **199:** 103-115.

85. Westhof, E. and L. Jaeger. 1992. RNA pseudoknots. Curr. Opin. Struct. Biol. **2:** 327-333.

86. Whittaker, K.L. and H.D. Lipshitz. 1995. Mechanisms and functions of RNA localization to the anterior pole of the *Drosophila* oocyte and early embryo. in: Localized RNAs, ed. H.D. Lipshitz. R.G. Landes Co./Springer-Verlag: Austin, Texas, p. 41-61.

87. Wilusz, J., S.M. Pettine, and T. Shenk. 1989. Functional analysis of point mutations in the AAUAAA motif of the SV40 late polyadenylation signal. Nucl. Ac. Res. **17:** 3899-3908.

88. Yue, L. and A.C. Spradling. 1992. *hu-li tai shao*, a gene required for ring canal formation during *Drosophila* oogenesis, encodes a homolog of adducin. Genes Dev. **6:** 2443-2454.

89. Zaccai, M. and H.D. Lipshitz. 1996. Differential distributions of two adducin-like protein isoforms in the *Drosophila* ovary and early embryo. Zygote **4:** 159-166.

90. Zaccai, M. and H.D. Lipshitz. 1996. Role of *Adducin-like* (*hu-li tai shao*) mRNA and protein localization in regulating cytoskeletal structure and function during *Drosophila* oogenesis and early embryogenesis. Dev. Genet. **19:** 249-257.

91. Zalokar, M., C. Audit, and I. Erk. 1975. Developmental defects of female-sterile mutants of *Drosophila melanogaster*. Dev. Biol. **47:** 419-432.

92. Zalokar, M. and I. Erk. 1976. Division and migration of nuclei during early embryogenesis of *Drosophila melanogaster*. J. Microsc. Biol. Cell **25:** 97-106.

TABLE AND TABLE LEGEND

Table 1. *Adducin-like* splice forms (compared to N4 sequence). Comparison of the exon structure of N4 and the presumed exon structure of R1, R2, and N32 cDNAs. Exon numbers in the first column correspond to those of Yue and Spradling (1992). Base numbers correspond to the cDNA sequence of Adducin-like published in Ding et al., (1993). + indicates that the full exon is present, otherwise the base numbers of the corresponding N4 sequence are given. For each cDNA class, the total cDNA length given is for the longest clone.

Table 1. *Adducin-like* splice forms (compared to N4 sequence)

Exon	Bases	Length	N4	R1	R2	N32
(novel) 5'UTR 1						+
1. 5'UTR 2	1-331	331 bp	+	85-331	73-127	
2. 5'UTR 2	332-380	49 bp	+	+	+	
3. 5'UTR 2, coding	381-976	596 bp	+	+	+	+
4. coding	977-1689	713 bp	+	+	+	+
5. coding	1690-1812	123 bp	+	+	+	+
6. coding	1813-1923	111 bp	+	+		
7. coding	1924-2218	295 bp	+	+		
8. coding	2219-2299	81 bp	+	+		
9. coding	2300-2371	72 bp	+	+		
10.coding, 3'UTR 1	2372-4239 (4208 if polyA tail is excluded)	1868 bp (1837 bp)	+			
Coding extension 1 (novel)	GEN VQN GDH SEA HLS TFS QSS KEF QDV STD GSP KKD KKK KKG LRT PSF LKK KKE KKK AEA*			+		
Coding extension 2 (novel)	VEI ITF EDM KQT KTT NLK EIE GK*				+	+
3'UTR 2 (novel)				+		
3'UTR 3 (novel)					+	+
3'UTR 4 (novel)						+
total cDNA length			4239	2617	1945	2320

FIGURES AND FIGURE LEGENDS

Figure 1. Schematic comparison of Adducin-like cDNAs. Arrows represent splice sites. Coding sequences are shown in solid colors, while the untranslated regions at either end are represented by striped boxes. Note that all cDNAs share 5'UTR sequence and open reading frame sequence, and that the R2 3'UTR is a truncated version of the N32 3'UTR. Striped green: shared 5'UTR sequence. Striped yellow: 5'UTR sequence unique to N32. Solid red: shared open reading frame sequence. Solid light pink: coding extension of R1. Solid turquoise: coding extension of R2 and N32. Striped light blue: N4 3'UTR. Striped purple: R1 3'UTR. Striped magenta: R2 and N32 3'UTRs.

Figure 1. Schematic comparison of Adducin-like cDNAs

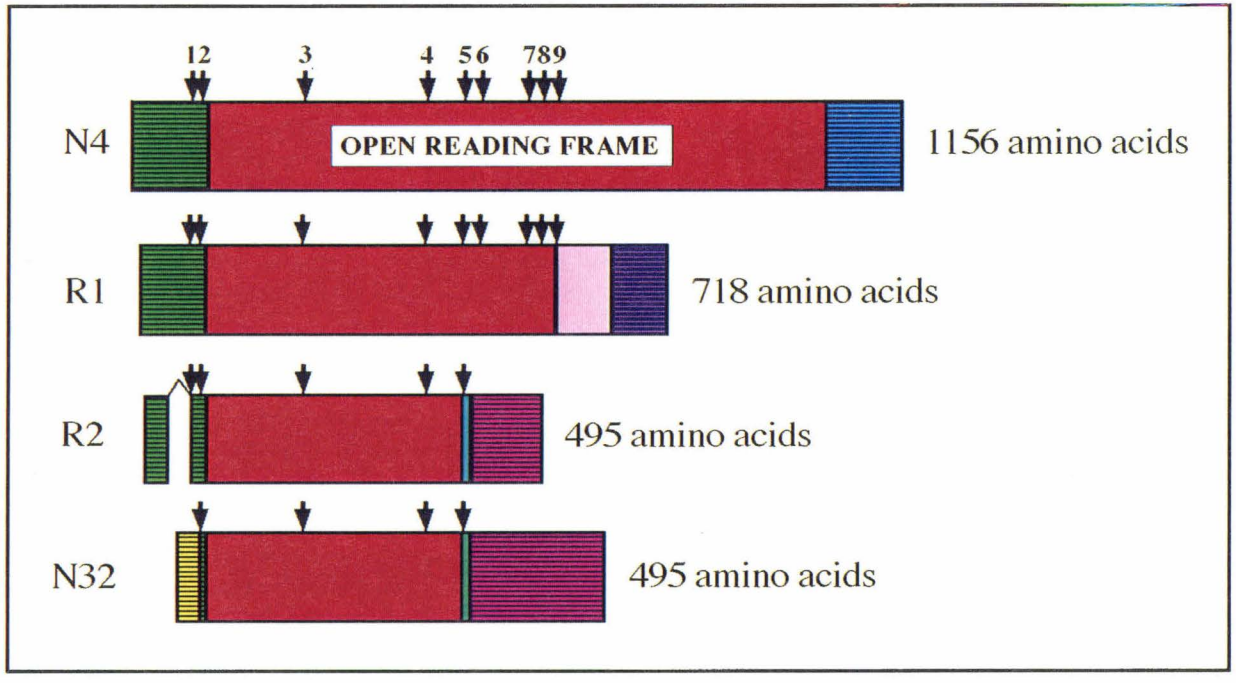

Solid color=coding region; striped color=UTR

Splice site (numbers refer to introns)

Figure 2. Sequence comparison of Adducin-like cDNAs. Dots indicate that the nucleotide sequence is identical to the Adducin-like N4 cDNA sequence. Dashes indicate that the sequence is not present since it has been eliminated by splicing. N4 splice sites are shown in bold type, with the number above each splice site referring to the deleted intron. The shared ATG translation start site is shown in underlined bold type. Polyadenylation signals are indicated by bold type.

Figure 2. Sequence comparison of Adducin-like cDNAs

Key: ..... *identical to N4 sequence*
------ *spliced across here*
ACGTAC *bold character indicates N4 splice site*
ATG *bold underlining indicates translation start*
AATAAA *potential polyadenylation sites are in bold*

```
N4      1  GAAAAACAAATATCGACCCATTGACATGCGTCAGGTTTGTCCATCCCTAACAAAATCGTAGTACGAAATATCGAAAACGAAACACATCACGCGGGCGAAA
R1      1                                                                                              .............
R2      1                                                                                          ...........

N4    101  TTTCGTGAAGTTCAGCATTTACAAATTTCTCCCTCTGTGGCGTATGTGTGTTTGTACGAATTAGCGGCTGAAAACCAAAAACCGAGGTGCGAGAGCGAGA
R1     17  ...............................................................................................
R2     29  .........................----------------------------------------------------------------------

N4    201  ATACGTTTATAAAAAACGCGTGCGTTTCTCCTCTAACACATACAGTGAGTGTGACCGTTGTATTTGTGACCTGTGCCTGTGTTAGCGGCCACTGGAGGAT
R1    117  ...............................................................................................
R2           -----------------------------------------------------------------------------------------------
N32     1                                                                                      CCCCCCCAGTCGA

                                          1                                                2
N4    301  CAACGAATTTAAAAGAATACTAAAAGTACCGGGACATCAATATAAAAGTATTATAACCACGCAACAAATTCAATTTTAAGCATTTTAACTGAAATCATGA
R1    217  ...............................................................................................
R2     56  ------------------------------.................................................................
N32    14  AAATTTTCCAGCTGAGCGTCAAGTTGAAGAAGAACTTATTCTAAATTCGGGAAAAACCCTTTTTCTCCATTTAATTGCAG.....................
N4    401  CTGAAGTTGAGCAACCGCCACAGAATGGCATAGATCCCACTGCCGGCGAAGATGATGACAATAGCAAAGCACGTCCCGCGGATATTGAACAGGATATGCG
R1    317  ...............................................................................................
R2    125  ...............................................................................................
N32   114  ...............................................................................................
N4    501  CGAAATGGAGCGTCGCAAGCGAGTCGAGGCTATAATGGGCTCGAAACTGTTCCGCGAGGAGCTGGAGCGTATCGTGGACTCGGCGCGCGATGGAGGTGCT
R1    417  ...............................................................................................
R2    225  ...............................................................................................
N32   214  ...............................................................................................
N4    601  GGCGCTAGTGGAATCCTGCAGCAGCTGTCGGACATTGTGGGCGTACCAGTGTCCAGGGTGGGCAGCGTCTTCAAGAGCAGCAACTGCATGGTGCCAATCA
R1    517  ...............................................................................................
R2    325  ...............................................................................................
N32   314  ...............................................................................................
N4    701  ACGATATACGCGGCGTCGAGTCCATGGGCTATGCCAAGGGCGAGAAGATACTCCGGTGCAAGCTGGCCGCCACATTCCGTCTGCTCGATCTGTACGGCTG
R1    617  ...............................................................................................
R2    425  ...............................................................................................
N32   414  ...............................................................................................
N4    801  GACCCAGGGTCTGGGGGCACAGATCACCGCCCGACTCAAGGTCGATCAGGAGTACTTCCTGGTTAACCCATACGGCCTGCTTTACCACGAGATCACTGCC
R1    717  ...............................................................................................
R2    525  ...............................................................................................
N32   514  ...............................................................................................
```

Figure 2, page ii: Sequence comparison of Adducin-like cDNAs

```
                                                                                         3
N4     901   TCAGCGCTGAACAAGGTGGATATGCAAGGACAGATTGTGGAGCAGGGCACCACCAACTTTGGCGGCAACAAGAGTCACTTTGTCCTCCATTCGGTGGTAC
R1     817   ....................................................................................................
R2     625   ....................................................................................................
N32    614   ....................................................................................................
N4    1001   ATGCTGCCCGTCCAGATATTCGATGCGCCATCTATATCGGCTGCAGTCCAGTCGTGGCTATTTCCTCACTAAAGACGGGTCTATTGCCCTTGACCAAGGA
R1     917   ....................................................................................................
R2     725   ....................................................................................................
N32    714   ....................................................................................................
N4    1101   TGCCTGTGTGCTGGGCGAGATCACCACTCACGCTTATACTGGTCTATTCGACGAGGAGGAGCGCAATCGATTGGTCCGCAGCCTTGGTCCCAACTCCAAG
R1    1017   ....................................................................................................
R2     825   ....................................................................................................
N32    814   ....................................................................................................
N4    1201   GTAATTCTGTTAACTAATCACGGTGCTTTGTGCTGCGGAGAGACCATCGAGGAAGCCTTCTTCGCCGCCTGTCACATTGTACAGGCGTGTGAGACGCAAC
R1    1117   ..C.................................................................................................
R2     925   ..T.................................................................................................
N32    914   ..G.................................................................................................
N4    1301   TGAAGCTGTTGCCCGTCGGTTTGGATAACTTGGTGCTGATTCCAGAGGAGTCGCGCAAGGCCATTTACGAGCAGTCGCGCCGGCCGCCGGAGGATCTGGA
R1    1217   ....................................................................................................
R2    1025   ....................................................................................................
N32   1014   ....................................................................................................
N4    1401   GAAGAAGTTTGCCGCCGTCGCCGCTGCCGAAGATGGTGCTGCTACTGCTGAAAAGGATGCAGCCGAAGCAGTACCCAAGGTTGGCAGTCCGCCCAAGTGG
R1    1317   ....................................................................................................
R2    1125   ....................................................................................................
N32   1114   ....................................................................................................
N4    1501   CGTGTGGGTGGTGCTGAATTTGAGGCCTTGATGCGCATGCTGGACAATGCTGGCTATCGCACTGGCTATATCTACCGTCATCCACTGATCAAATCGGATC
R1    1417   ....................................................................................................
R2    1225   ....................................................................................................
N32   1214   ....................................................................................................
                                                                                                      4
N4    1601   CTCCCAAGCCTAAGAACGATGTCGAACTACCGCCAGCTGTTTCATCACTGGGCTATCTTCTTGAGGAGGAGGAACTCTTCCGTCAAGGGATCTGGAAGAA
R1    1517   ....................................................................................................
R2    1325   ....................................................................................................
N32   1314   ....................................................................................................
N4    1701   GGGAGATATTCGCAAAGGCGGCGATCGCAGTCGGTGGCTCAACTCGCCAAACGTTTACCAAAAGGTCGAGGTTCTGGAGACCGGCACTCCGGATCCCAAG
R1    1617   ....................................................................................................
R2    1425   ....................................................................................................
N32   1414   ....................................................................................................
```

Figure 2, page iii: Sequence comparison of Adducin-like cDNAs

```
                                  5
N4    1801  AAGATTACAAAGTGGGTGGCTGAGGGTTCCCCCACCCACTCAACGCCAGTGAGGATAGAAGATCCACTCCAGTTTGTGCCTGCAGGAACCAATCCAAGGG
R1    1717  ..................................................................................................
R2    1525  ............GTAGAAATCATTACTTTCGAAGATATGAAGCAAACCAAAACCACCAACCTTAAGGAGATTGAGGGAAAATAGTTGAAATTGTTGGACA
N32   1514  ............GTAGAAATCATTACTTTCGAAGATATGAAGCAAACCAAAACCACCAACCTTAAGGAGATTGAGGGAAAATAGTTGAAATTGTTGGACA
                                      6
N4    1901  AATTTAAGCGTGTCCAGCAACTAATTAAGGACAACCGCCGGGCAGATAAGATTTCAGCCGGACCACAGTCGCATATTCTGGAGGGCGTGACATGGGACGA
R1    1817  ..................................................................................................
R2    1625  CCGAATCCTTCAACTCTTTACAGACATTCCACTTGCTATCCCCATATATAATTTCCATTTCGTTAGCACTCAGTTTTAGTTTCAACTTTGCCACTAAGCT
N32   1614  CCGAATCCTTCAACTCTTTACAGACATTCCACTTGCTATCCCCATATATAATTTCCATTTCGTTAGCACTCAGTTTTAGTTTCAACTTTGCCACTAAGCT
N4    2001  GGCGAGCCGACTCAAGGATGCAACGGTCTCGCAGGCCGGCGATCATGTCGTCATGATGGGTGCTGCCTCCAAAGGAATCATTCAGCGTGGCTTCCAGCAC
R1    1917  ..................................................................................................
R2    1725  GCAACTATATTCACGCATAAAATTTTTAGAGTTTAAGTAAATGAAAGTAATCAATATACAAATTCTATATATTTATATACTTTGGAAATAGAATTAAAAC
N32   1714  GCAACTATATTCACGCATAAAATTTTTAGAGTTTAAGTAAATGAAAGTAATCAATATACAAATTCTATATATTTATATACTTTGGAAATAGAATTAAAAC
N4    2101  AATGCCACTGTCTACAAGGCACCGTATGCTAAGAACCCATTCGATAACGTCACAGACGATGAACTCAATGAATACAAACGCACGGTGGAGCGCAAAAAGA
R1    2017  ..................................................................................................
R2    1825  TCGGGCTAAACCAAAATTATTTTACGTGCTTTGCTAGCAAGCAAACAAATATTGTGTAATGTGCATTAATCAAATAAATAAAATAAACAAGAAATAAAAA
N32   1814  TCGGGCTAAACCAAAATTATTTTACGTGCTTTGCTAGCAAGCAAACAAATATTGTGTAATGTGCATTAATCAAATAAATAAAATAAACAAGAAATAAAAA
                          7                                                                               8
N4    2201  AATCGGTGCATGGTGAATATACCGACACAGACTTTTCGGAATCCGAAGCGGTCCTGCAGGCGGGGACAAAGAAATACCCACAAAGCGAACCCGAGACCGA
R1    2117  ..................................................................................................
R2    1925  AAAAAAAAAAAAAAAAAAAAA
N32   1914  TTTGCATAGATGATTTTGTGCCTCATTTAGGGATTTGCGCTGCCTCACCAAACAAGACAATAGCGCTAAAACAATGCAAAGAAAGAGAAAGAAATTTGCT
                                                                                                  9
N4    2301  GCACCAGGTCATTGAGATCCAAACACAGCAAGCGCCAGTGCCAAGGCAGGCGGAAGTCGTGCTGAGCGATGCACTTGTCTCTCAACTGGCTCAAAAGTAT
R1    2217  ..............................................................GTGAAAACGTACAAAATGGCGATCATTCG
N32   2025  ATGAATACTAATCACTATGTAATAAATAAAACATTTTTTAATTTACCGAATCAATGATTTCATATTTAACCGCATTATTTTTCATTCATAAAATTTTTCT
N4    2401  GCGTTCCTTTATTCGCCTGGCCAATACATGTATGCCTGCATGAAAATGGCTCCATTAATGCAGAAGGTTTATGTTATACACAAGGTCGAGCCCGTCAGCA
R1    2317  GAGGCACACTTGAGCACCTTCTCGCAGAGCAGTAAAGAGTTCCAGGATGTCTCCACGGACGGATCCCCCAAGAAAGACAAGAAGAAGAAGAAGGGTCTGC
N32   2125  TTGCATGTTTTATGGTATCTTTCTTTTATTCTCTTTGTGATTGGTTTTCATTGTTATTCAAGGCACCAAATCATTTATGCTTGTTATTTTAGTTAATTTA
N4    2501  AGCACAACTATCCGCCAGTTAACGATGGCAATATGAGTATTCATCACAACGAAAGTGGAGCCGGATTCATGGCCCAAGAGTCCAGCGTTATTAGTAGCAC
R1    2417  GCACACCATCGTTTTTGAAAAAGAAGAAGGAGAAGAAGAAGGCCGAGGCCTAAGCTGACCATCAGCGTGATCCGTAGGAGTAGCAATCTTGACCAACCTC
N32   2225  TGTTTATTTGATCATTGAAAAGTTTGATATCTAGGAACATATTCTTATGTATGTTAAAAATAAACATTTCGAAAACCACAAAAAAAAAAAACAAAAAAAA
N4    2601  CCCCGTACGCAATGCCTTGGCATCTGTATCATTGCCGGAAGAGAGGAATCATTCTATTTTGGGCTTATCATCGACTCCGTATCGCACCATCTCGCATTTC
R1    2517  CCACCATCAGCGGGAACCGAGAAAAATAACGACAATGATACCACGAGAAAATGGAAACTTTAGCCAGATCAGCAAAAGAAGCATTATATAAAAAAAAAAA
N32   2314  AAATAAA

N4    2701  GGGTTCAATTGTCCGCTTATTACGTCACCAACCATTCTCCTGCATCCCGAACATCGATCCATTTGGCAACGGGTGGCCGAGCAGCGCGAGAAGGTTGTGT
R1    2597  A
```

Figure 2, page iv: Sequence comparison of Adducin-like cDNAs

```
N4    2801    CCTTCATAGATCTCACAACATTGAGCTTGGACAACCGCAAGCTGCTCAATGTGGTGACATCAACGCATCCAACCCAGTGCCAATCGCAATCGCAATCCTT
N4    2901    TATCTCTGAGAAGCACATTCAGCTGGAAGTTACGCCACCGAAGCGAAAGCAGCGTGTCTACAGCGCCACCATCAGCAGTGGTCTAGACGACAGCCTCGAT
N4    3001    GAGCTGGACTCCCTGATGAGTGGCCTAGCCATCAATATGCCGCGCAGTCGGGAGCAGGACAGCGGTCTGTACCGCAGCTACACCTTTCTACCCAGCAATC
N4    3101    ATGCTCTGCCCAAGGATACAGATGCCAATAATAGGGATCAAACGGATCGGGAGCGACCAGAAGCGGAGCAGGAGGAAAGTTTTCACTGCGCAGGCGACAG
N4    3201    TGGTATTGGCGATTCCACCGGCAGGCGTCCGCGTCTGGCCACCACCAGCAATGATTCGTCTATTCAAGAGGCCGAAGCCTATACCCAGGGCAAGCACGTC
N4    3301    AAGTTGACCTTGAGCAGCTCACCCACGCCGACGGCCACACAGTCACCTGCAACCATCGAAATTCTTATCAACGTATCGCTGCGCAATGCCGAGTGCGTCC
N4    3401    AAACGGTCCAGACCCATGAGCAGGAGTTTCGCGCCAAGTTGGAGCGAGTAATCGACGAGGAGATCCACTATATTTCGCAGCAACTCGCATTTAAACAGCG
N4    3501    ACAGGCAGAGTTGCATGAACAACAGACTACATCGCGGGCTCCAATCGCTACGCCTTCTTTCACAACTATGCATCCGCCGGCACCGGCTTCTTCATCATCC
N4    3601    ATGGTTCACCGCAGCAACTCGGCACCAGAACTGTGCCACACCTATAGCTATGTGGCCGTGTGCGATTTGTCGACCAAACAGGATCAAGCCTCTCCCCAAC
N4    3701    TGCCAGCGGAGGGTGAGCCGTTGAATGATATACTCAGCAGTCTGGAGAAGGAACTGGAGCGTCTGCTGAATAGCGTGGTGACAGCACACATGCTGCACAA
N4    3801    CAAGGCCATCATACACGAGTGCCGGGCTCGCTTCTCGCAGCTGGCCGATGGAATTGTCAGCTCGTAGATACATATTATGATTTTGATGGAAAATTTACAT
N4    3901    CTTCGCTTTTGTTGTGATATTTGAAATCGACAACAGTGAAATGATTGTATAAAGCAACTAGATTAAGTTTAATGATGATAATTTGGAAACCTTCAAATCG
N4    4001    AACTAATGCATTTTTTACTTCTTTGTTCTCTTAATTTAAATGTTAAGACTGTAACTTAAGCACAATATGGAAATGCAAAGTTAAAACTGAATCTGAGCCA
N4    4101    ACCATTGTACATTTAAACATCTGTGAAATTGTTAAGTTTAATTTTTGTCGAATCTTGATTTTCGTTTCATATTTTTATAATTAAAATATAATAAATATAG
N4    4201    TTTTCATTAAAAAAAAAAAAAAAAAAAAAAAAAAAAAA
```

Figure 3. Comparison of Adducin-like protein sequences. Dots indicate that the amino acid residues indicated are identical to the predicted Adducin-like N4 peptide sequence. Stop codons are shown as asterisks.

Figure 3: Comparison of Adducin-like protein sequences

```
N4       1   MTEVEQPPQNGIDPTAGEDDDNSKARPADIEQDMREMERRKRVEAIMGSKLFREELERIVDSARDGGAGASGILQQLSDIVGVPVSRVGSVFKSSNCMVP
R1       1   ..........................................................................................................
R2       1   ..........................................................................................................
N32      1   ..........................................................................................................

N4     101   INDIRGVESMGYAKGEKILRCKLAATFRLLDLYGWTQGLGAQITARLKVDQEYFLVNPYGLLYHEITASALNKVDMQGQIVEQGTTNFGGNKSHFVLHSV
R1     101   ..........................................................................................................
R2     101   ..........................................................................................................
N32    101   ..........................................................................................................

N4     201   VHAARPDIRCAIYIGCSPVVAISSLKTGLLPLTKDACVLGEITTHAYTGLFDEEERNRLVRSLGPNSKVILLTNHGALCCGETIEEAFFAACHIVQACET
R1     201   ..........................................................................................................
R2     201   ..........................................................................................................
N32    201   ..........................................................................................................

N4     301   QLKLLPVGLDNLVLIPEESRKAIYEQSRRPPEDLEKKFAAVAAAEDGAATAEKDAAEAVPKVGSPPKWRVGGAEFEALMRMLDNAGYRTGYIYRHPLIKS
R1     301   ..........................................................................................................
R2     301   ..........................................................................................................
N32    301   ..........................................................................................................

N4     401   DPPKPKNDVELPPAVSSLGYLLEEEELFRQGIWKKGDIRKGGDRSRWLNSPNVYQKVEVLETGTPDPKKITKWVAEGSPTHSTPVRIEDPLQFVPAGTNP
R1     401   ..........................................................................................................
R2     401   ..........................................................................VEIITFEDMKQTKTTNLKEIEGK*
N32    401   ..........................................................................VEIITFEDMKQTKTTNLKEIEGK*

N4     501   REFKRVQQLIKDNRRADKISAGPQSHILEGVTWDEASRLKDATVSQAGDHVVMMGAASKGIIQRGFQHNATVYKAPYAKNPFDNVTDDELNEYKRTVERK
R1     501   ..........................................................................................................
R2     501

N4     601   KKSVHGEYTDTDFSESEAVLQAGTKKYPQSEPETEHQVIEIQTQQAPVPRQAEVVLSDALVSQLAQKYAFLYSPGQYMYACMKMAPLMQKVYVIHKVEPV
R1     601   ..................................................GENVQNGDHSEAHLSTFSQSSKEFQDVSTDGSPKKDKKKKKG

N4     701   SKHNYPPVNDGNMSIHHNESGAGFMAQESSVISSTPVRNALASVSLPEERNHSILGLSSTPYRTISHFGFNCPLITSPTILLHPEHRSIWQRVAEQREKV
R1     701   LRTPSFLKKKKEKKKAEA*

N4     801   VSFIDLTTLSLDNRKLLNVVTSTHPTQCQSQSQSFISEKHIQLEVTPPKRKQRVYSATISSGLDDSLDELDSLMSGLAINMPRSREQDSGLYRSYTFLPS

N4     901   NHALPKDTDANNRDQTDRERPEAEQEESFHCAGDSGIGDSTGRRPRLATTSNDSSIQEAEAYTQGKHVKLTLSSSPTPTATQSPATIEILINVSLRNAEC

N4    1001   VQTVQTHEQEFRAKLERVIDEEIHYISQQLAFKQRQAELHEQQTTSRAPIATPSFTTMHPPAPASSSSMVHRSNSAPELCHTYSYVAVCDLSTKQDQASP

N4    1101   QLPAEGEPLNDILSSLEKELERLLNSVVTAHMLHNKAIIHECRARFSQLADGIVSS*
```

Figure 4. Conservation of peptide sequence between *Drosophila* R1 Adducin-like and human adducin proteins. Residues that are boxed are identical between *Drosophila* R1 Adducin-like and one or more human adducins. Green: amino acid sequence conservation between R1 Adducin-like and all three human adducin proteins. Yellow: amino acid sequence conservation between R1 Adducin-like and one or two of the human adducins.

Figure 4. Conservation of peptide sequence between *Drosophila* R1 Adducin-like and human adducin proteins

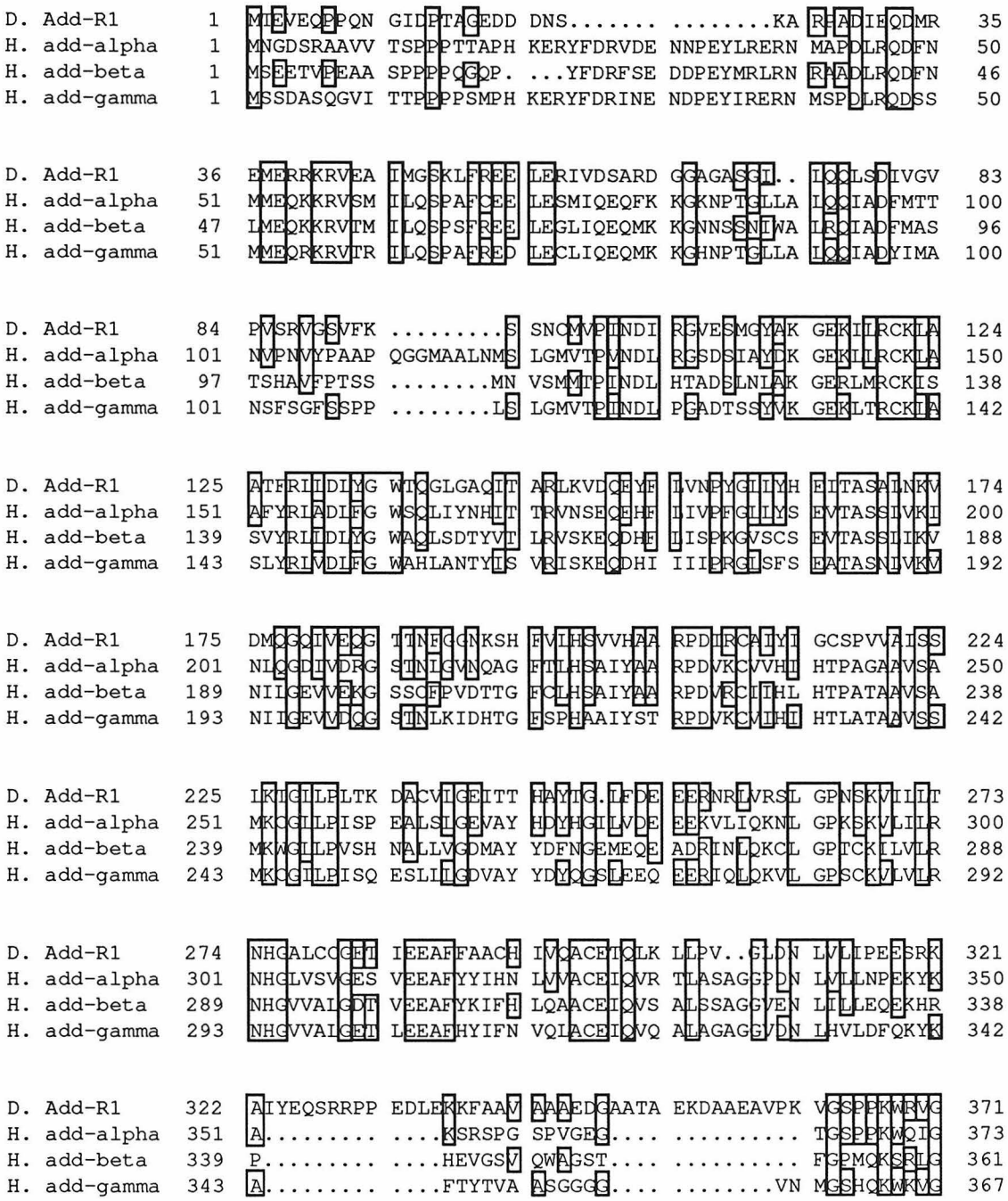

Figure 4, p. ii: Conservation of peptide sequence between *Drosophila* R1 Adducin-like and human adducin proteins

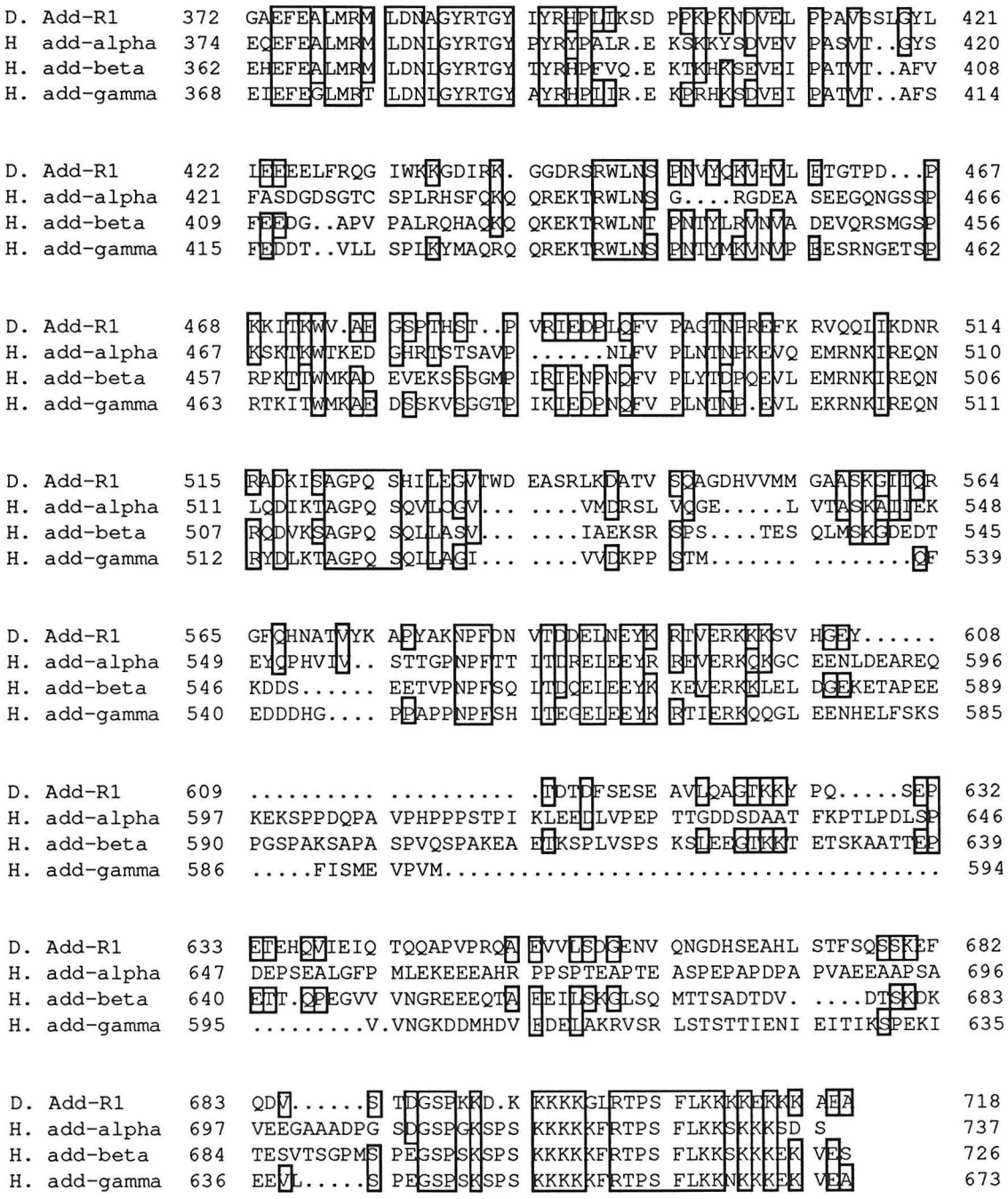

Figure 5A. Conservation of the major site for calmodulin binding and PKA and PKC phosphorylation in *Drosophila* and human adducin proteins. Amino acids conserved between any of the proteins are boxed. The serine residue which is the target for phosphorylation in the MARCKS-related sequence is shown in bold face and is also marked with an asterisk.

Figure 5B. Alternate alignments of the *Drosophila* and human adducins with the human MARCKS protein sequence. Amino acids conserved between *Drosophila* R1 Adducin-like, human adducins, and MARCKS are boxed. Serines known to be phosphorylated are shown in bold. The repeated sequence motifs of SFKK/L in the MARCKS protein are underlined.

Figure 5A. Conservation of the major site for calmodulin binding and PKA and PKC phosphorylation in *Drosophila* and human adducin proteins

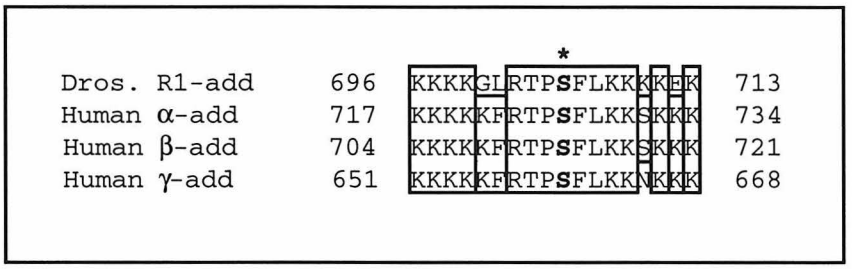

Figure 5B. Alternate alignments of the *Drosophila* and human adducins with the human MARCKS protein sequence

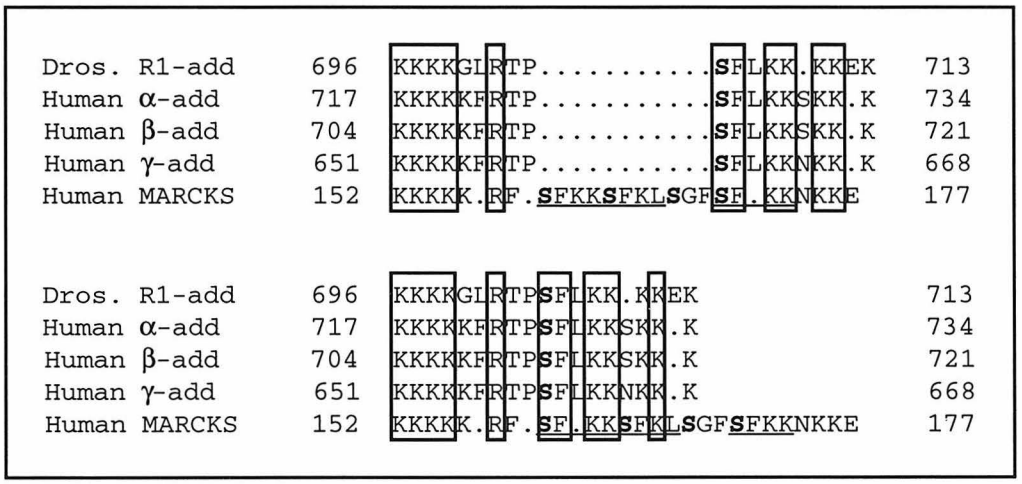

Figure 6. Possible conservation of a PKA-phosphorylated serine residue between *Drosophila* R1 and human α-adducin. Human α-adducin is phosphorylated by protein kinase A at the serine residue shown in bold type and marked by an asterisk. Note that human β-adducin is not phosphorylated at this serine residue or at the other serine residues immediately adjacent. It is not possible to determine from the sequence homology alone whether *Drosophila* R1 Adducin-like (or N4 Adducin-like, which has identical sequence in this region of the protein) is also likely to be phosphorylated at this serine residue. Residues which are identical between *Drosophila* R1 and human α-adducin are boxed together. Boxes around human β-adducin residues indicate identity with *Drosophila* R1 residues.

Figure 6. Possible conservation of a PKA-phosphorylated serine residue between *Drosophila* R1 and human α-adducin

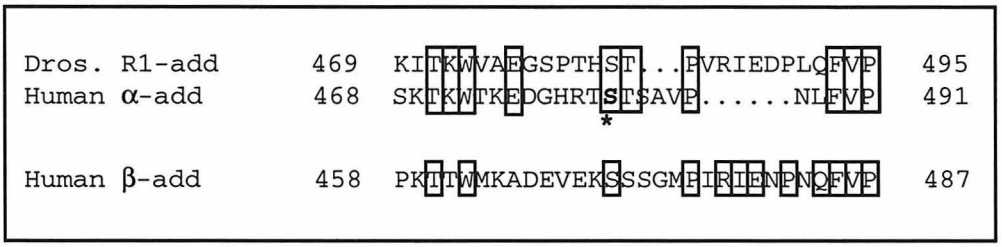

Figure 7. Localization patterns of endogenous transcripts with different 3'UTRs. *In situ* hybridization of DNA probes specific for each Adducin-like 3'UTR (N4, R1, R2/N32) to ovarioles from wild-type females. (A) During the early stages of oogenesis, transcripts with the N4 3'UTR are found in discrete locations within the germarium (most likely the presumptive oocyte). In young egg chambers, transcripts with the N4 3' UTR are found in the most posterior cell (the oocyte). (B) In a stage 8 egg chamber, transcripts with the N4 3'UTR are restricted to the oocyte cortex. Here the posterior of the oocyte is in a slightly different focal plane than the anterior, causing the localization pattern to be less visible at the posterior. (C) At stage 9 (center egg chamber) transcripts with the N4 3'UTR are restricted to the anterior cortex of the oocyte. (D) In stage 10 egg chambers, transcripts with the N4 3'UTR are strongly expressed in nurse cells and are restricted within the oocyte to the anterior cortex. (E) In stage 12-14 egg chambers, transcripts carrying the N4 3'UTR remain restricted to the anterior cortex of the oocyte. (F) Transcripts with the R1 3'UTR are first detectable within the germarium. In early egg chambers, these transcripts appear to be distributed over the entire egg chamber, as would be the case if they were expressed within the monolayer of follicle cells surrounding the egg chamber. (G) Low levels of transcripts with the R1 3'UTR are present in the follicle cells and thus appear to be distributed over the entire stage 8 egg chamber. (H) At stage 9, transcripts with the R1 3'UTR are present in the follicle cells. (I) Stage 10 egg chambers show high levels of transcripts with the R1 3'UTR in the follicle cells. The posterior of the oocyte is in a slightly different focal plane than the anterior; expression of R1 transcripts is present at the posterior though it is not as visible in this photograph. (J) Transcripts with R1 3'UTRs are present in the follicle cells of stage 12-14 oocytes. Here the ventral side of the oocyte is in a slightly different focal plane, but expression of R1 transcripts is present at the same levels in ventral follicle cells as in dorsal follicle cells. (K) Transcripts carrying R2 3'UTRs are present at low levels throughout the germarium and early egg chambers. (L) At stage 8, transcripts with R2 3'UTRs are found

only within the nurse cells. (M) In stage 9 egg chambers, R2 transcripts are found within the nurse cells. (N) At stage 10, R2 transcripts are found within the nurse cells. (O) In stage 12-14 egg chambers, following nurse cell dumping, transcripts with R2 3'UTRs are distributed throughout the oocyte. For all egg chambers shown, the orientation is such that the anterior of the oocyte is to the left and the dorsal side is up.

Figure 7. Localization patterns of endogenous transcripts with different 3'UTRs

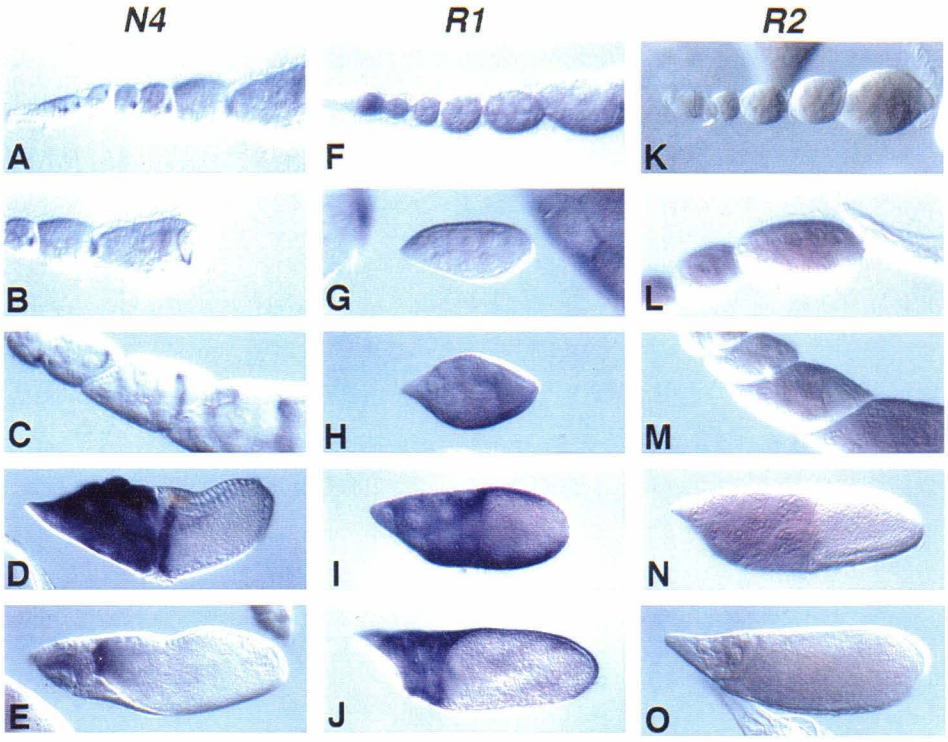

Figure 8. Comparison of localization patterns for endogenous *Adducin-like* N4 transcripts vs. pAdd3'UTR reporter transcripts. A-F, *in situ* hybridizations of DNA probe for the N4 coding region to ovarioles from w^{1118} females. G-L, *in situ* hybridizations of antisense *β-galactosidase* RNA probe to ovarioles from females homozygous for the pAdd3'UTR transgene. The pAdd3'UTR transgene produces reporter transcripts with the N4 *Adducin-like* 3'UTR. (A) *Adducin-like* transcripts are found at discrete locations within the germarium, and in the posteriormost cell (the oocyte) of early egg chambers. (B) At stage 8, *Adducin-like* transcripts are restricted to the oocyte cortex. (C) In stage 9 egg chambers, *Adducin-like* transcripts are localized to the anterior cortex of the oocyte. (D) At stage 10, the nurse cells show strong expression of *Adducin-like* transcripts. Within the oocyte, *Adducin-like* mRNA is confined to the anterior cortex. (E) In stage 10b-11 egg chambers, *Adducin-like* transcripts remain at the anterior. (F) Stage 12-14 egg chambers show *Adducin-like* transcripts distributed within the remainders of the nurse cells, and localized to the anterior of the oocyte. (G) In early egg chambers, reporter transcripts containing the N4 3'UTR are found only in the oocyte. The germarium is not shown here. (H) At stage 8, pAdd3'UTR reporter transcripts are found in the oocyte's cortex. (I) Stage 9 egg chambers show reporter transcripts restricted to the anterior of the oocyte. (J) At stage 10, reporter transcripts remain at the anterior of the oocyte and are also detectable in the nurse cells. (K) Reporter transcripts are found at the anterior of the stage 10b-11 oocyte and within the nurse cells. (L) In stage 12-14 egg chambers, reporter transcripts are found within the remnants of the nurse cells and restricted to the anterior of the oocyte. Anterior is to the left and dorsal is up, for all egg chambers.

Figure 8. Comparison of localization patterns for endogenous *Adducin-like* N4 transcripts vs. pAdd3UTR reporter transcripts

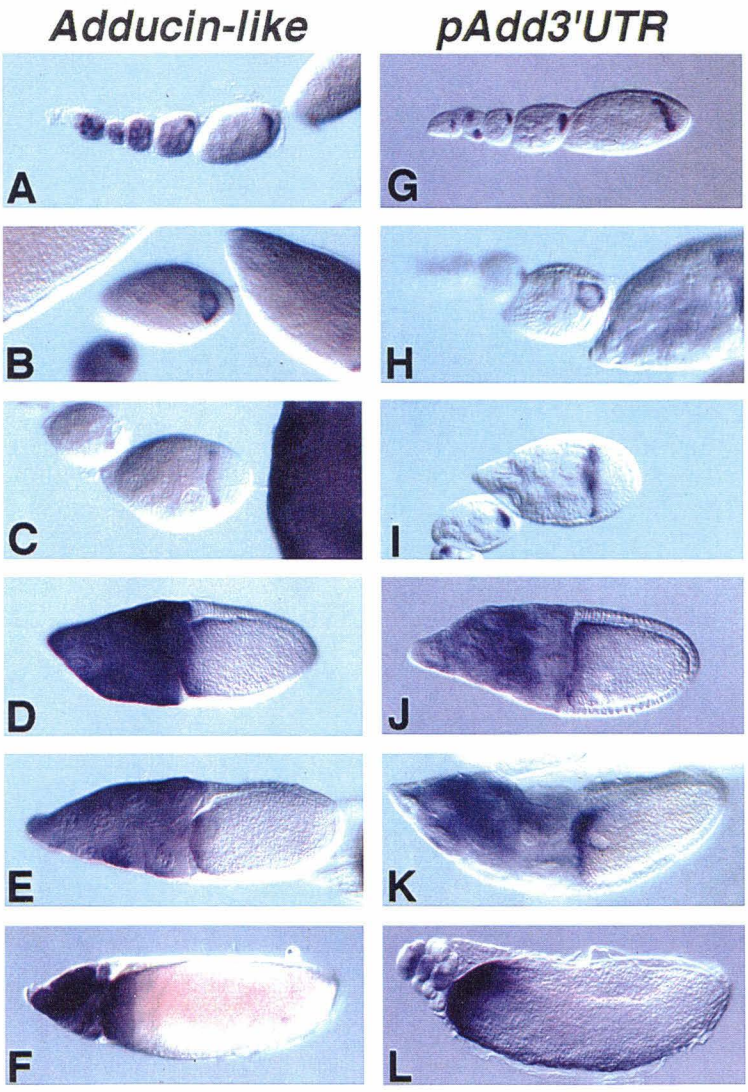

Figure 9. Schematic diagram of the pAdd3'UTR construct used for germline transformation. The 5' and 3' P-element ends are shown in solid black. The *hsp26* enhancer sequences are shown as a light gray dotted region. The *Sgs-3* enhancer and promoter are depicted by dark black stripes on a gray background, while the *lacZ* tag is shown as black stripes on a white background and the N4 3'UTR sequence is represented by white stripes on a black background. pUC sequences are shown as white, on the left of the plasmid, and sequences from the *white* gene are shown on the right of the plasmid. Restriction sites marking the boundaries between various elements are also shown.

Figure 9. Schematic diagram of the pAdd3'UTR construct used for germline transformation.

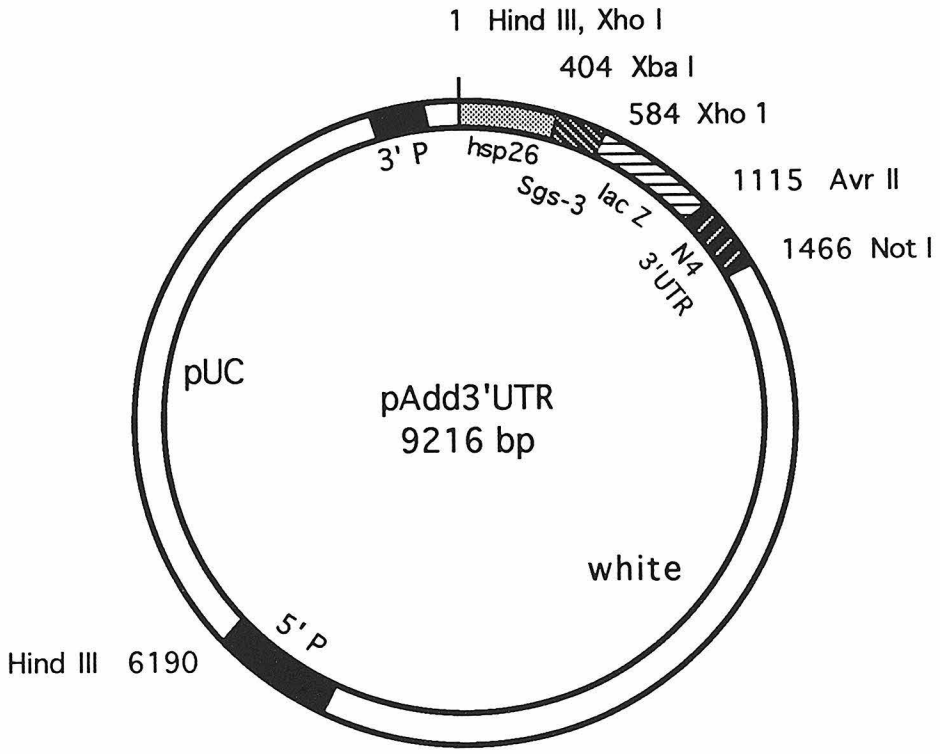

Figure 10. Localization of pAddtag3'UTR and pORFtagtub reporter transcripts. *In situ* hybridizations of antisense *β-galactosidase* RNA probes to ovarioles from transgenic females. A-E, egg chambers from females homozygous for the pAddtag3'UTR transgene. F-J, egg chambers from females homozygous for the pORFtagtub transgene. (A) pAddtag3'UTR reporter transcripts are found in discrete regions within the germarium and in the oocyte of early egg chambers. (B) At stage 7, pAddtag3'UTR reporter transcripts are restricted to the oocyte cortex. (C) In a stage 9 egg chamber, pAddtag3'UTR reporter transcripts are localized to the anterior cortex of the oocyte. (D) At stage 10, pAddtag3'UTR reporter transcripts are found in the nurse cells and at the anterior of the oocyte. (E) In a stage 12 egg chamber, pAddtag3'UTR reporter transcripts are maintained at the anterior of the oocyte. (F) No localization of pORFtagtub reporter transcripts is visible within the germarium or in early egg chambers. (G) pORFtagtub reporter transcripts are not detectable in a stage 8 egg chamber (middle of photograph). (H) pORFtagtub reporter transcripts are not localized at stage 9. (I) Strong expression of pORFtagtub reporter mRNA is detectable within the nurse cells at stage 10. (J) Expression of pORFtagtub reporter transcripts is detectable within the remnants of the nurse cells at stage 12, but no localization is present within the oocyte. For all egg chambers, anterior is to the left and dorsal is up.

Figure 10. Localization of pAddtag3'UTR and pORFtagtub reporter transcripts

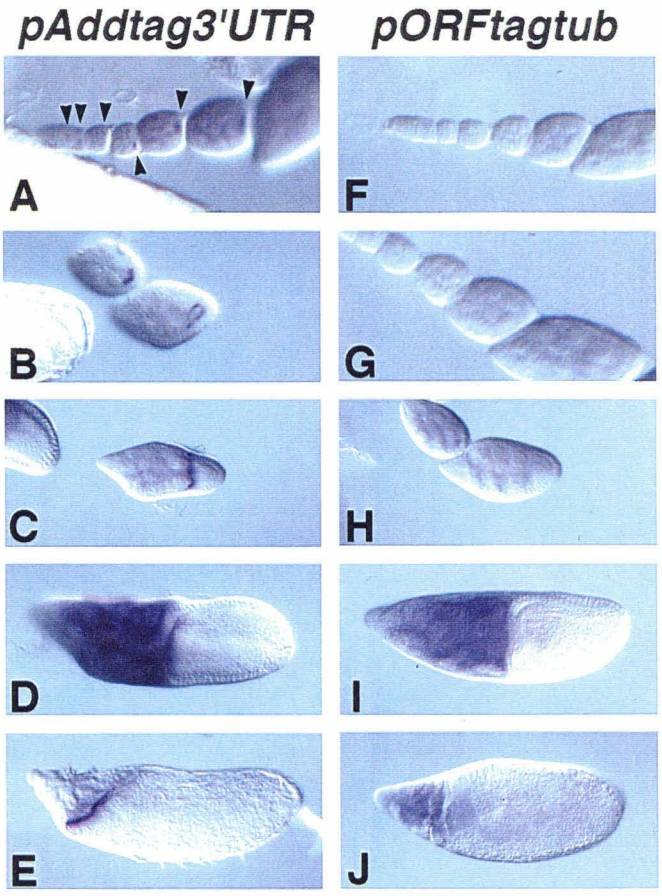

Figure 11. Schematic of reporter transcripts carrying mutated N4 3'UTRs. (A) Structure of reporter transcripts containing either 5' deletions or internal deletions. Light gray represents the *hsp26* enhancers; black stripes on gray background show the location of the *Sgs-3* enhancer/promoter; the white box represents the *lacZ* tag; and solid black shows the 3'UTR region of the transcript derived from *Adducin-like* N4. The transcription start site and direction are marked by an arrow. (B) Structure of reporter transcripts containing 3' deletions. All shading representations are the same as in (A), with the addition of a black-and-white striped box to represent the *α-tubulin* 3'UTR. The *tubulin* 3'UTR provides transcription termination and polyadenylation signals. (C) Summary of the deleted versions of the N4 3'UTR used in reporter transcripts. The scale on the top shows the ribonucleotide position within the N4 transcript 3'UTR, with 1 corresponding to the first nucleotide of the stop codon. The scale on the bottom shows the base position within the N4 cDNA clone.

Figure 11. Schematic of reporter transcripts carrying mutated N4 3'UTRs

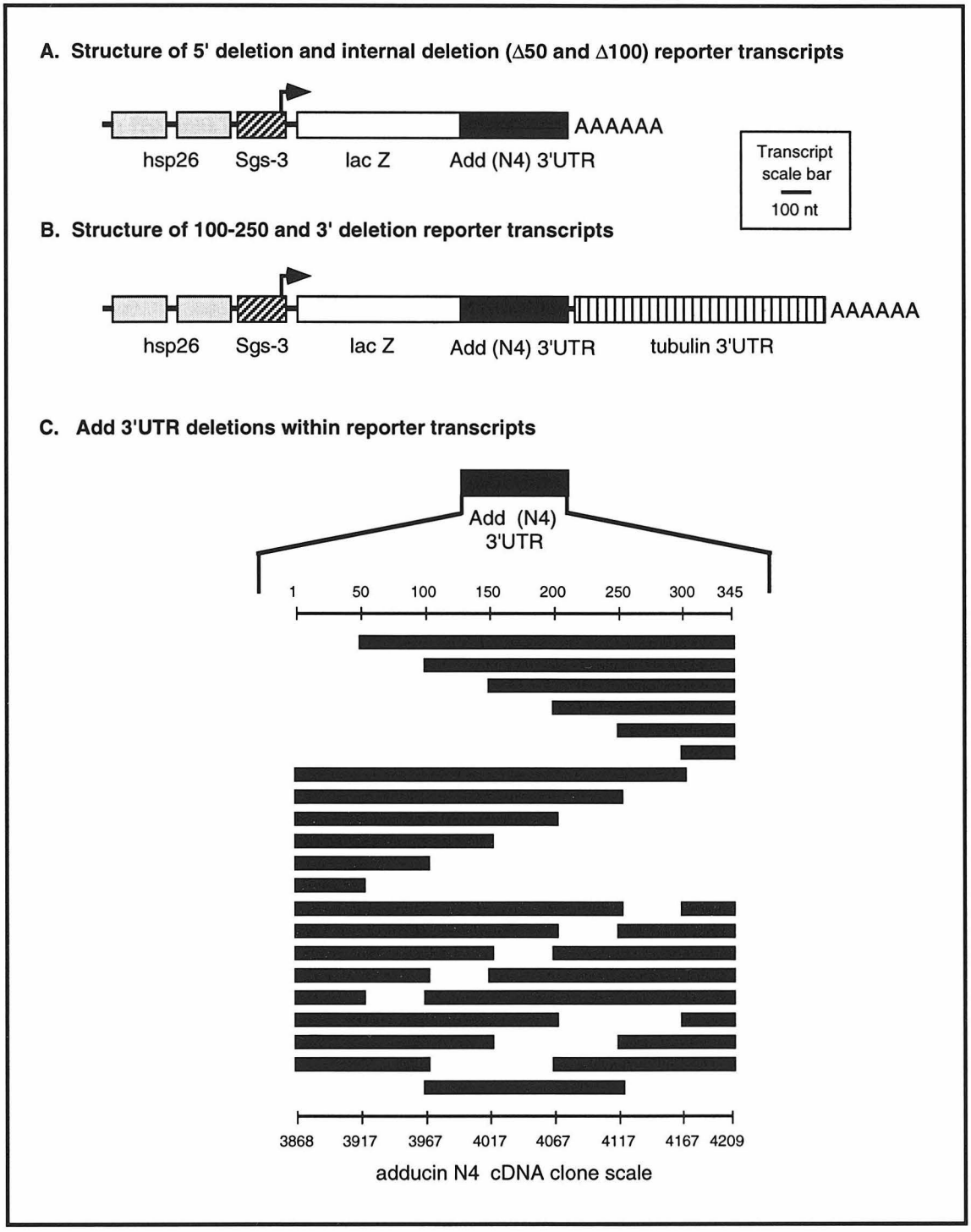

Figure 12. Early transport to the oocyte of reporter transcripts from pAdd3'UTR deletion transgenes. *In situ* hybridizations using an antisense *β-galactosidase* RNA probe on ovaries from transgenic females. See Figure 12 key, on the following page, for a complete summary. The germarial region and early egg chambers are shown from fly lines carrying each transgene. Arrowheads indicate localization. The position of the *cis*-acting localization element ALE1 (nucleotides 150-250 within the N4 3'UTR) is shown underneath the schematic summary.

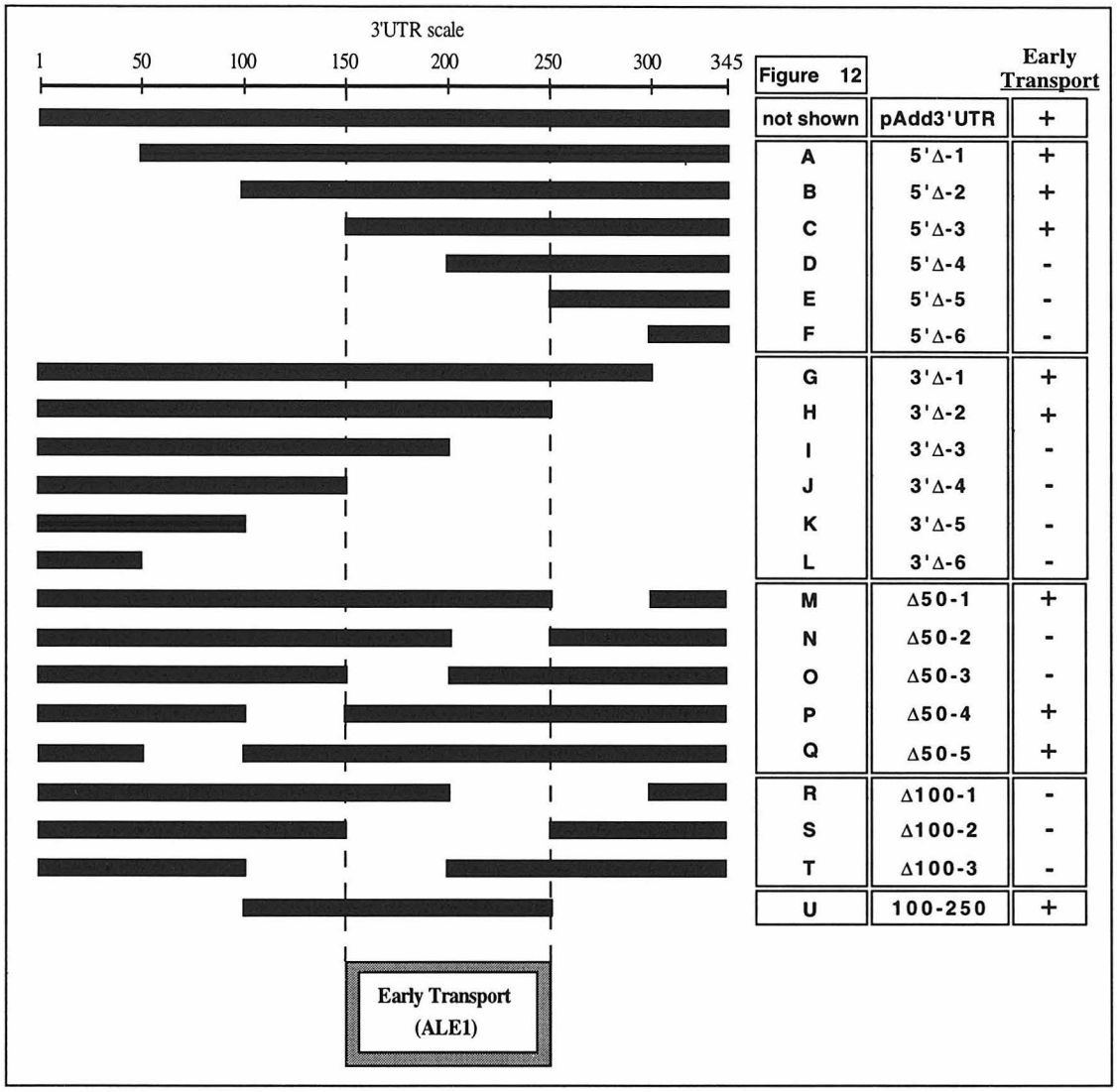

Figure 12		Early Transport
not shown	pAdd3'UTR	+
A	5'Δ-1	+
B	5'Δ-2	+
C	5'Δ-3	+
D	5'Δ-4	-
E	5'Δ-5	-
F	5'Δ-6	-
G	3'Δ-1	+
H	3'Δ-2	+
I	3'Δ-3	-
J	3'Δ-4	-
K	3'Δ-5	-
L	3'Δ-6	-
M	Δ50-1	+
N	Δ50-2	-
O	Δ50-3	-
P	Δ50-4	+
Q	Δ50-5	+
R	Δ100-1	-
S	Δ100-2	-
T	Δ100-3	-
U	100-250	+

Figure 12. Early transport to the oocyte of reporter transcripts from pAdd3'UTR deletion transgenes

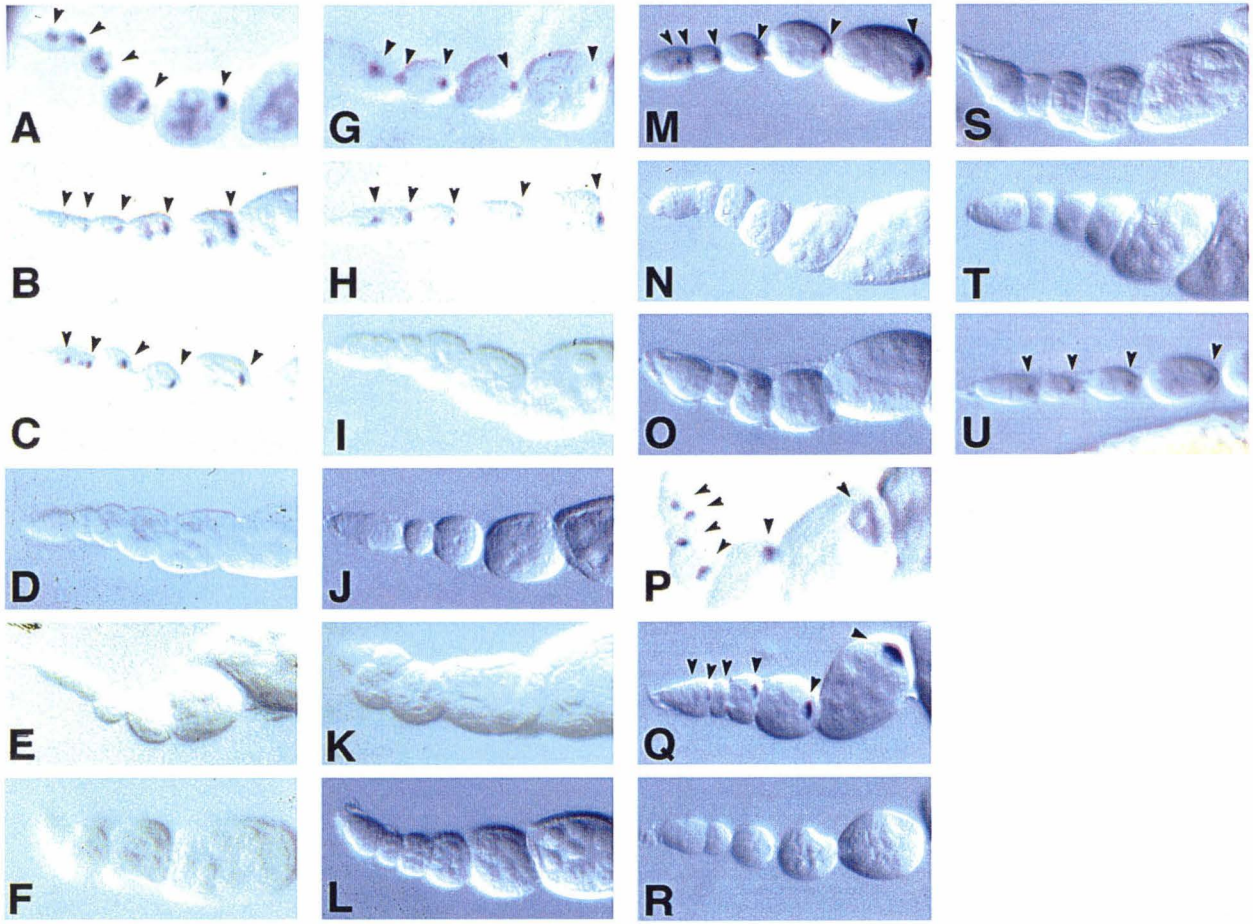

Figure 13. Localization of reporter transcripts from pAdd3'UTR deletion transgenes to the oocyte cortex at stage 8. *In situ* hybridizations using an antisense *β-galactosidase* RNA probe on ovaries from transgenic females. See Figure 13 key, on the following page, for a complete summary. Stage 8 egg chambers are shown from transgenic fly lines that were successful in early transport of reporter RNA. The position of the *cis*-acting localization element ALE1 is shown underneath the schematic summary.

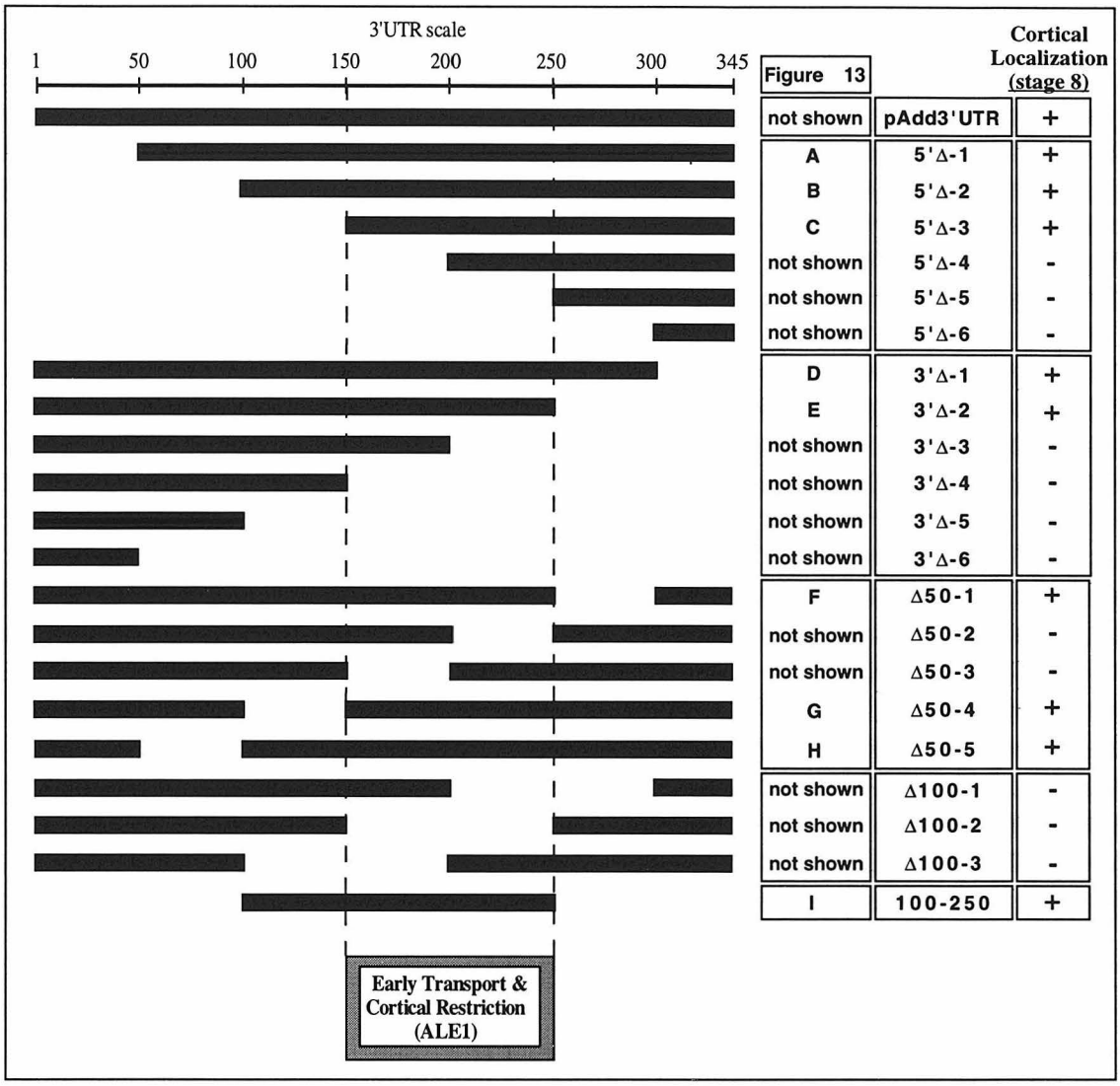

Figure 13		Cortical Localization (stage 8)
not shown	pAdd3'UTR	+
A	5'Δ-1	+
B	5'Δ-2	+
C	5'Δ-3	+
not shown	5'Δ-4	-
not shown	5'Δ-5	-
not shown	5'Δ-6	-
D	3'Δ-1	+
E	3'Δ-2	+
not shown	3'Δ-3	-
not shown	3'Δ-4	-
not shown	3'Δ-5	-
not shown	3'Δ-6	-
F	Δ50-1	+
not shown	Δ50-2	-
not shown	Δ50-3	-
G	Δ50-4	+
H	Δ50-5	+
not shown	Δ100-1	-
not shown	Δ100-2	-
not shown	Δ100-3	-
I	100-250	+

Figure 13. Localization of reporter transcripts from pAdd3'UTR deletion transgenes to the oocyte cortex at stage 8

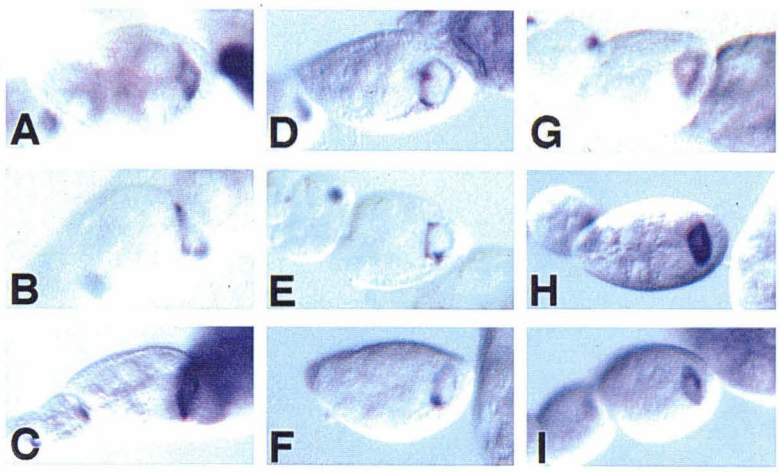

Figure 14. Localization of reporter transcripts from pAdd3'UTR deletion transgenes to the anterior cortex of the oocyte at stage 9-10a. *In situ* hybridizations using an antisense *β-galactosidase* RNA probe on ovaries from transgenic females. See Figure 14 key, on the following page, for a complete summary. Stage 9-10a egg chambers from transgenic fly lines that were successful in early transport of reporter RNA are shown. The positions of ALE1 and other *cis*-acting localization elements acting at stage 9-10a are shown underneath the schematic summary.

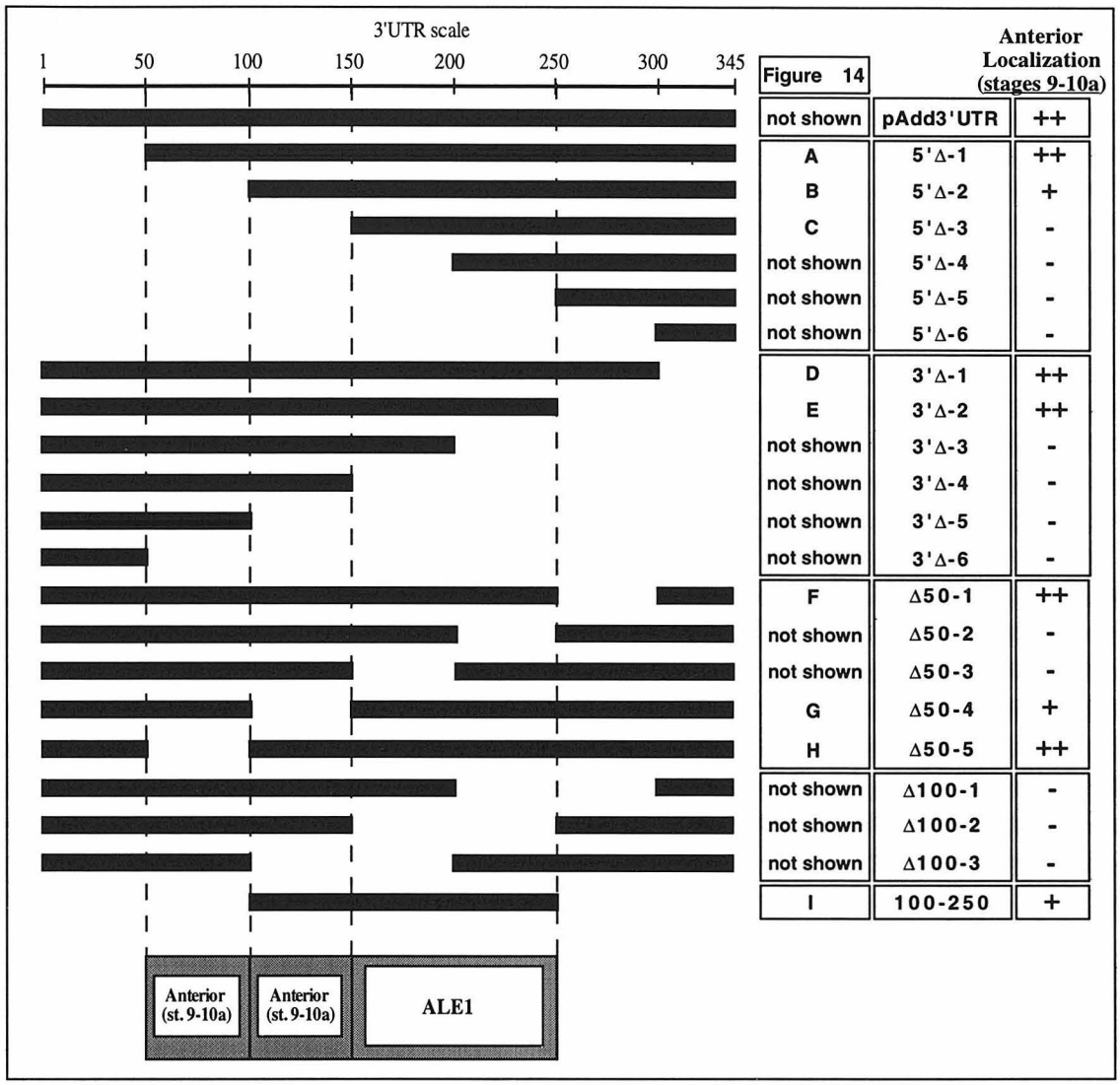

Figure 14		Anterior Localization (stages 9-10a)
not shown	pAdd3'UTR	++
A	5'Δ-1	++
B	5'Δ-2	+
C	5'Δ-3	-
not shown	5'Δ-4	-
not shown	5'Δ-5	-
not shown	5'Δ-6	-
D	3'Δ-1	++
E	3'Δ-2	++
not shown	3'Δ-3	-
not shown	3'Δ-4	-
not shown	3'Δ-5	-
not shown	3'Δ-6	-
F	Δ50-1	++
not shown	Δ50-2	-
not shown	Δ50-3	-
G	Δ50-4	+
H	Δ50-5	++
not shown	Δ100-1	-
not shown	Δ100-2	-
not shown	Δ100-3	-
I	100-250	+

Figure 14. Localization of reporter transcripts from pAdd3'UTR deletion transgenes to the oocyte cortex at stage 9-10a

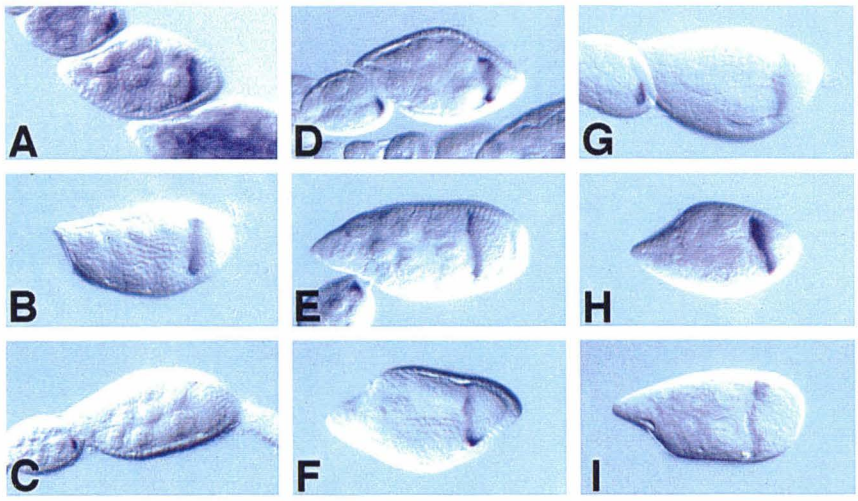

Figure 15. Localization of reporter transcripts from pAdd3'UTR deletion transgenes to the anterior cortex of the oocyte at stage 10b-11. *In situ* hybridizations using an antisense *β-galactosidase* RNA probe on ovaries from transgenic females. See Figure 15 key, on the following page, for a complete summary. Stage 10b-11 egg chambers from transgenic fly lines that were successful in early transport of reporter RNA are shown. The positions of ALE1 and other *cis*-acting localization elements acting at stage 10b-11 are shown underneath the schematic summary.

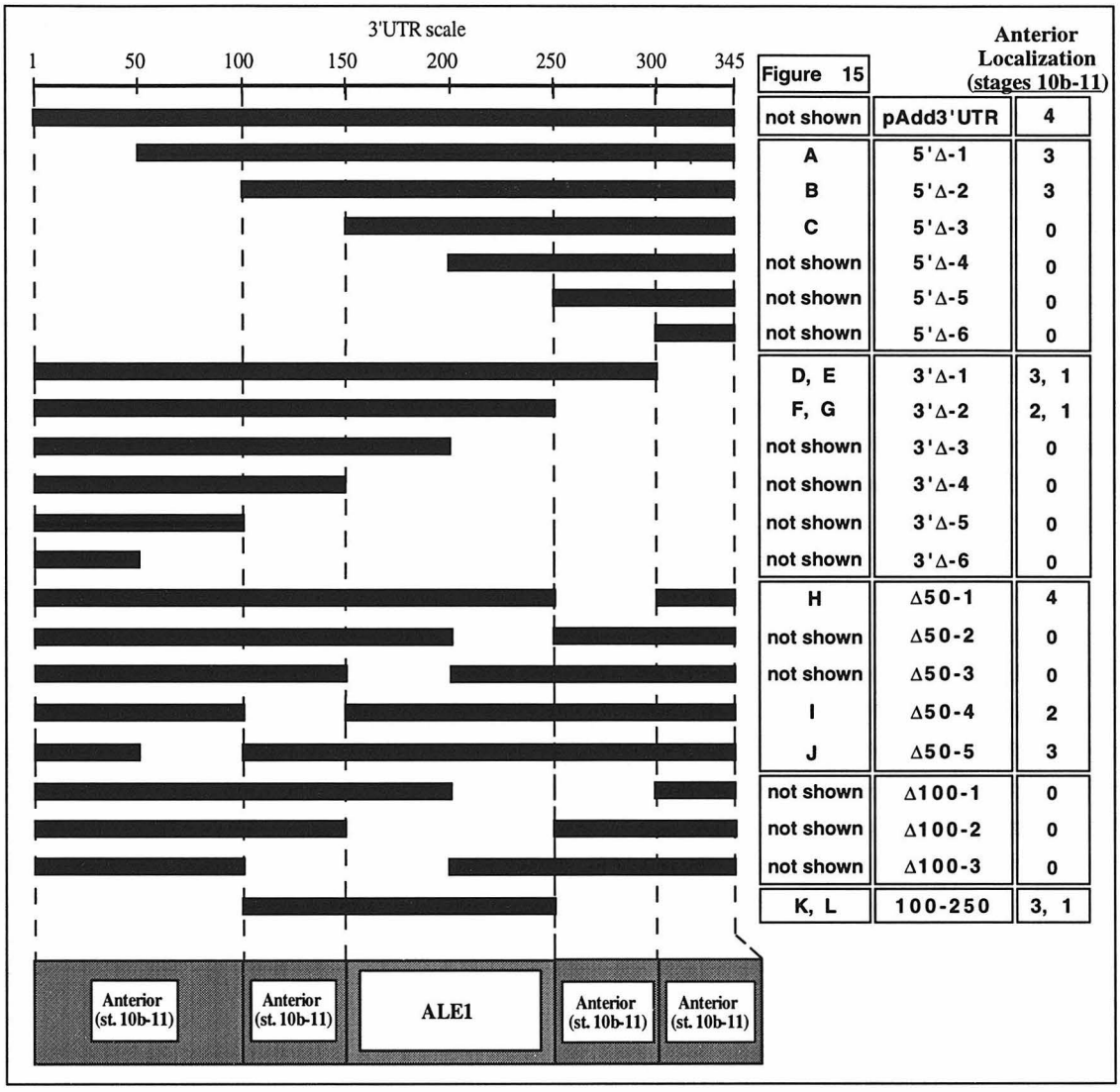

Figure 15		Anterior Localization (stages 10b-11)
not shown	pAdd3'UTR	4
A	5'Δ-1	3
B	5'Δ-2	3
C	5'Δ-3	0
not shown	5'Δ-4	0
not shown	5'Δ-5	0
not shown	5'Δ-6	0
D, E	3'Δ-1	3, 1
F, G	3'Δ-2	2, 1
not shown	3'Δ-3	0
not shown	3'Δ-4	0
not shown	3'Δ-5	0
not shown	3'Δ-6	0
H	Δ50-1	4
not shown	Δ50-2	0
not shown	Δ50-3	0
I	Δ50-4	2
J	Δ50-5	3
not shown	Δ100-1	0
not shown	Δ100-2	0
not shown	Δ100-3	0
K, L	100-250	3, 1

4= normal anterior localization
3= anterior + delocalization
2= weak anterior localization
1= anterior + ectopic localization
0= delocalized

Figure 15. Localization of reporter transcripts from pAdd3'UTR deletion transgenes to the oocyte cortex at stage 10b-11

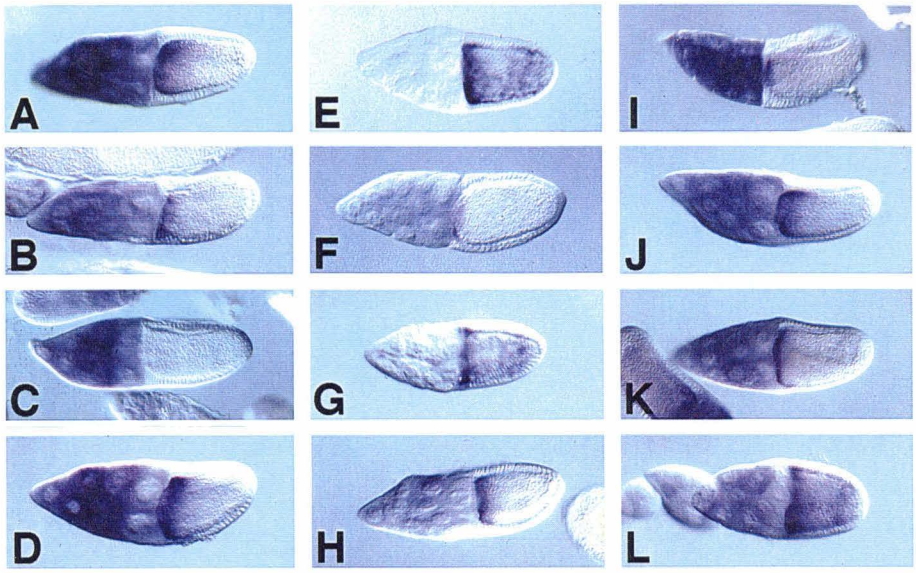

Figure 16. Localization of reporter transcripts from pAdd3'UTR deletion transgenes to the anterior cortex of the oocyte at stage 12-14. *In situ* hybridizations using an antisense *β-galactosidase* RNA probe on ovaries from transgenic females. See Figure 16 key, on the following page, for a complete summary. Stage 12-14 egg chambers from selected transgenic fly lines that were successful in early transport of reporter RNA are shown. The positions of ALE1 and other *cis*-acting localization elements acting at stage 12-14 are shown underneath the schematic summary.

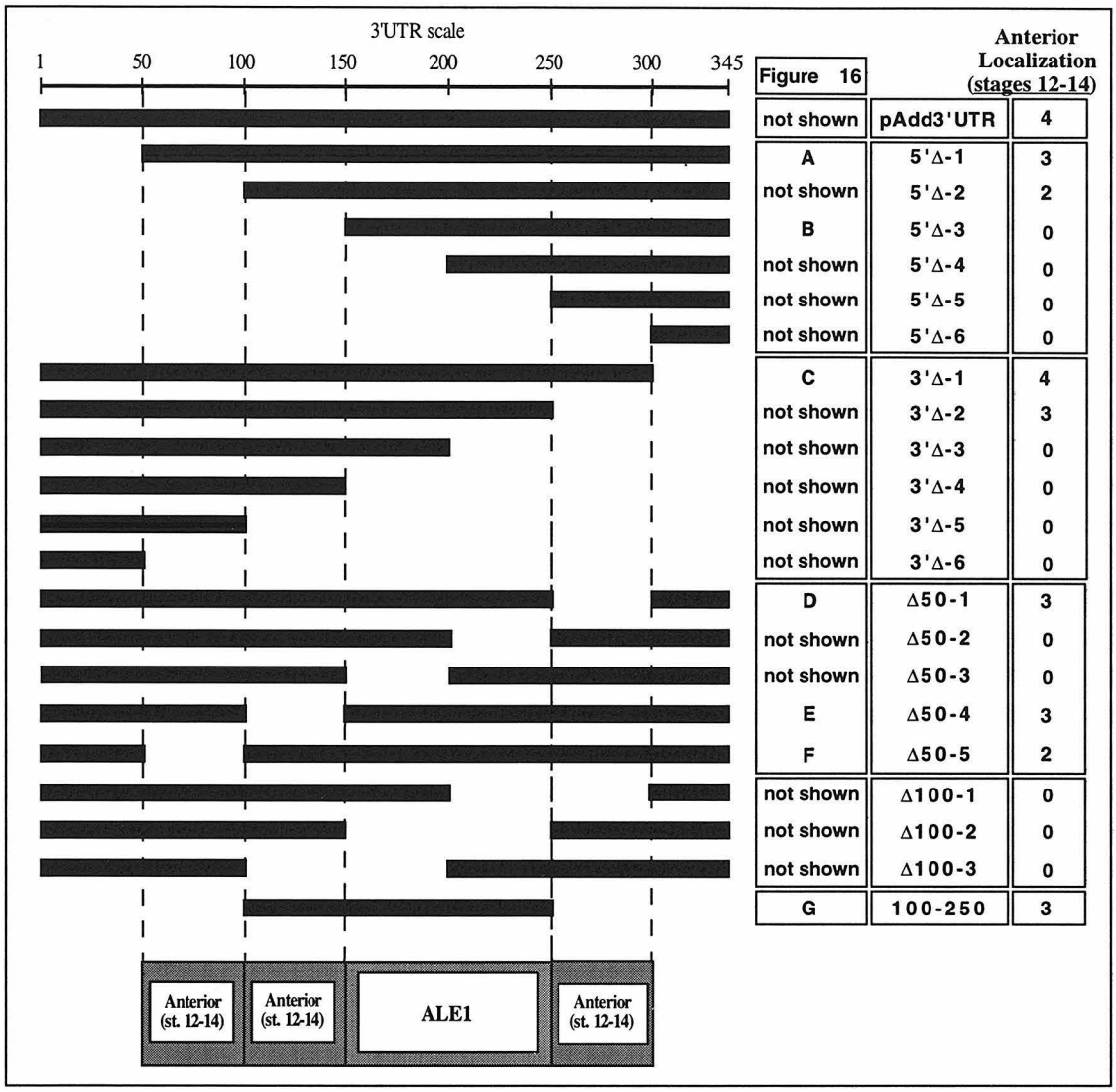

Figure 16		Anterior Localization (stages 12-14)
not shown	pAdd3'UTR	4
A	5'Δ-1	3
not shown	5'Δ-2	2
B	5'Δ-3	0
not shown	5'Δ-4	0
not shown	5'Δ-5	0
not shown	5'Δ-6	0
C	3'Δ-1	4
not shown	3'Δ-2	3
not shown	3'Δ-3	0
not shown	3'Δ-4	0
not shown	3'Δ-5	0
not shown	3'Δ-6	0
D	Δ50-1	3
not shown	Δ50-2	0
not shown	Δ50-3	0
E	Δ50-4	3
F	Δ50-5	2
not shown	Δ100-1	0
not shown	Δ100-2	0
not shown	Δ100-3	0
G	100-250	3

4= normal anterior localization
3= anterior + delocalization
2= weak anterior localization
1= anterior + ectopic localization
0= delocalized

Figure 16. Localization of reporter transcripts from pAdd3'UTR deletion transgenes to the oocyte cortex at stage 12-14

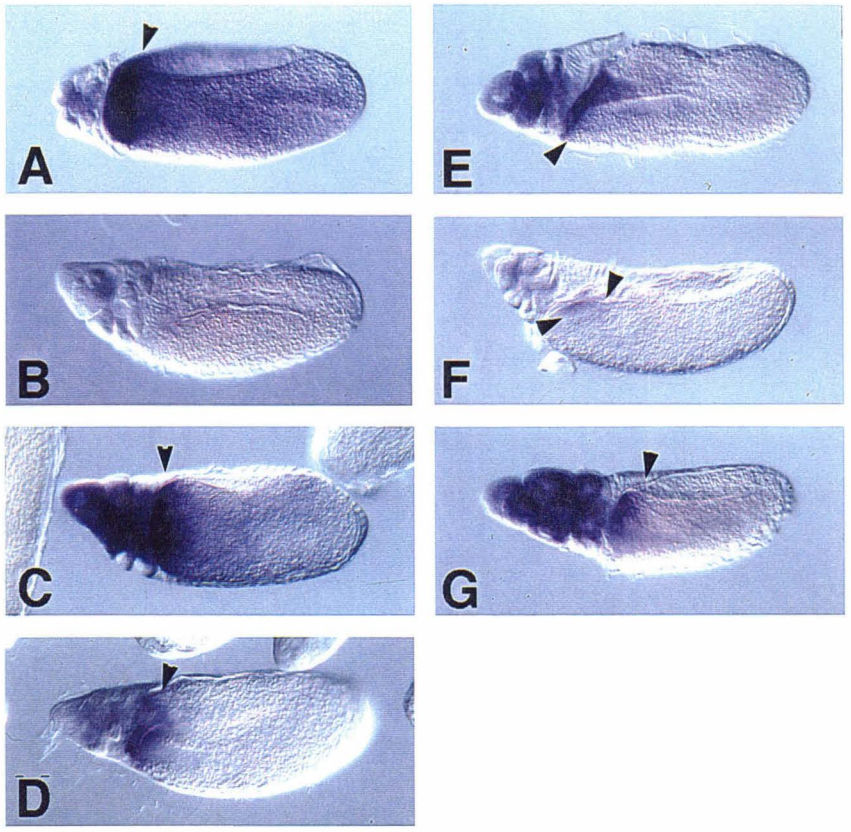

Figure 17. Summary of *in situ* hybridization results for N4 3'UTR deletion transgenes. Key to coding: T=transport from nurse cells into oocyte; C=localization to cortex of oocyte; A=localization to anterior cortex of oocyte. ++=process of transport or localization occurs normally; +=process is mostly normal but some delocalization of reporter mRNA occurs, or signal is weak, +*=process is more significantly impaired; ectopic localization or more delocalization of reporter RNA occurs; -=process does not occur. Since nonspecific nurse cell dumping of RNAs (and other macromolecules and organelles) occurs at stage 10b-11, the coding for stage 10b-11 is only A++, A+, A+*, or A-, and not T+ or T-. This shift in coding reflects the fact that reporter RNA is definitely present in the oocyte due to bulk transport, but anterior localization may or may not occur.

Figure 17. Summary of in situ hybridization results for N4 3'UTR deletion transgenes

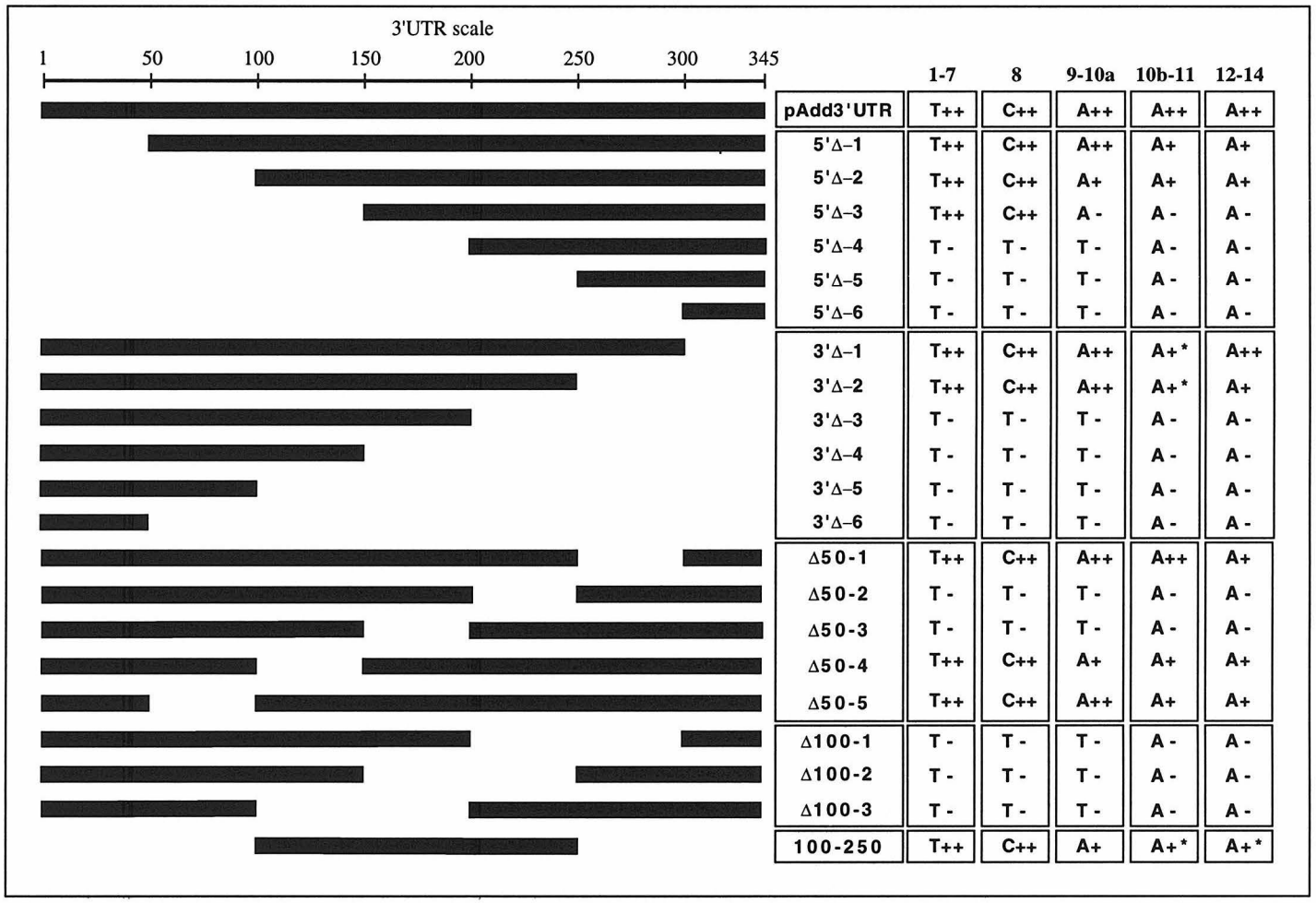

	1-7	8	9-10a	10b-11	12-14
pAdd3'UTR	T++	C++	A++	A++	A++
5'Δ–1	T++	C++	A++	A+	A+
5'Δ–2	T++	C++	A+	A+	A+
5'Δ–3	T++	C++	A -	A -	A -
5'Δ–4	T -	T -	T -	A -	A -
5'Δ–5	T -	T -	T -	A -	A -
5'Δ–6	T -	T -	T -	A -	A -
3'Δ–1	T++	C++	A++	A+*	A++
3'Δ–2	T++	C++	A++	A+*	A+
3'Δ–3	T -	T -	T -	A -	A -
3'Δ–4	T -	T -	T -	A -	A -
3'Δ–5	T -	T -	T -	A -	A -
3'Δ–6	T -	T -	T -	A -	A -
Δ50-1	T++	C++	A++	A++	A+
Δ50-2	T -	T -	T -	A -	A -
Δ50-3	T -	T -	T -	A -	A -
Δ50-4	T++	C++	A+	A+	A+
Δ50-5	T++	C++	A++	A+	A+
Δ100-1	T -	T -	T -	A -	A -
Δ100-2	T -	T -	T -	A -	A -
Δ100-3	T -	T -	T -	A -	A -
100-250	T++	C++	A+	A+*	A+*

KEY: T = transport from nurse cells into oocyte
C = localization in cortex of oocyte
A = localization to anterior pole of oocyte

++ = process normal
+ = normal, but some delocalization, or signal is weak
+* = normal, but some delocalization and/or ectopic localization
- = process does not occur

Figure 18. Summary of localization elements within the N4 3'UTR. Different elements affect the N4 mRNA localization pathway at different stages. For each phase of localization of N4 mRNA, regions which are necessary (as defined by deletion analysis) for wild-type N4 transcript localization are shown in solid black. Regions that are sufficient to direct localization of a heterologous reporter mRNA in a wild-type N4 localization pattern are depicted in solid gray. Those regions which are only partly sufficient to direct wild-type localization of a heterologous reporter transcript are shown as striped boxes. For early transport and cortical localization through stage 8, the 100-250 region is sufficient, but only the 150-250 region is necessary. At stages 9-10a, the 100-250 region is partly sufficient to direct anterior localization, and the 50-250 region is necessary. In late oogenesis (stages 10b-14), the 100-250 region is still only partly sufficient to direct and maintain anterior localization, and the entire 3'UTR contains necessary sequences.

Figure 18. Summary of localization elements within the N4 3'UTR

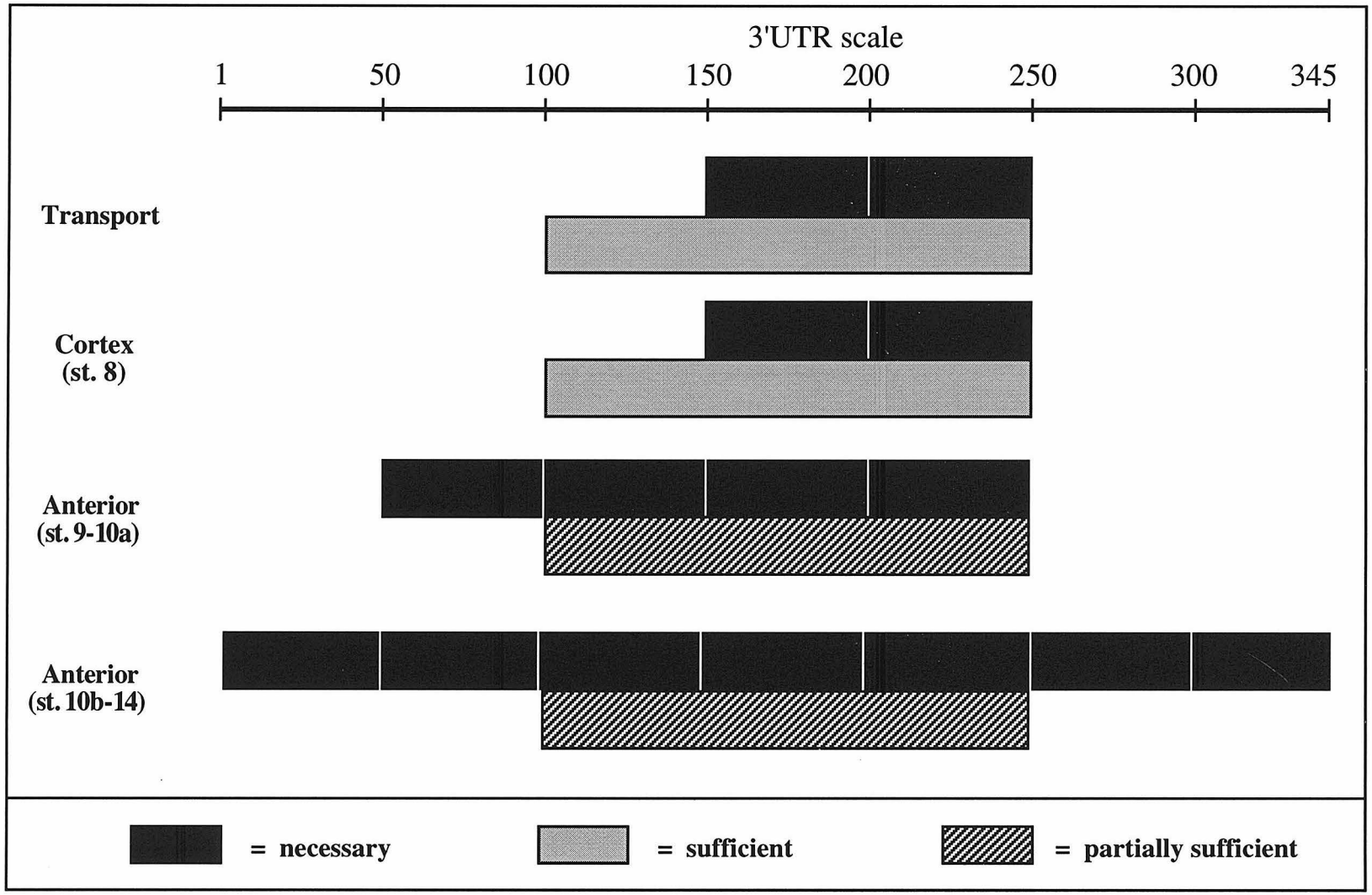

Figure 19. Predicted secondary structure of the N4 transcript 3'UTR. The five loops within the predicted stem-loop structure are designated by Roman numerals I-V. Positions corresponding to the 50-nt increments used in making deletion constructs are noted. The start and end of the ALE1 sequence (nt 150-250) are indicated by arrows.

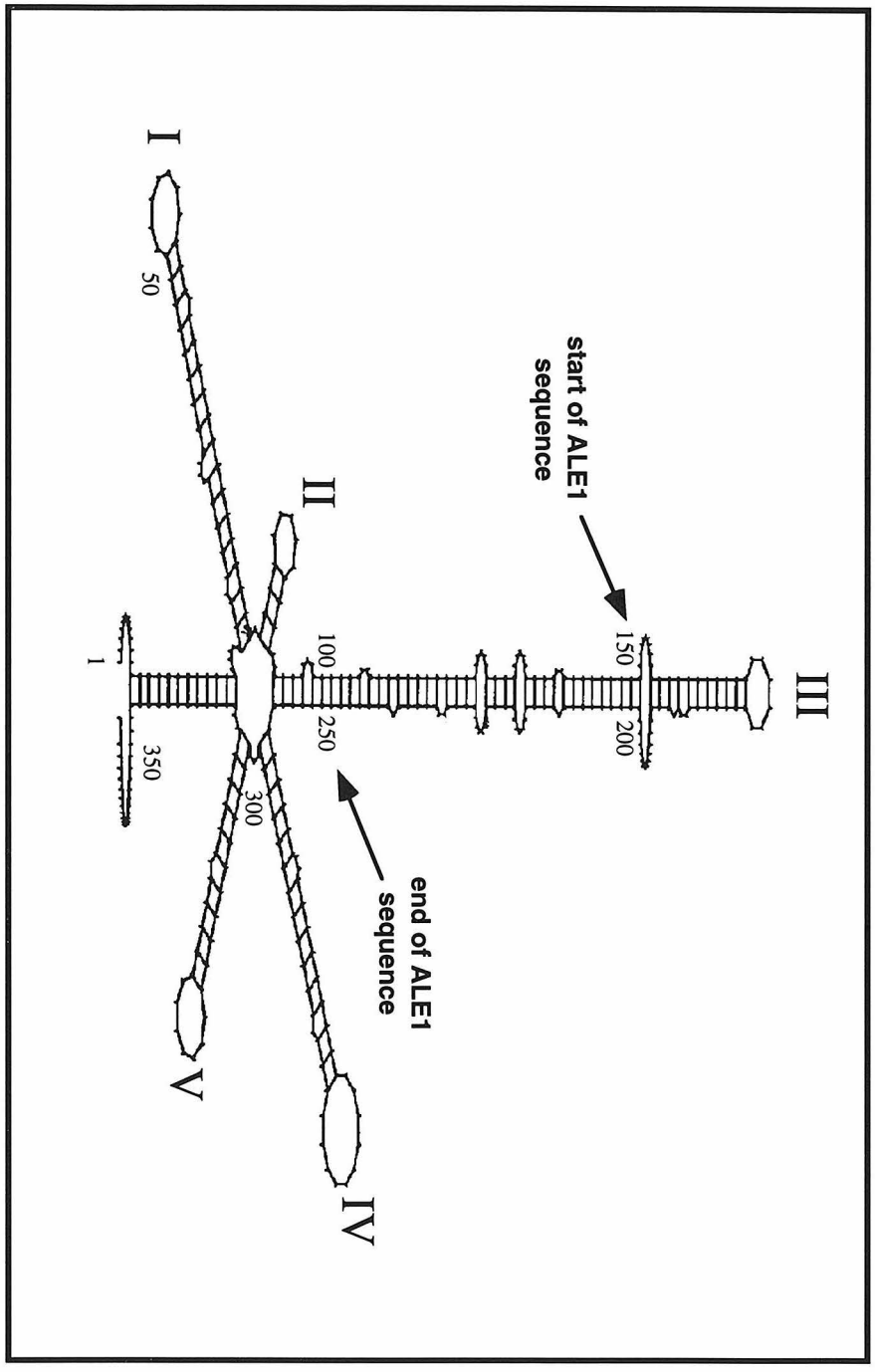

Figure 19. Predicted secondary structure of the N4 transcript 3'UTR

Figure 20. RT-PCR of total RNA from selected transgenic females. (A) Agarose gel electrophoresis of RT-PCR products from total RNA prepared from transgenic females, using primers designed to amplify reporter sequence between the 5' end of the lacZ tag and the 3' end of the N4 3'UTR. Four different transgenic lines were examined, which were expected to express reporter transcripts containing either the full-length N4 3'UTR or specific deletions of the N4 3'UTR. Marker sizes are shown on the left side of the gel, and RT-PCR product sizes (874, 774, 674, and 574 base pairs) on the right side. Lanes: M=molecular weight marker, 1= pAdd3'UTR transgene, 2= 5'Δ-2 transgene, 3= 5'Δ-4 transgene, 4= 5'Δ-6 transgene. In each numbered lane there is a single band present of the expected size. (B) Schematic showing the different regions of the N4 3'UTR present in each transgene, and noting whether the specific transgenes examined are able to generate RT-PCR products as well as early transport of reporter RNA into the oocyte. In all cases, RT-PCR products of the expected sizes were detected, regardless of whether early transport occurred. Thus the detection of early transport, for at least these specific trangenes and probably also for the others, depends on whether the reporter RNA is successfully targeted to the oocyte by *cis*-acting signals, and not on whether the RNA is stable or unstable.

Figure 20. RT-PCR of total RNA from selected transgenic females

A

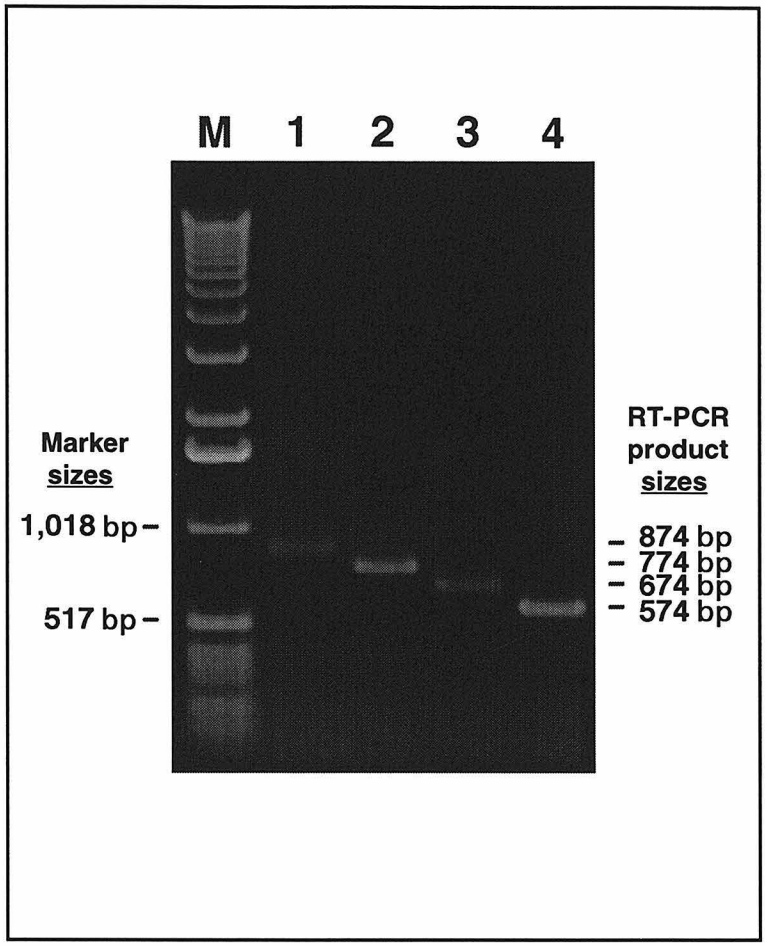

B

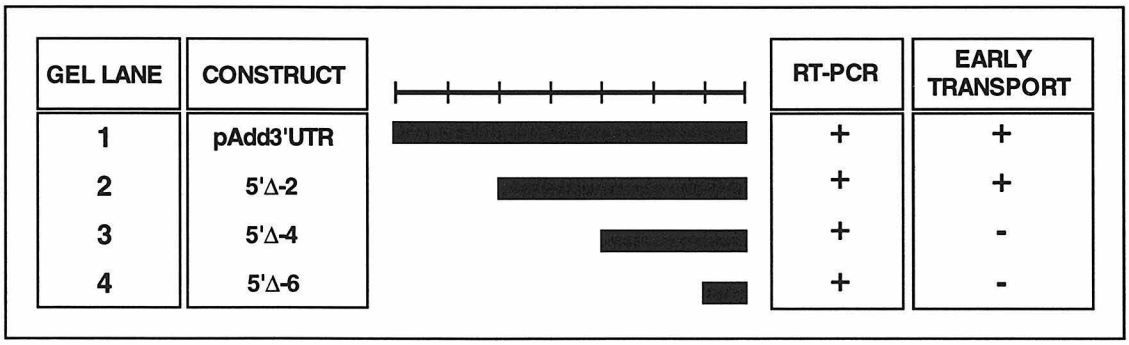

GEL LANE	CONSTRUCT	RT-PCR	EARLY TRANSPORT
1	pAdd3'UTR	+	+
2	5'Δ-2	+	+
3	5'Δ-4	+	-
4	5'Δ-6	+	-

Figure 21. Localization of reporter transcripts containing the full-length N4 3'UTR in *swallow* (*sww*) ovaries. *In situ* hybridizations of antisense *β-galactosidase* RNA probe to ovaries from females homozygous for the pAdd3'UTR transgene, and either homozygous for w^{1118}, or homozygous for sww^{1}, or heterozygous for sww^{1} and sww^{6}. A-G, reporter transcript localization is normal at all stages in an essentially wild-type background. H-N, reporter transcript localization is normal in a sww^{1} mutant background until late stage 9 (panel J), when localization to the anterior is not quite as tight as normal. At stage 10b (panel L), reporter transcripts are found only at the anterodorsal "corner" of the oocyte and do not spread out along the entire anterior cortex as in wild-type. By stage 11 (panel M) the RNA has delocalized from the anterior of the oocyte. At stage 12-13 (panel N) reporter RNA is completely delocalized and staining is visible only in the remnants of the nurse cells. O-U, reporter transcript localization is normal in a sww^{1}/sww^{6} mutant background until late stage 9 (panel Q), when reporter RNA is found at the anterior of the oocyte but localization is impaired. The effects of the transheterozygous background on reporter RNA localization are quite noticeable at stage 10 (panel R), when reporter RNA is distributed over the anteriormost 20% of the oocyte rather than being confined tightly to the anterior cortex. Arrowheads here mark the boundary of posterior spreading of reporter RNA at stage 10. At stage 10b (panel S), reporter RNA is not only found at the anterodorsal corner (rather than along the entire anterior cortex), it is also spreading posteriorly along the dorsal side of the oocyte. By stage 11, there is very little RNA left at the anterodorsal corner (panel T). Finally, reporter RNA is completely delocalized during the last stages of oogenesis in the sww^{1}/sww^{6} mutant ovaries (stage 12, panel U).

Figure 21. Localization of reporter transcripts containing the full-length N4 3'UTR in *swallow* (*sww*) ovaries

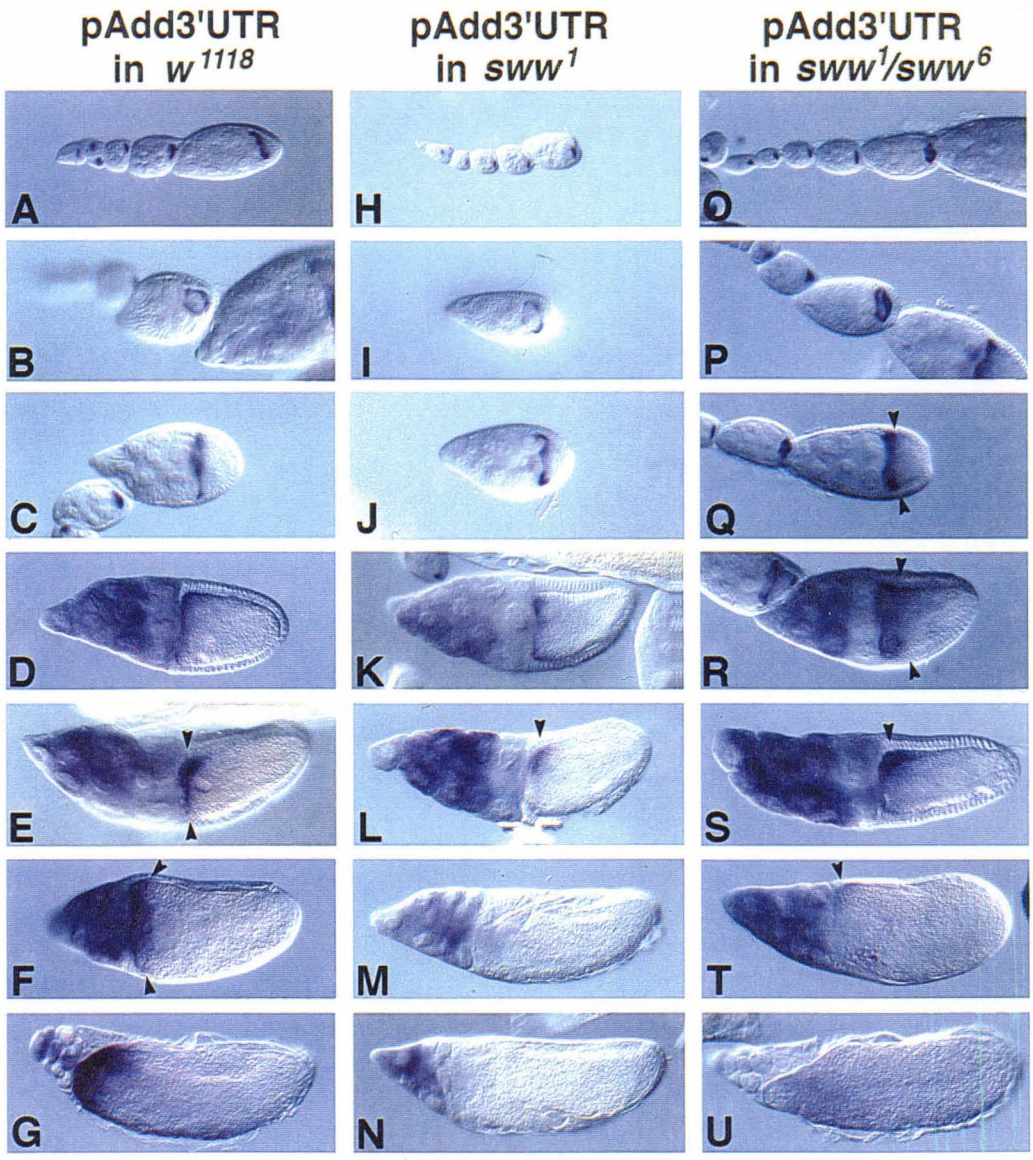

CHAPTER 3

Mitochondrially Encoded 16S Large Ribosomal RNA Is Concentrated in the Posterior Polar Plasm of Early *Drosophila* Embryos but Is Not Required for Pole Cell Formation

This chapter was published in Developmental Biology 163: 503-515 (1994).

DEVELOPMENTAL BIOLOGY 163, 503-515 (1994)

Mitochondrially Encoded 16S Large Ribosomal RNA Is Concentrated in the Posterior Polar Plasm of Early *Drosophila* Embryos but Is Not Required for Pole Cell Formation

DALI DING,[1,3] KELLIE L. WHITTAKER,[1] AND HOWARD D. LIPSHITZ[2]

Division of Biology 156-29, California Institute of Technology, Pasadena, California 91125

Accepted February 16, 1994

In a molecular screen for polar-localized RNAs in *Drosophila*, we identified the mitochondrially encoded 16S large ribosomal RNA (16S RNA) as an RNA that is highly concentrated at the posterior pole of early embryos. This high posterior accumulation decreases sharply during the first hour of embryogenesis and reaches the uniform level found throughout the remainder of the embryo by the time pole cells form 1.5 hr after fertilization. At the cellular blastoderm stage the 16S RNA is uniformly distributed basal to the nuclei of all somatic cells and is present only at low levels in the pole cells and in the apical regions of the somatic cells. Transcripts produced by the 12S small rRNA gene are also concentrated in the posterior polar plasm and exhibit the same dynamic changes in distribution as the 16S RNA. In contrast, NADH dehydrogenase subunit 1 RNA, which is transcribed from the same strand of the mitochondrial genome just downstream of the 12S and 16S genes, does not exhibit a high posterior concentration but is uniformly distributed throughout early embryos. Posterior localization of 16S RNA is normal in embryos produced by mothers carrying mutations which affect posterior patterning without disrupting the polar plasm or polar granule integrity. However, posterior localization of 16S RNA is abolished in embryos produced by females carrying maternal-effect mutations that disrupt the posterior polar plasm and the polar granules. Ectopic localization of the *oskar* RNA to the anterior pole of the oocyte and early embryo results in anterior assembly of polar plasm and anterior budding of functional pole cells. We show that 16S and 12S RNAs are not concentrated at the anterior pole of such embryos. This leads to the conclusion that, although the 16S and 12S RNAs are concentrated in the posterior polar plasm during normal development, functional pole cells can form in the absence of high levels of these RNAs. These data argue against previous hypotheses that the 16S RNA serves an obligatory function in pole cell formation.

INTRODUCTION

Formation of primordial germ cells (PGCs) in animal species ranging from worms to amphibians is dependent on localized germ plasm (Eddy, 1975, for a review). In *Drosophila*, the germ plasm (also called the polar plasm) is a posteriorly localized, yolk-free cytoplasmic cap that is continuous with the cortical cytoplasm of the egg and early embryo. One and a half hours after fertilization, pole cells (the *Drosophila* PGCs) bud from the posterior pole of the embryo, incorporating part of the polar plasm. It has been demonstrated that the polar plasm is both necessary and sufficient for pole cell formation in *Drosophila*. When components of the posterior polar plasm are disrupted by uv irradiation or pricking, or by mutations, pole cells do not form (for reviews, see Ding and Lipshitz, 1993b; Eddy, 1975; Lasko, 1992; Lipshitz, 1991). When transplanted to the anterior pole of the early embryo, polar plasm induces ectopic pole cells that can give rise to a functional germ line (Illmensee and Mahowald, 1974, 1976; Niki, 1986). Polar plasm contains electron-dense, non-membrane-bound organelles (called polar granules) that reside within 4 μm of the posterior tip and have been proposed to contain the cytoplasmic determinant(s) for pole cells (Mahowald, 1977).

Since *Drosophila* polar plasm is formed during oogenesis, genetic studies of the posterior polar plasm have focused on characterization of grandchildless mutations, maternal-effect mutations that produce progeny lacking a functional germ line. A number of these mutations have been found to disrupt the polar plasm, germ cell formation, and development of the abdomen (Ding and Lipshitz, 1993b; Lasko, 1992, for reviews). Two additional genes, *pumilio* and *nanos*, also appear to encode components of the polar plasm; however, these are re-

[1] These authors made equal contributions to the research reported here.

[2] To whom correspondence should be addressed. Fax: 818-564-8709. E-mail: lipshitzh@starbase1.caltech.edu.

[3] Present address: Amgen, Inc., 1840 DeHavilland Drive, Thousand Oaks, CA 91320-1789.

0012-1606/94 $6.00

quired for abdominal patterning but not for pole cell formation (Lehmann and Nüsslein-Volhard, 1987, 1991). Additional components of the polar plasm have been identified by molecular approaches (reviewed in Ding and Lipshitz, 1993b). These include RNAs encoded by *cyclin B*, *orb*, and *Hsp83* (Ding and Lipshitz, 1993a; Ding *et al.*, 1993b; Lantz *et al.*, 1992; Lehner and O'Farrell, 1990; Raff *et al.*, 1990), RNA and protein encoded by *germ cell-less* (Jongens *et al.*, 1992), and a 95-kDa protein (Waring *et al.*, 1978). The specific functions of *cyclin B*, *orb*, *Hsp83*, and the 95-kDa protein in the polar plasm are not known. In the case of *germ cell-less*, antisense-inactivation experiments indicate that it may be required specifically for pole cell formation (Jongens *et al.*, 1992).

It has been reported that the mitochondrial 16S large ribosomal RNA (referred to as 16S RNA hereafter) might also function as a component of the posterior polar plasm required for pole cell formation. This conclusion was based on the observation that injection of *in vitro*-transcribed 16S RNA rescues the ability of embryos to form pole cell-like cells after uv irradiation of the posterior polar plasm (Kobayashi and Okada, 1989). However, while possessing many of the characteristics of pole cells, these cells are not fully functional and cannot give rise to an operating germline. Recently we found that 16S RNA is concentrated at the posterior pole of early embryos (Ding and Lipshitz, 1993a). It has also recently been reported that a subset of the 16S RNA is extramitochondrial and might be associated with the polar granules (Kobayashi *et al.*, 1993). This last study also noted posterior concentration of the 16S RNA in early embryos, but reported a uniform distribution for 12S rRNA and the NADH dehydrogenase subunit 1 (*ND-1*) RNA.

Here, we show that, while the *ND-1* RNA is uniformly distributed in early embryos, both the 16S and the 12S RNAs are highly concentrated at the posterior pole. We demonstrate that posterior localization of the 16S RNA is dependent on genes that are required for polar plasm integrity and pole cell formation, but does not correlate well with either the distribution or the activity of mitochondria in early embryos. Ectopic localization of *oskar* RNA to the anterior pole of the oocyte and early embryo results in assembly of functional polar plasm anteriorly and the formation of ectopic, functional, anterior pole cells (Ephrussi and Lehmann, 1992). However, we show that 16S and 12S RNAs are not concentrated at the anterior pole of such embryos, indicating that germ plasm and functional germ cells can form in the the absence of high levels of 16S and 12S RNA. These data argue against the hypothesis (Kobayashi *et al.*, 1993; Kobayashi and Okada, 1989) that the 16S RNA functions as a necessary component of the polar plasm in early embryos.

MATERIALS AND METHODS

Identification of the 16S RNA as a Posteriorly Localized RNA

A cDNA representing the 16S RNA was identified in our differential screen for cDNAs representing maternally synthesized polar-localized RNAs in the early embryo (Ding and Lipshitz, 1993a). Probes made from the cDNA and used for whole-mount tissue *in situ* hybridization recognized an abundant RNA concentrated at the posterior pole of early embryos. Additional cDNAs were isolated by screening a 0- to 1-hr embryonic cDNA library with probe made from this initial cDNA (Ding and Lipshitz, 1993a). Sequence analysis of these cDNAs indicated that they represent the mitochondrial 16S large ribosomal RNA (Garesse, 1988; Kobayashi and Okada, 1990).

Isolation of the 12S Ribosomal RNA Gene

Four 12S-specific primers were designed based on *Drosophila yakuba* sequence (Clary and Wolstenholme, 1985), for use in a two-step nested PCR amplification: 12S I: 5′-TTA AAG TTT TAT TTT GGC TTA AAA ATT TGT TAT TAG TTT G-3′ and 12S II: 5′-TCA TTC TAG ATA CAC TTT CCA GTA CAT CTA CTA TGT TAC G-3′, yielding a predicted fragment of approximately 788 bp; 12S 5A: 5′-TGG TGC CAG CAG TCG CGG TTA TAC-3′ and 12S 3A: 5′-TAA GAG CGA CGG GCG ATG TGT AC-3′, yielding a fragment of approximately 550 bp. These sizes were approximate because primers based on *D. yakuba* sequence were used to amplify 12S mitochondrial rDNA from *Drosophila melanogaster*. The initial 100-μl reaction contained 1 μg of *D. melanogaster* total DNA, 0.5 m*M* 12S I primer, 0.5 m*M* 12S II primer, 0.75 m*M* $MgCl_2$, 50 m*M* KCl, 10 m*M* Tris-HCl, pH 8.4, 0.1 mg/ml gelatin, 200 m*M* dNTP mix, and 2.5 units of *Taq* polymerase. The reaction was run for 1.5 min at 94°C, 1.5 min at 56°C, and 2 min at 72°C for 30 cycles using a Perkin–Elmer DNA thermal cycler. The reamplification reaction was run under the same conditions, except that it contained 10 ng of the 788-bp fragment as template, 0.5 m*M* 12S 5A primer, and 0.5 m*M* 12S 3A primer. PCR amplification using the 12S I and II primers produced a single fragment of about 790 bp; this was gel-purified and used as template in a second round of amplification with the 12S 5A and 3A primers, which gave a single fragment of about 550 bp. This 550-bp fragment was gel-purified and subjected to sequencing, confirming its identity. Subsequently the 550-bp fragment was labeled with digoxigenin and used as a probe for whole-mount RNA tissue *in situ* hybridization.

Isolation of the ND-1 Gene

Two *ND-1*-specific primers were designed based on the *D. melanogaster* mitochondrial DNA sequence (Garesse, 1988): *ND-1*-5B: 5'-CAT AAC GAA ATC GAG GTA AAG TTC CTC GAA CTC A-3' and *ND-1*-3A: 5'-ATA CTG TTA TAG TAG CTG GTT GGT CGT CTA ATT C-3'. These primers were used for enzymatic amplification (PCR) of a 485-bp internal fragment of the *ND-1* gene from *Drosophila* total DNA. PCR conditions were as for the 12S gene, but using the *ND-1*-specific primers. A single strong band of the predicted size was visible after separation of the reaction products on an agarose gel; the DNA in this band was purified using a GeneClean kit (Bio 101, Inc.). Sequencing of the purified DNA confirmed that it indeed comprised the expected amplified fragment of the *ND-1* gene; it was subsequently labeled with digoxigenin for use as probe in whole-mount RNA tissue *in situ* hybridization.

Isolation of the nanos Gene

Primers specific for the second exon of the *nanos* gene were designed based on the published sequence (Wang and Lehmann, 1991): nos 5' internal: 5'-CTG ACT GGA TCC ATG CGG CTG GCT CGA TGC AGG ATG TG-3' and nos 3' internal: 5'-TCA GTC GAA TTC CTC TTT GGC CTT GCT GTT GTA ACG C-3'. The 5' primer included a novel *Bam*HI restriction site, and the 3' primer included a novel *Eco*RI site, to facilitate subsequent cloning. These primers were used for PCR amplification of a 466-bp fragment of the *nanos* gene from *D. melanogaster* total DNA. PCR conditions were the same as for 12S mitochondrial rDNA, except for the identity of the primers. The amplified 491-bp fragment (including the novel restriction sites) was gel-purified and reamplified using the same primers. Restriction mapping with *Pst*I confirmed the identity of the amplified DNA, which was then labeled with digoxigenin and used as a probe for *in situ* hybridization.

Analysis of Mitochondrial Activity in Early Embryos

Mitochondrial activity was analyzed by staining live embryos with 10 μg/ml rhodamine-123 (Chen *et al.*, 1982; Johnson *et al.*, 1980) in 1.1× basic incubation medium (BIM) (Limbourg and Zalokar, 1973), following a permeabilization procedure for live embryos developed by Strecker *et al.* (1994). This procedure has been shown to result in uniform dye penetration without any adverse effects on embryogenesis, patterning, or viability (Strecker *et al.*, 1994). Embryos were collected for 20 min, permeabilized with octane (Strecker *et al.*, 1994), and incubated in a shallow depression slide for 10 min with 10 μg/ml rhodamine-123 in 1.1× BIM. The dye was then removed and the embryos were washed twice with fresh 1.1× BIM and then covered with HC-56 halocarbon oil (Halocarbon Products Corp., Hackensack, NY). The remaining droplets of BIM were vacuumed off using a drawn-out micropipette connected to a vacuum aspirator (Inman, 1984). A coverslip was placed over the embryos and they were then examined under a Zeiss confocal microscope, using an argon laser with an excitation wavelength of 488 nm.

RNA Tissue in Situ Hybridization to Whole-Mount Embryos and Ovaries

Whole-mount RNA tissue *in situ* hybridization was based on the method of Tautz and Pfeifle (1989) modified as described (Ding *et al.*, 1993a). Visualization was carried out using either Vectastain (Vector Laboratories) or Genius (Boehringer-Mannheim Biochemicals) kits according to the manufacturers' instructions. Since both strands of the mitochondrial DNA are transcribed, we compared the *in situ* hybridization pattern obtained using randomly primed probe to that exhibited by single-sided PCR-generated probe for the 16S, the 12S, and the *ND-1* RNAs. There were no detectable differences in the results obtained for any of these transcripts using either of these methods.

Fly Strains

Mutant embryos were obtained from females homozygous for osk^{166} (Lehmann and Nüsslein-Volhard, 1986), $capu^{HK}$, $spir^{RP}$ (Manseau and Schüpbach, 1989), nos^{L7}, pum^{680} (Lehmann and Nüsslein-Volhard, 1987), vas^{PD}, $stau^{HL}$, vls^{RB}, tud^{WC8} (Schüpbach and Wieschaus, 1986). Embryos with *oskar* RNA mislocalized to the anterior pole were obtained from females heterozygous for a P-element insertion carrying the *oskar-bicoid 3'UTR* construct (Ephrussi and Lehmann, 1992).

RESULTS

16S RNA Is Uniformly Distributed in the Oocyte during Most of Oogenesis but Is Concentrated at the Posterior Pole of Early Embryos

During *Drosophila* oogenesis, four incomplete mitoses of a single cystoblast in the germarium of the ovariole lead to the formation of an interconnected 16-cell germ line cyst (King, 1970). One of the 16 cells becomes the oocyte, while the remaining 15 become the nurse cells, in which most of the nonyolk components of the oocyte are synthesized and then transported into the oocyte via the connecting ring canals. This process occurs in the vitellarium of the ovariole and has been divided into 14 distinct stages (King, 1970). High levels of 16S RNA are first detected in region 3 of the germarium (equivalent

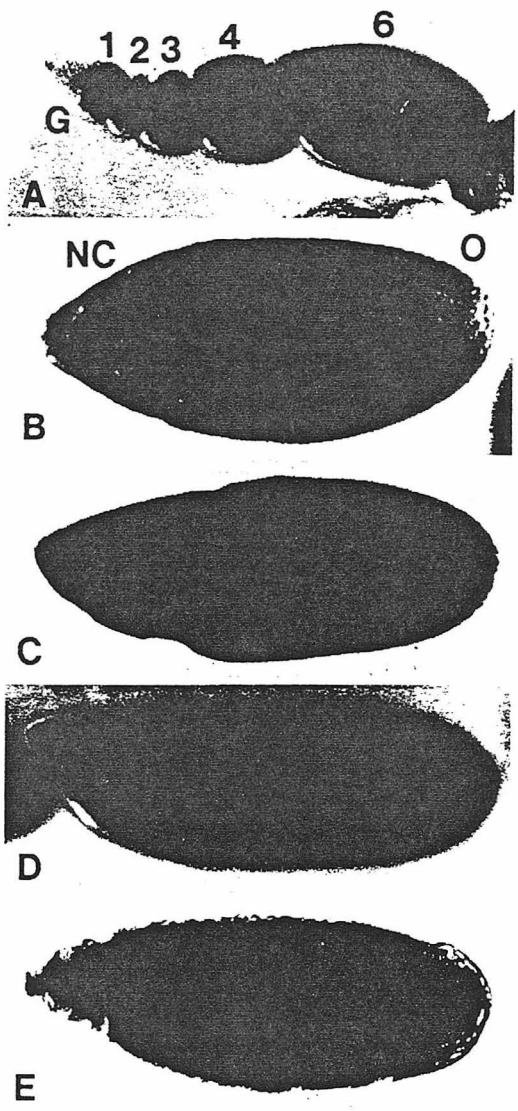

FIG. 1. Distribution of 16S RNA during oogenesis. *In situ* hybridization of 16S cDNA probe to ovarioles from wildtype females. (A) During the early stages of oogenesis, 16S RNA is detected in all the cells in region 3 of the germarium (G). From stage 1 of oogenesis (vitellogenesis) on, 16S RNA accumulates in all 16 cells of the nurse cell-oocyte complex (shown are stages 1, 2, 3, 4, and 6). (B) A stage 10A egg chamber shows high levels of 16S RNA in nurse cells (NC) and slightly lower levels in the oocyte (O). (C) In a stage 11 egg chamber, nurse cells contain high levels of 16S RNA, which is being transported into the oocyte. (D) A stage 10 egg chamber showing the somatic follicle cells, which are heavily stained with 16S cDNA probe. (E) In stage 12 oocytes, 16S RNA is distributed uniformly at high levels throughout the oocyte.

to oogenesis stage 1) (Fig. 1A). In stages 2 through 10A follicles in the vitellarium, 16S RNA is present at a high level in the nurse cells and is detected at a lower level in the oocyte (Figs. 1A and 1B). Nurse cell expression persists through stages 10B and 11, and accumulation of 16S RNA in the oocyte begins at stage 10B (Fig. 1C). The somatically derived follicle cells are also heavily labeled with probe that recognizes the 16S RNA (Fig. 1D). By stage 12, when nurse cells have completely emptied their contents into the oocyte, 16S RNA is present at high levels throughout the oocyte (Fig. 1E). Between stage 12 of oogenesis and egg deposition shortly after fertilization higher levels of 16S RNA accumulate at the posterior tip of the oocyte (Fig. 2A). Oocytes at stages later than stage 12 are not readily fixed and devitellinized, and thus we were unable to determine unambiguously whether 16S RNA becomes localized to the posterior pole of the oocyte before or after fertilization. However, the fact that all embryos exhibit high levels of posteriorly localized 16S RNA immediately after fertilization (Fig. 2A) suggests that this RNA is likely to be concentrated posteriorly during late oogenesis. The timing of posterior localization of 16S RNA is similar to that of the *germ cell-less* transcript, which becomes posteriorly localized at an undetermined time between stage 11 and egg deposition (Jongens *et al.*, 1992).

In early embryos immediately after egg deposition, 16S RNA is present at high levels at the posterior tip of the embryo and at a much lower, uniform concentration throughout the rest of the embryo (Fig. 2A). During the early cleavage stages, the high posterior concentration of 16S RNA decreases rapidly. By the time that pole cell buds appear, the intensity of 16S RNA at the posterior tip of the embryo has dropped significantly, becoming only slightly higher than elsewhere in the embryo (Fig. 2B). The pole cell buds are not labeled at this stage (Fig. 2B), indicating that little 16S RNA is incorporated into the pole cells. After pole cell formation, the concentration of 16S RNA in the cortical cytoplasm at the posterior tip is the same as that throughout the cortex of the embryo, while the pole cells exhibit much lower 16S RNA levels (Fig. 2C). During the syncytial and cellular blastoderm stages, 16S RNA remains evenly distributed along the anteroposterior axis in the basal somatic cytoplasm; only low levels are present in the pole cells and in the apical somatic cytoplasm (Fig. 2D).

Control experiments with strand-specific probes indicate that the observed distribution reflects that of 16S RNA rather than transcripts synthesized from the complementary strand of the mitochondrial genome (data not shown; see Materials and Methods). In addition, hybridization of a genomic Southern blot with 16S probe indicated that there is no nuclear copy of the 16S RNA gene (data not shown) and, therefore, that the tran-

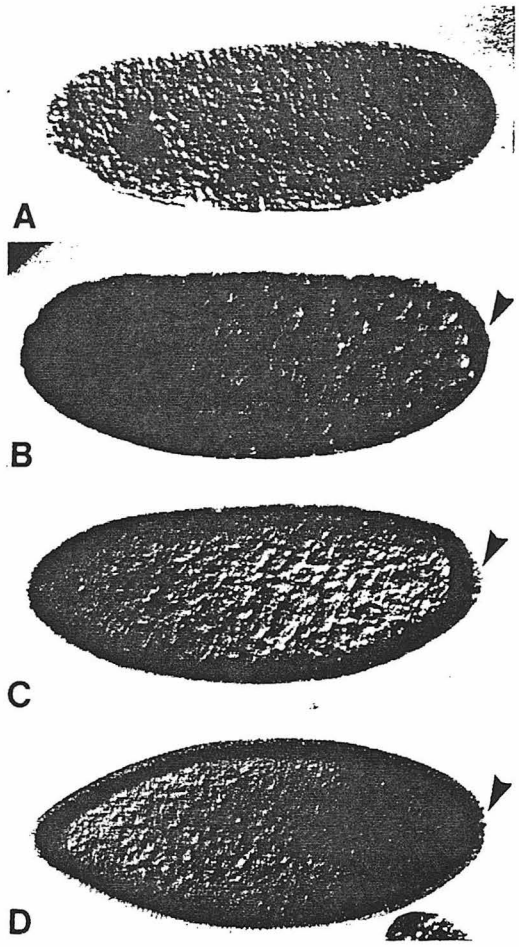

FIG. 2. Localization of 16S RNA during early embryogenesis. *In situ* hybridization of 16S cDNA probe to wildtype embryos. (A) In an embryo immediately after fertilization, 16S RNA is present throughout the embryo, but is found at a higher concentration at the posterior pole. (B) The high posterior concentration of 16S RNA decreases rapidly during the cleavage stages. When pole cells form, there is only slightly more RNA at the posterior end than the rest of the embryo. The pole cell buds (arrowhead) exhibit very low levels of 16S RNA. (C) At the syncytial blastoderm stage, 16S RNA is uniformly distributed throughout the somatic part of the embryo. Levels in the pole cells (arrowhead) remain low. (D) At the cellular blastoderm stage, 16S RNA is present in the basal cytoplasm of the somatic cells, while the levels in the pole cells (arrowhead) are low. For all embryos, anterior is to the left and dorsal is toward the top of the page.

scripts detected must have been synthesized in mitochondria. This last result is consistent with the Southern blot and chromosome polytene *in situ* hybridization data reported by Kobayashi and Okada (1989).

12S RNA Is Concentrated at the Posterior Pole of Early Embryos

The mitochondrial genome also encodes the 12S small ribosomal RNA (Clary and Wolstenholme, 1985; Garesse, 1988). Given our data on the concentration of 16S RNA in the posterior polar plasm, it was of interest to determine whether this distribution pattern is specific for the 16S RNA or whether both the 16S and 12S RNAs exhibit posterior concentration. Our results show that the 12S RNA is also concentrated at the posterior pole of early embryos in a pattern and, with dynamics, indistinguishable from that of the 16S RNA (Fig. 3A). As for the

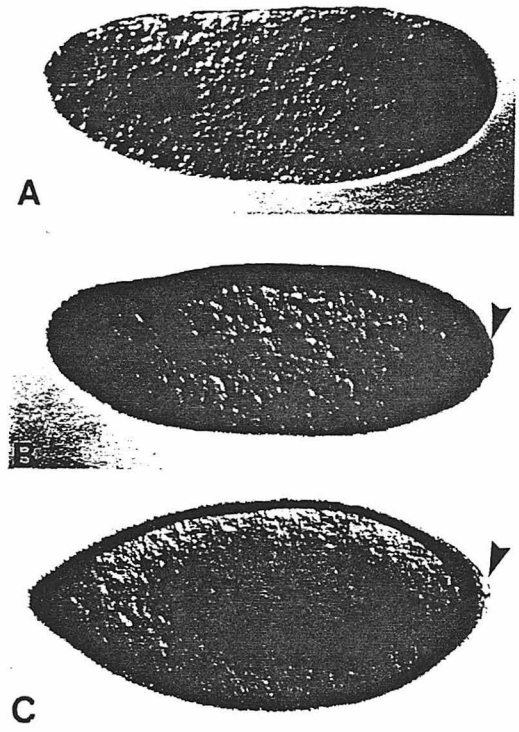

FIG. 3. Distribution of 12S rRNA in early embryos. *In situ* hybridization of 12S probe to wildtype embryos. (A) In an embryo immediately after fertilization, 12S RNA is present throughout the embryo, but is found at a higher concentration at the posterior pole. (B) The high posterior concentration of 12S RNA decreases rapidly during the cleavage stages and, by the early syncytial blastoderm stage, 12S RNA is only marginally more abundant at the posterior pole than in the rest of the somatic cortical cytoplasm of the embryo. Levels in the pole cells (arrowhead) remain low. (D) At the cellular blastoderm stage, 12S RNA is present in the basal cytoplasm of the somatic cells, while levels in the pole cells (arrowhead) remain low. For all embryos, anterior is to the left and dorsal is toward the top of the page.

16S RNA, the high posterior concentration of 16S RNA decreases rapidly during the early cleavage stages. By the early syncytial blastoderm stage, the concentration of 12S RNA in the cortical cytoplasm at the posterior tip is only marginally higher than that throughout the rest of the cortex of the embryo, and the pole cells contain only low levels of 12S RNA (Fig. 3B). During the syncytial and cellular blastoderm stages, 12S RNA remains evenly distributed in the somatic cytoplasm along the anteroposterior axis, where it is concentrated basally, as is the 16S RNA (Fig. 3C, cf. Fig. 2D).

Control experiments with strand-specific probes indicate that the observed distribution reflects that of 12S RNA rather than that of transcripts synthesized from the complementary strand of the mitochondrial genome (data not shown; see Materials and Methods). Our data contrast with those of Kobayashi *et al.* (1993), who reported a uniform distribution of 12S RNA in early embryos. Since both the 16S and 12S RNAs are very abundant in early embryos (Ding and Lipshitz, 1993a), it is possible that the embryos examined by those authors were overstained, thus obscuring the concentration of 12S RNA in the posterior polar plasm.

ND-1 RNA Is Distributed Uniformly in Early Embryos

To compare the distribution of an additional mitochondrially encoded transcript to that of 16S and 12S RNAs, we carried out whole-mount *in situ* detection of the *ND-1* RNA. We chose to analyze *ND-1* RNA distribution because Kobayashi and Okada (1989) had previously used the *ND-1* gene as a control in their experiments. *ND-1* RNA is synthesized from the same strand of the mitochondrial DNA as the 16S and 12S RNAs and the *ND-1* gene resides just downstream of the 16S RNA gene, being separated from it only by the Leu (CUN) tRNA gene (Clary and Wolstenholme, 1985; Garesse, 1988). Unlike the posterior-localized 16S and 12S RNAs, the *ND-1* RNA is uniformly distributed throughout the early cleavage stage embryo (Fig. 4, cf. Figs. 2 and 3). This indicates that the nonuniform distribution observed for the 16S and 12S RNAs is not a general rule for all mitochondrial transcripts. Neither is posterior concentration a property solely of the mitochondrial ribosomal RNAs since we have previously shown that the *cytochrome oxidase subunit 1 (CO1)* messenger RNA is concentrated at both poles of the early embryo (Ding and Lipshitz, 1993a). Thus, not only are the distributions of the large and small mitochondrial rRNAs identical and distinct from that of the protein-coding *ND-1* RNA, but there are also differences in the distribution patterns of different mitochondrial messenger RNAs during the same stages of embryogenesis.

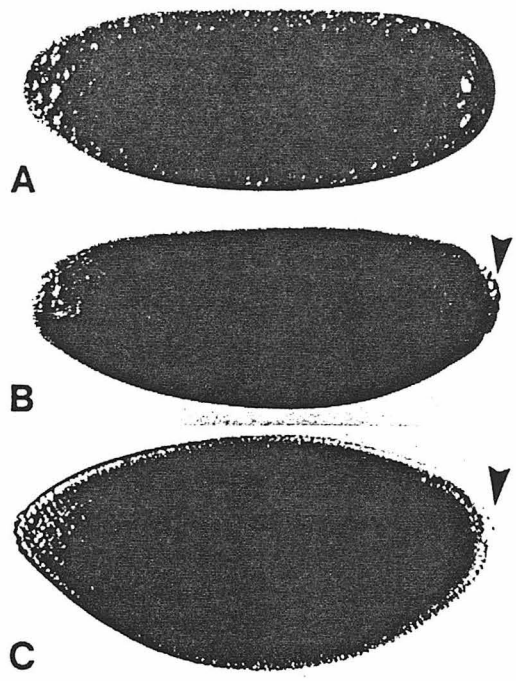

FIG. 4. Localization of *ND-1* RNA during early embryogenesis. *In situ* hybridization of *ND-1* cDNA probe to wildtype embryos. (A) In an early cleavage stage embryo, *ND-1* RNA is distributed uniformly throughout the embryo. (B) At the syncytial blastoderm stage, the *ND-1* RNA is distributed uniformly in the somatic part of the embryo and is present at a slightly reduced level in the pole cells (arrowhead). (C) At the cellular blastoderm stage, *ND-1* RNA is present throughout the cytoplasm of the somatic part of the embryos, while levels in the pole cells (arrowhead) have dropped. For all embryos, anterior is to the left and dorsal is toward the top of the page.

Mitochondrial Distribution and Activity in Early Embryos Do Not Correlate with the 16S and 12S RNA Distribution Pattern

The high posterior concentration of 16S and 12S RNAs in early cleavage stage embryos is not a consequence of a high concentration of mitochondria posteriorly since it has been shown that mitochondria are uniformly distributed in early embryos (Akiyama and Okada, 1992). A second possibility is that the high posterior concentration of 16S and 12S RNAs is a reflection of elevated activity of mitochondria in the posterior polar plasm relative to the rest of the cortical cytoplasm. Consequently, we assayed mitochondrial activity in permeabilized living embryos (Strecker *et al.*, 1994) using the voltage-sensitive dye, rhodamine-123 (Chen *et al.*, 1982; Johnson *et al.*, 1980). In contrast to the uniform

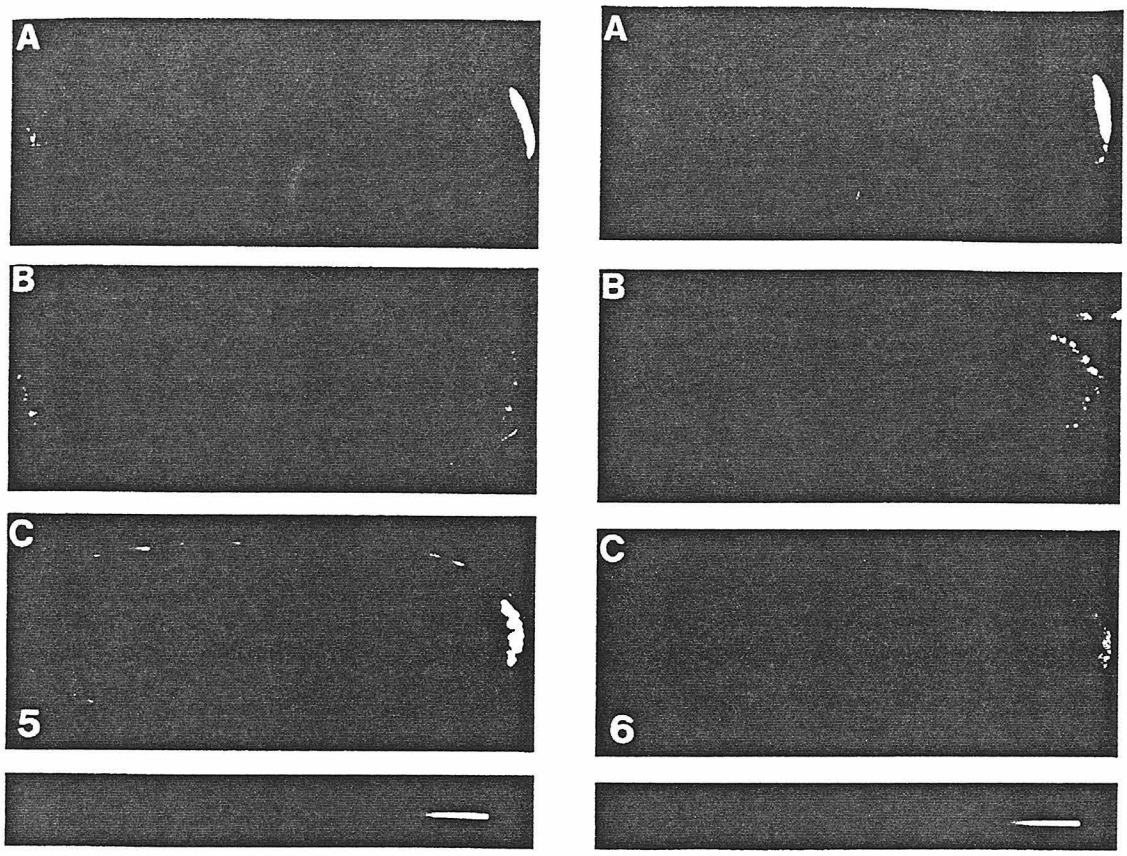

FIG. 5. Distribution of mitochondrial activity in early embryos. Pseudocolor confocal images of rhodamine-123-stained live embryos. (A) An early cleavage embryo shows a posteriorly localized "cap" of high mitochondrial membrane potential and a somewhat increased membrane potential at the anterior (cf. Figs. 2A and 3A). (B) In mid cleavage, mitochondrial activity remains high at the posterior pole and is high in the pole cell buds (cf. Figs. 2B and 3B). (C) In a cellular blastoderm stage embryo, high mitochondrial activity is restricted to the pole cells (cf. Figs. 2D and 3D).

FIG. 6. Distribution of mitochondrial activity in early embryos from *pumilio*, *cappuccino*, and *tudor* females. Pseudocolor confocal images of rhodamine-123-stained live embryos. (A) In an early cleavage stage embryo from a *pumilio* mother, the posterior cap of mitochondrial activity is tightly concentrated, as in wildtype (cf. Fig. 5A). (B) An early cleavage stage embryo from a *cappuccino* mother shows a high posterior level of mitochondrial membrane potential, but the distribution is more diffuse than that in wildtype (cf. Fig. 5A). Anterior levels of mitochondrial activity are slightly elevated, as in wildtype. (C) In an early cleavage stage embryo from a *tudor* female, the mitochondrial activity is high at the posterior pole but is more diffusely distributed than that in wildtype (cf. Fig. 5A). Anterior levels of mitochondrial activity are also elevated, as seen in wildtype embryos.

mitochondrial distribution, mitochondrial activity was found to be both spatially and temporally regulated (Fig. 5). During early cleavage, there is a tight "cap" of mitochondria with very high membrane potential in the posterior polar plasm, as well as a more diffuse cap of mitochondria with a somewhat elevated membrane potential in the anterior of the embryo (Fig. 5A). At these stages, the density of mitochondria in these regions is essentially uniform (Akiyama and Okada, 1992). High levels of anterior and posterior mitochondrial activity persist through mid cleavage (roughly 1 hr after fertilization), and the pole cell buds exhibit high levels of mitochondrial activity when they form (Fig. 5B). While the pole cells continue to exhibit very high respiratory activity through the cellular blastoderm stage, anterior mitochondrial activity drops to background levels by this stage (Fig. 5C). Our results differ from those reported by Akiyama and Okada (1992), who did not observe elevated anterior and posterior mitochondrial activity in mid cleavage embryos (see also below). The

protocol we used to permeabilize living embryos has been shown to result in uniform penetration of dye (Strecker *et al.*, 1994), giving us confidence that our results reflect true differences in mitochondrial activity rather than an artifact caused by variable penetration of rhodamine-123.

Thus, the posterior pole of the early cleavage stage embryo exhibits an elevated mitochondrial respiratory activity and a high concentration of 16S and 12S RNA. However, mitochondrial respiratory activity and the 16S and 12S RNA distribution do not correlate subsequently, since pole buds and pole cells exhibit high levels of rhodamine-123 staining but only low levels of 16S and 12S RNA (Figs. 2B–2D). This uncoupling of mitochondrial activity and RNA levels is further supported by the fact that rhodamine-123 staining is high at the posterior pole of embryos produced by females carrying grandchildless mutations while these same mutations completely eliminate posterior concentration of 16S RNA (Figs. 6 and 7; see below).

Mitochondrial Activity Is Largely Unaffected by Grandchildless Mutations

Next we analyzed the effects of two grandchildless mutations on mitochondrial activity as assayed by rhodamine-123 staining. These two mutations, *cappuccino* and *tudor*, reduce the posterior polar plasm, eliminate the polar granules, and prevent pole cell formation. *cappuccino* functions early in polar plasm and polar granule assembly (see Lasko, 1992, for review), while *tudor* functions later (Ephrussi and Lehmann, 1992). The *tudor* protein has recently been detected inside mitochondria during early embryogenesis (Bardsley *et al.*, 1993). In addition, we assayed the effects of the *pumilio* mutation on rhodamine-123 staining. *pumilio* RNA is concentrated in the posterior polar plasm of the early embryo (Barker *et al.*, 1992; Macdonald, 1992), but *pumilio* function is not required for maintenance of polar granule integrity or pole cell formation.

Rhodamine-123 staining in embryos from *pumilio* mothers was indistinguishable from that in wildtype (Fig. 6A, cf. Fig. 5A). In embryos produced by *cappuccino* and *tudor* mutant females, rhodamine-123 staining was high at the posterior pole (Figs. 6B and 6C). However, the posterior signal in embryos from these mutant females was less tightly localized than in wildtype embryos, being distributed through the posterior sixth of the cortical cytoplasm (Fig. 6, cf. Fig. 5). This observation is consistent with the elimination of the posterior polar plasm as a morphologically distinct entity in these mutants (Boswell and Mahowald, 1985; Lehmann and Nüsslein-Volhard, 1986; Schüpbach and Wieschaus, 1986). Thus, wildtype embryos, as well as embryos from *pumilio*, *cappuccino*, and *tudor* females, exhibit an elevated activity of posteriorly located mitochondria. However, in the embryos produced by *cappuccino* and *tudor* mutant females, the reduction in the volume of the cytoplasmic cap at the posterior pole results in the active mitochondria being less tightly restricted to the posterior tip. Our results differ from those presented by Akiyama and Okada (1992), who reported no detectable effect of grandchildless mutants on the distribution of active posterior mitochondria. Curiously, their embryos derived from mutant females appear to exhibit the presence of posterior polar plasm, although it is known to be eliminated in these mutants (Boswell and Mahowald, 1985; Lehmann and Nüsslein-Volhard, 1986; Schüpbach and Wieschaus, 1986).

Our results demonstrate that the high-level activation of posteriorly located mitochondria in early embryos does not require the posterior polar plasm. Rather, some other cue must be used to activate these mitochondria and they are then restricted to posterior polar plasm of wildtype embryos by one or more of the components of the polar plasm.

Posterior Localization of the 16S RNA Is Disrupted by Grandchildless Mutations

We then examined the effects of the *cappuccino*, *tudor*, and *pumilio* mutations, as well as an additional five maternal-effect mutations which cause defects in pole cell formation and/or posterior patterning, on 16S RNA distribution. For all mutations that affect the integrity of polar granules, pole cell formation, and abdominal development (*cappuccino*, *spire*, *oskar*, *vasa*, *valois*, *tudor*, and *staufen*), the 16S RNA is present at uniform levels throughout the embryo at early cleavage stages and the high posterior concentration is completely abolished (Fig. 7). In contrast, mutations that affect abdominal patterning but not polar granule integrity or pole cell formation (*nanos* and *pumilio*) result in embryos in which the posterior localization of 16S RNA is normal (Fig. 8).

Thus, components of the polar plasm are required to establish and/or maintain the high posterior concentration of the 16S RNA in early embryos.

Ectopic Anterior Polar Plasm and Pole Cells Can Form in the Absence of a High Anterior Concentration of 16S and 12S RNA

A key component of the polar plasm is encoded by the *oskar* RNA, which is localized to the posterior pole of the oocyte and early embryo (Ephrussi *et al.*, 1991; Kim-Ha *et al.*, 1991). The *oskar* gene resides near the top of the polar plasm assembly pathway (Ephrussi and Lehmann, 1992). Ectopic localization of *oskar* RNA to the

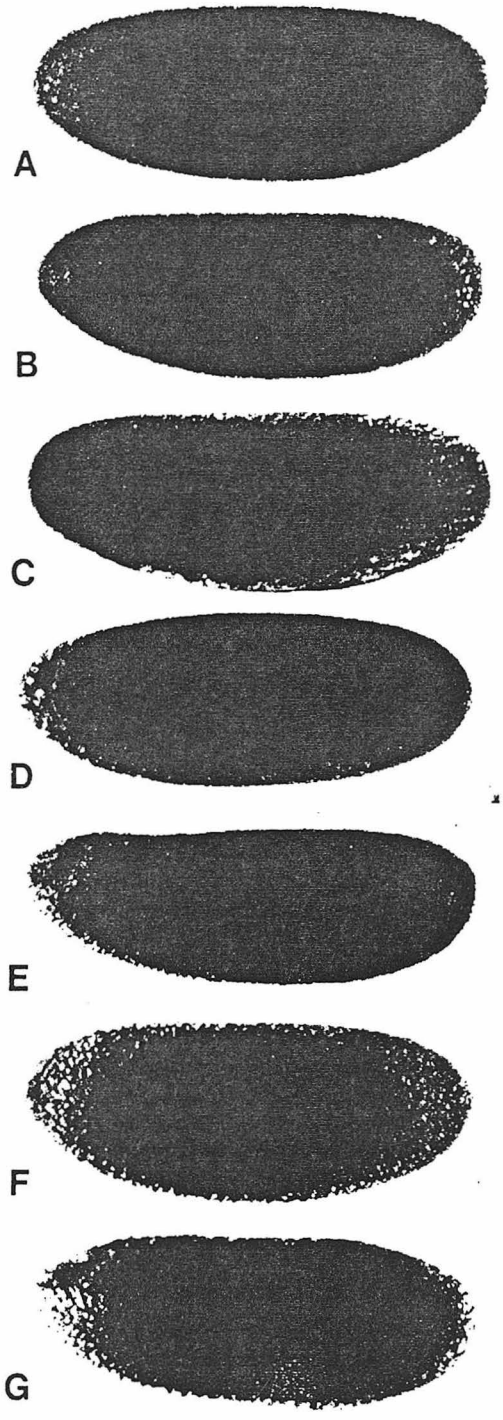

anterior pole of the oocyte and early embryo under the control of the *bicoid 3'UTR* results in anterior assembly of polar granules (Bardsley *et al.*, 1993), polar plasm, and the formation of functional pole cells at this ectopic location (Ephrussi and Lehmann, 1992). In addition, *vasa* protein (Ephrussi and Lehmann, 1992), *nanos* RNA (Ephrussi and Lehmann, 1992), and *Hsp83* RNA (Ding *et al.*, 1993b) are relocalized anteriorly in such embryos and are taken up into the ectopic pole cells that form there (reviewed in Ding and Lipshitz, 1993b). Given our observation that 16S RNA is delocalized by grandchildless mutants (see above) and reports that pole cell-like cells could be induced at the anterior pole by injection of 16S RNA along with uv-irradiated posterior cytoplasm (Kobayashi and Okada, 1989), we examined embryos from *osk-bcd 3'UTR* females for possible anterior concentration of 16S RNA. 16S RNA is not concentrated anteriorly in these embryos (Figs. 9A-9C): 96% exhibited no significant anterior concentration of 16S RNA despite showing clear posterior concentration; 4% exhibited 16S RNA concentrated at both poles (n = 129). The 12S RNA is also not concentrated anteriorly in such embryos (data not shown). Control embryos, derived from the same batch and processed in parallel, were examined for *nanos* RNA as well as for the ability to form ectopic pole cells: 96% of the embryos with *nanos* RNA localized posteriorly also exhibited significant anterior *nanos* RNA localization (Figs. 9D-9F); 4% showed *nanos* RNA concentrated only at the posterior pole (n = 116). The stage 3 to 5 embryos we examined also clearly formed ectopic anterior pole buds and pole cells (Figs. 9E-9F). Thus, we are led to conclude that functional polar granules, polar plasm, and pole cells can form in the absence of a high concentration of 16S and 12S RNA.

DISCUSSION

We have shown that the mitochondrially encoded 16S and 12S ribosomal RNAs are concentrated at the posterior pole of early cleavage stage embryos. The dynamics of 16S and 12S RNA expression and localization do not correlate well with either the distribution of mitochondria or their activity. Mutations that disrupt the integrity of the posterior polar plasm, the polar granules, and the ability to form pole cells have a limited effect on the

FIG. 7. Distribution of 16S RNA in embryos from grandchildless-*knirps* mutant females. 16S RNA is shown in early cleavage stage embryos derived from females homozygous for mutations that disrupt the posterior polar plasm and the integrity of the polar granules (A-G). These are (A) *cappuccino*, (B) *spire*, (C) *staufen*, (D) *oskar*, (E) *vasa*, (F) *tudor*, and (G) *valois*. Maternal 16S RNA is not present at higher levels at the posterior pole, but it is still present at uniform levels throughout the anteroposterior axis of the embryo. For all embryos, anterior is to the left and dorsal is toward the top of the page.

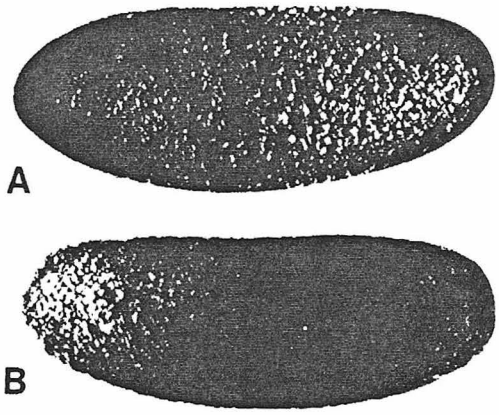

FIG. 8. Distribution of 16S RNA in embryos from *nanos* and *pumilio* mutant females. Posterior localization of 16S RNA is normal in early cleavage stage embryos produced by females mutant for *nanos* (A) or *pumilio* (B), which eliminate components of the posterior polar plasm without affecting the integrity of the polar granules. Shown are early cleavage stage embryos with anterior to the left and dorsal toward the top of the page.

distribution of active mitochondria at the posterior pole. In contrast, all of these mutations completely eliminate posterior concentration of the 16S RNA. Further, ectopic anterior formation of functional polar granules and polar plasm in embryos from *oskar-bicoid 3'UTR* females does not result in ectopic anterior concentration of the 16S and 12S RNAs. Indeed, functional ectopic pole cells form in such embryos in the absence of high concentrations of 16S and 12S RNAs. Thus, pole cell formation is not dependent on a local concentration of these RNAs. Here, we discuss the significance of these results and compare them with the results of previous studies of the 16S RNA and the posterior polar plasm.

The 16S and 12S RNAs Are Concentrated in the Posterior Polar Plasm of Early Embryos

We have shown that both the 16S and 12S RNAs are transiently concentrated at high levels in the posterior polar plasm of early embryos. This cannot simply be a result of a higher density of mitochondria in this region since the mitochondrial density in the posterior polar plasm is not elevated relative to the rest of the embryo (Akiyama and Okada, 1992). Further, we have shown that the high posterior concentration of these RNAs is also not simply a correlate of higher respiratory activity of mitochondria in the polar plasm. While, in early cleavage embryos, mitochondrial activity (as assayed in living embryos with rhodamine-123), 16S, and 12S RNA concentrations are high at the posterior pole, highly active mitochondria are found in the pole buds and pole cells, both of which exhibit very low levels of 16S and 12S RNA. Mitochondrial activity can further be shown to be uncoupled from posterior localization of 16S RNA by our analysis of grandchildless mutants. These eliminate the posterior polar plasm as a morphologically distinct entity (Boswell and Mahowald, 1985; Lehmann and Nüsslein-Volhard, 1986; Schüpbach and Wieschaus, 1986) and we have shown here that they also completely eliminate posterior polar concentration of 16S RNA. However, these grandchildless mutations do not alter the high activity level of posterior mitochondria; they produce only a minor effect on the spatial distribution of the active mitochondria, as might have been expected given the absence of posterior polar plasm in these embryos. Were the 16S RNA dispersed in a pattern identical to that of the active mitochondria in these mutants, the posterior 16S RNA level would have appeared significantly higher than that in the rest of the cortical cytoplasm. However, these mutants result in complete delocalization of the 16S RNA from the posterior pole. Thus, we are led to conclude that the high concentration of 16S RNA in the posterior polar plasm is not a reflection either of a high density of mitochondria or of high activity of mitochondria in this region. This concentration of the 16S RNA, however, is absolutely dependent on the presence and integrity of the posterior polar plasm.

Polar Plasm Concentration of the 16S and 12S RNAs Is Not Required for Pole Cell Formation

Kobayashi and Okada (1989) reported that the injection of *in vitro*-transcribed 16S RNA into the cytoplasm at the posterior of uv-irradiated embryos restored their ability to form pole cell-like cells which, while not fully functional, had many of the properties of germ cells. When injected anteriorly together with uv-irradiated posterior cytoplasm, hybrid selected 16S RNA could induce pole cell-like cells anteriorly (Kobayashi and Okada, 1989). These authors found that 16S RNA is more abundant in a subcellular fraction containing few mitochondria (P3) than in a mitochondrial fraction (P2), suggesting that a subset of 16S RNA is outside of the mitochondria in the cytoplasm of early embryos (Kobayashi and Okada, 1989). Recently, Kobayashi *et al.* (1993) have reported electron microscopic RNA *in situ* hybridization experiments supporting the notion that a subset of 16S RNA at the posterior pole of the early embryo may be associated with the polar granules in the cytoplasm.

Our analyses of the 16S and 12S RNAs have shown that both of these RNAs are concentrated in the posterior polar plasm, forming a tight cap at the posterior pole of early embryos, a pattern similar to that of other

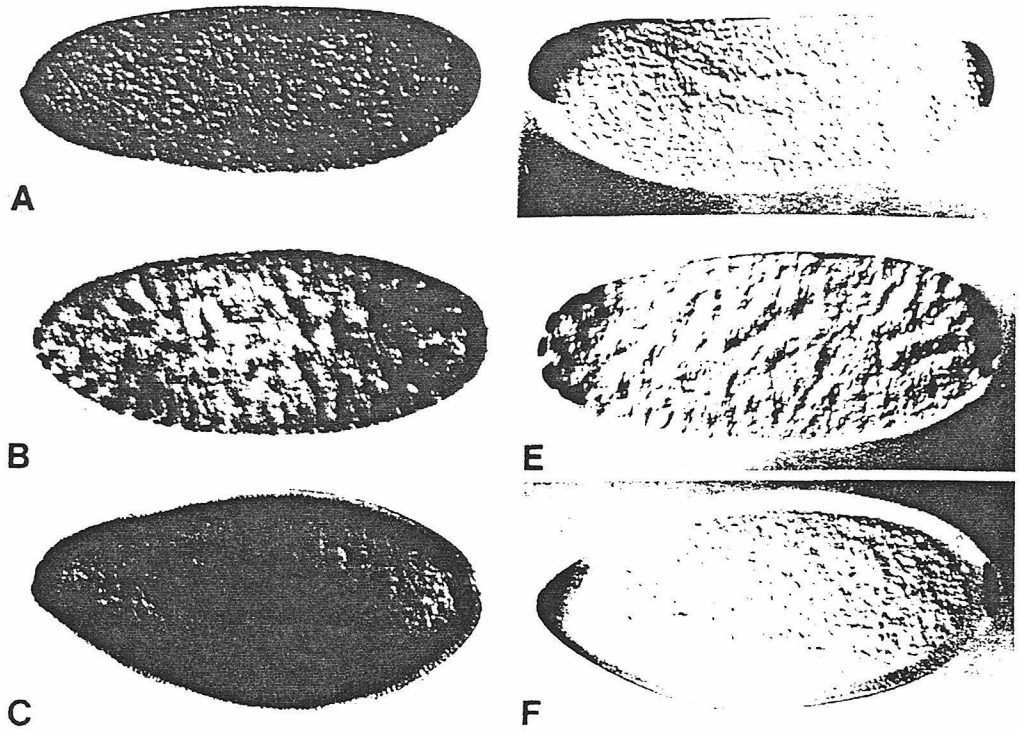

FIG. 9. Distribution of 16S (A-C) and *nanos* (D-F) RNAs in embryos produced by *oskar-bicoid 3'UTR* females. In embryos immediately after fertilization, 16S RNA (A) is concentrated at the posterior pole as in wildtype (cf. Fig. 2A) but is not concentrated at the anterior pole. In contrast, *nanos* RNA (D) is localized at both poles. The high posterior concentration of 16S RNA decreases rapidly during the cleavage stages and, when pole cells form, there is only slightly more 16S RNA (B) at the posterior end than in the rest of the embryo. The dynamics of this process are indistinguishable from those in wildtype (cf. Fig. 2B). In contrast, *nanos* RNA remains at both poles (E). At the cellular blastoderm stage, 16S RNA (C) is present in the basal cytoplasm of the somatic cells and levels are low in the pole cells, again resembling wildtype (cf. Fig. 2D). In contrast, *nanos* RNA is taken up into the pole cells at both poles (F). For all embryos, anterior is to the left and dorsal is toward the top of the page.

RNAs that are likely to be components of the polar plasm such as transcripts of *nanos*, *oskar*, and *germ cell-less* (Ephrussi *et al.*, 1991; Jongens *et al.*, 1992; Kim-Ha *et al.*, 1991; Wang and Lehmann, 1991). In addition, we have demonstrated that posterior concentration of the 16S RNA is dependent on the integrity of the posterior polar plasm and the polar granules since it does not occur in embryos derived from grandchildless mutant females.

While these data support the hypothesis that 16S RNA is a component of the posterior polar plasm, they do not prove that the 16S RNA must be concentrated there for pole cell formation to occur. In order to test this possibility more directly, we examined both the 16S and 12S RNA distributions in embryos derived from females carrying an *oskar-bicoid 3'UTR* construct designed to ectopically localize *oskar* RNA to the anterior pole of oocytes and early embryos (Ephrussi and Lehmann, 1992). This results in anterior localization of *vasa* protein (Ephrussi and Lehmann, 1992), *nanos* RNA (Ephrussi and Lehmann, 1992), and *Hsp83* RNA (Ding and Lipshitz, 1993b; Ding *et al.*, 1993b), anterior assembly of polar granules and polar plasm, and formation of ectopic, anterior, fully functional pole cells (Ephrussi and Lehmann, 1992). If high-level concentration of 16S and/or 12S RNAs were obligatory for pole cell formation, one would have expected these RNAs to be ectopically concentrated at the anterior pole of embryos derived from *oskar-bicoid 3'UTR* females. In fact, however, our data clearly demonstrate that neither the 16S nor the 12S RNAs are concentrated at the anterior pole of such embryos.

The simplest interpretation of these results is that, while the 16S (and possibly the 12S) RNA is concentrated at the posterior pole of early embryos in a polar plasm-dependent fashion (Fig. 7), and may even be associated with polar granules (Kobayashi *et al.*, 1993), this is not necessary for pole cell formation. Of some significance in this regard is the fact that attempts to inactivate the 16S RNA in the posterior polar plasm, either by injection of *in vitro*-transcribed antisense RNA (Kobayashi and Okada, 1989) or by injection of mixtures of high concentrations of antisense oligodeoxynucleotides complementary to the conserved loops of the 16S RNA (D. Ding, K. L. Whittaker, S. M. Parkhurst, and H. D. Lipshitz, unpublished data), have failed to produce any phenotypic effects. An alternative hypothesis, that the 16S RNA functions above (prior to) *oskar* in the polar plasm assembly hierarchy (and that, therefore, the requirement for its function is bypassed in the *oskar-bicoid 3'UTR* situation), is unlikely in light of a comparison of the dynamics of *oskar* and 16S localization to the posterior pole of the oocyte and early embryo: *oskar* RNA is localized to the posterior of the oocyte by stage 9 of oogenesis (Ephrussi *et al.*, 1991; Kim-Ha *et al.*, 1991), and it remains posteriorly concentrated through early embryogenesis. In contrast, we have shown that 16S RNA is not concentrated to the posterior pole until much later. Thus the temporal aspects of *oskar* and 16S RNA localization are consistent with the former functioning prior to the latter, rather than the opposite.

The ability of injected 16S RNA to partially restore the pole cell formation pathway (Kobayashi and Okada, 1989) cannot at present be explained. It is not possible at present to exclude rigorously the hypothesis that the 16S RNA acts in an independent pathway involved in polar plasm and pole cell formation. However, such a scenario is made unlikely by the fact that hybrid selected 16S RNA can only induce pole cell-like cells anteriorly when co-injected with uv-irradiated posterior polar plasm (Kobayashi and Okada, 1989). Such polar plasm would include, among other things, highly active mitochondria (since uv irradiation does not affect their activity; Akiyama and Okada, 1992) as well as molecules required for polar plasm assembly and pole cell formation (e.g., *oskar* RNA and protein, *vasa* protein; reviewed in Ding and Lipshitz, 1993b).

Whatever the explanation for the effects of 16S RNA on uv-irradiated embryos, our present data prove that functional polar plasm and pole cells can form in the absence of a localized concentration of 16S RNA.

We thank the Bowling Green and Indiana *Drosophila* Stock Centers, as well as A. Ephrussi and R. Lehmann for providing *Drosophila* stocks, W. Fisher and J. Angus for technical assistance, S. Parkhurst for advice and help, T. Strecker for help with the rhodamine-123 experiments and for sharing her embryo-permeabilization protocol, J. Revel for assistance with confocal microscopy, and the following for critical comments on the manuscript: G. Attardi, S. Halsell, S. Parkhurst, T. Strecker, D. Weigel, and M. L. Yip. D.D. was supported, in part, by graduate fellowships from the California Foundation for Biochemical Research and the Howard Hughes Medical Institute. K.L.W. was supported, in part, by an NIH predoctoral training grant. This research was supported by a U.S. Public Health Service Program Project Grant (GM40499) to H.D.L. Additional support was provided by a gift for the support of genetics research from Millard and Muriel Jacobs and a grant from the Gustavus and Louise Pfeiffer Research Foundation, to whom H.D.L. wishes to express his gratitude.

REFERENCES

Akiyama, T., and Okada, M. (1992). Spatial and developmental changes in the respiratory activity of mitochondria in early *Drosophila* embryos. *Development* 115, 1175–1182.

Bardsley, A., McDonald, K., and Boswell, R. E. (1993). Distribution of *tudor* protein in the *Drosophila* embryo suggests separation of functions based on site of localization. *Development* 119, 207–219.

Barker, D. D., Wang, C., Moore, J., Dickinson, L. K., and Lehmann, R. (1992). *Pumilio* is essential for function but not for distribution of the *Drosophila* abdominal determinant *nanos*. *Genes Dev.* 6, 2312–2326.

Boswell, R. E., and Mahowald, A. P. (1985). *tudor*, a gene required for assembly of the germ plasm in *Drosophila melanogaster*. *Cell* 43, 97–104.

Chen, L. B., Summerhayes, I. C., Johnson, L. V., Walsh, M. L., Bernal, S. D., and Lampidis, T. J. (1982). Probing mitochondria in living cells with rhodamine 123. *Cold Spring Harbor Symp. Quant. Biol.* 46, 141–155.

Clary, D. O., and Wolstenholme, D. R. (1985). The ribosomal RNA genes of *Drosophila* mitochondrial DNA. *Nucleic Acids Res.* 13, 4029–4045.

Ding, D., and Lipshitz, H. D. (1993a). A molecular screen for polar-localized maternal RNAs in the early embryo of *Drosophila*. *Zygote* 1, 257–271.

Ding, D., and Lipshitz, H. D. (1993b). Localized RNAs and their functions. *BioEssays* 10, 651–658.

Ding, D., Parkhurst, S. M., and Lipshitz, H. D. (1993a). Different genetic requirements for anterior RNA localization revealed by the distribution of *Adducin-like* transcripts during *Drosophila* oogenesis. *Proc. Natl. Acad. Sci. USA* 90, 2512–2516.

Ding, D., Parkhurst, S. M., Halsell, S. R., and Lipshitz, H. D. (1993b). Dynamic *Hsp83* RNA localization during *Drosophila* oogenesis and embryogenesis. *Mol. Cell. Biol.* 13, 3773–3781.

Eddy, E. M. (1975). Germ plasm and the differentiation of the germ line. *Int. Rev. Cytol.* 43, 329–380.

Ephrussi, A., Dickinson, L. K., and Lehmann, R. (1991). *oskar* organizes the germ plasm and directs localization of the posterior determinant *nanos*. *Cell* 66, 37–50.

Ephrussi, A., and Lehmann, R. (1992). Induction of germ cell formation by *oskar*. *Nature* 358, 387–392.

Garesse, R. (1988). *Drosophila melanogaster* mitochondrial DNA: Gene organization and evolutionary considerations. *Genetics* 118, 649–663.

Illmensee, K., and Mahowald, A. P. (1974). Transplantation of posterior polar plasm in *Drosophila*: Induction of germ cells at the anterior pole of the egg. *Proc. Natl. Acad. Sci. USA* 71, 1016–1020.

Illmensee, K., and Mahowald, A. P. (1976). The autonomous function of germ plasm in a somatic region of *Drosophila* egg. *Exp. Cell Res.* 97, 127–140.

Inman, R. B. (1984). Methodology for the study of the effect of drugs on development and DNA replication in *Drosophila melanogaster* embryonic tissue. *Biochim. Biophys. Acta* 783, 205–215.

Johnson, L. V., Walsh, M. L., and Chen, L. B. (1980). Localization of mitochondria in living cells with rhodamine 123. *Proc. Natl. Acad. Sci. USA* **77**, 990–994.

Jongens, T. A., Hay, B., Jan, L. Y., and Jan, Y. N. (1992). The *germ cell-less* gene product: A posteriorly localized component necessary for germ cell development in *Drosophila*. *Cell* **70**, 569–584.

Kim-Ha, J., Smith, J. L., and Macdonald, P. M. (1991). *oskar* mRNA is localized to the posterior pole of the *Drosophila* oocyte. *Cell* **66**, 23–35.

King, R. C. (1970). "Ovarian Development in *Drosophila melanogaster*." Academic Press, New York.

Kobayashi, S., Amikura, R., and Okada, M. (1993). Presence of mitochondrial large ribosomal RNA outside mitochondria in germ plasm of *Drosophila melanogaster*. *Science* **260**, 1521–1524.

Kobayashi, S., and Okada, M. (1989). Restoration of pole-cell forming ability to u.v.-irradiated *Drosophila* embryos by injection of mitochondrial lrRNA. *Development* **107**, 733–742.

Kobayashi, S., and Okada, M. (1990). Complete cDNA sequence encoding mitochondrial large ribosomal RNA of *Drosophila melanogaster*. *Nucleic Acids Res.* **18**, 4592.

Lantz, V., Ambrosio, L., and Schedl, P. (1992). The *Drosophila orb* gene is predicted to encode sex-specific germline RNA-binding proteins and has localized transcripts in ovaries and early embryos. *Development* **115**, 75–88.

Lasko, P. F. (1992). Molecular-movements in oocyte patterning and pole cell differentiation. *BioEssays* **14**, 507–512.

Lehmann, R., and Nüsslein-Volhard, C. (1986). Abdominal segmentation, pole cell formation and embryonic polarity require the localised activity of *oskar*, a maternal gene in *Drosophila*. *Cell* **47**, 141–152.

Lehmann, R., and Nüsslein-Volhard, C. (1987). Involvement of the *pumilio* gene in the transport of an abdominal signal in the *Drosophila* embryo. *Nature* **329**, 167–170.

Lehmann, R., and Nüsslein-Volhard, C. (1991). The maternal gene *nanos* has a central role in posterior pattern formation of the *Drosophila* embryo. *Development* **112**, 679–693.

Lehner, C. F., and O'Farrell, P. H. (1990). The roles of *Drosophila cyclins A* and *B* in mitotic control. *Cell* **61**, 535–547.

Limbourg, B., and Zalokar, M. (1973). Permeabilization of *Drosophila* eggs. *Dev. Biol.* **35**, 382–387.

Lipshitz, H. D. (1991). Axis specification in the *Drosophila* embryo. *Curr. Opin. Cell Biol.* **3**, 966–975.

Macdonald, P. M. (1992). The *Drosophila pumilio* gene: An unusually long transcription unit and an unusual protein. *Development* **114**, 221–232.

Mahowald, A. P. (1977). The germ plasm of *Drosophila*: An experimental system for the analysis of determination. *Am. Zool.* **17**, 551–563.

Manseau, L., and Schüpbach, T. (1989). *cappuccino* and *spire*: Two unique maternal-effect loci required for both anteroposterior and dorsoventral patterns of the *Drosophila* embryo. *Genes Dev.* **3**, 1437–1452.

Niki, Y. (1986). Germline autonomous sterility of P-M dysgenic hybrids and their application to germline transfers in *Drosophila melanogaster*. *Dev. Biol.* **113**, 255–258.

Raff, J. W., Whitfield, W. G. F., and Glover, D. M. (1990). Two distinct mechanisms localize *cyclin B* transcripts in syncytial *Drosophila* embryos. *Development* **110**, 1249–1261.

Schüpbach, T., and Wieschaus, E. (1986). Maternal-effect mutations altering the anterior-posterior pattern of the *Drosophila* embryo. *Roux's Arch. Dev. Biol.* **195**, 302–317.

Strecker, T. R., McGhee, S., Shih, S., and Ham, D. (1994). Permeabilization, staining and culture of living *Drosophila* embryos. *Biotechnic Histochem.* **69**, 25–30.

Tautz, D., and Pfeifle, C. (1989). A non-radioactive *in situ* hybridization method for the localization of specific RNAs in *Drosophila* embryos reveals translational control of the segmentation gene *hunchback*. *Chromosoma* **98**, 81–85.

Wang, C., and Lehmann, R. (1991). *nanos* is the localized posterior determinant in *Drosophila*. *Cell* **66**, 637–647.

Waring, G., Allis, C. D., and Mahowald, A. P. (1978). Isolation of polar granules and the identification of polar granule-specific protein. *Dev. Biol.* **66**, 197–206.